
Electronic Thesis and Dissertation Repository

1-17-2014 12:00 AM

Growth of the Marine Fish-Killing Phytoflagellate, *Heterosigma Akashiwo* Under Emerging Coastal Regimes: Temperature, Eutrophication and Ocean Acidification

Cayla M. Bronicheski, *The University of Western Ontario*

Supervisor: Dr. Charles G. Trick, *The University of Western Ontario*

A thesis submitted in partial fulfillment of the requirements for the Master of Science degree in Biology

© Cayla M. Bronicheski 2014

Follow this and additional works at: <https://ir.lib.uwo.ca/etd>

 Part of the [Biology Commons](#), [Marine Biology Commons](#), and the [Plant Biology Commons](#)

Recommended Citation

Bronicheski, Cayla M., "Growth of the Marine Fish-Killing Phytoflagellate, *Heterosigma Akashiwo* Under Emerging Coastal Regimes: Temperature, Eutrophication and Ocean Acidification" (2014). *Electronic Thesis and Dissertation Repository*. 1871.
<https://ir.lib.uwo.ca/etd/1871>

This Dissertation/Thesis is brought to you for free and open access by Scholarship@Western. It has been accepted for inclusion in Electronic Thesis and Dissertation Repository by an authorized administrator of Scholarship@Western. For more information, please contact wlsadmin@uwo.ca.

**GROWTH OF THE MARINE FISH-KILLING PHYTOFLAGELLATE,
HETEROSIGMA AKASHIWO UNDER EMERGING COASTAL REGIMES:
TEMPERATURE, EUTROPHICATION AND OCEAN ACIDIFICATION**

(Thesis format: integrated article)

by

Cayla M. Bronicheski

Graduate Program in Biology
Collaborative with the Centre for Environment and Sustainability

A thesis submitted in partial fulfillment
of the requirements for the degree of
Master of Science

The School of Graduate and Postdoctoral Studies
Western University
London, Ontario, Canada

© Cayla M. Bronicheski 2014

ABSTRACT

Coastal oceans are fundamental to human economies, nutrition and recreation. Anthropogenic stressors have led to the acceleration of the nitrogen cycle, the accumulation of inorganic carbon in the earth's atmosphere, the loss of UV-scavenging upper atmospheric ozone and the overall accumulation of deep elements from the earth's crust to surface exposure. These changes have caused ocean acidification and eutrophication events in coastal waters and the impacts of these events on primary production and ocean biodiversity are not yet fully understood.

This study examined the effects of predicted future ocean conditions (salinity, temperature, reduced seawater pH and modified nitrogen supplies), on the growth, photosynthesis and fatty acid composition of a key harmful algal bloom producing phytoflagellate predicted to dominate in the future ocean, *Heterosigma akashiwo*. Results from *H. akashiwo* NWFSC were compared to the marine diatom *Thalassiosira weissflogii* and the marine cyanobacterium, *Synechococcus* sp. Experimental pH levels represented ambient seawater (pH 8.1 or pH 8.2), and ecologically relevant pH levels predicted for the years 2050 and 2100 (pH 7.4 and pH 7.8, respectively).

Findings showed that *H. akashiwo* experienced maximal growth rates at 20 practical salinity units, which increased with increasing temperatures predicted in a global climate change scenario (from 14.7 °C-24.4 °C). Altering pH environments did not demonstrate any notable change in growth rates of *H. akashiwo* compared to the other phytoplankton species. Rather, altering the nutrient environment (which occurs in coastal upwelling regimes) was the main driving force to change *H. akashiwo* productivity and intracellular fatty acid composition. Results from this research can provide a foundation for predicting future ocean acidification impacts on marine ecosystems, economies and fisheries productivity.

Keywords: marine phytoplankton, coastal ecosystems, harmful algal blooms, cyanobacteria, diatoms, *Synechococcus*, *Thalassiosira weissflogii*, *Heterosigma akashiwo*, ocean acidification, eutrophication, global change

Co-Authorship Statement

Chapter 2 (Growth kinetics of *Heterosigma akashiwo* under combinations of temperature and salinity) is a collaborative work with Mr. Chris Ikeda (San Francisco State University – The Romberg Tiburon Center for Environmental Studies). As research partners, we designed, prepared and carried out the research together. We independently wrote up the research in consultation with our respective supervisors.

This thesis is dedicated to my loving family:

David, Loretta, Carissa and Christopher.

You have taught me that I can do anything I put my mind to. I am so grateful for all that you do for me, for all of the sacrifices you've made, and all of the opportunities you've given me to get me to this point in my life. Thank you for always believing in me and for your unconditional support in all of my endeavors. Your ongoing love and encouragement is what inspires me to pursue my dreams.



ACKNOWLEDGEMENTS

Northrop Frye, Canadian Icon of cultural criticism, tells a story appropriate to the path of my research. In this story a dog sits in the middle of a great library. Observers note “All the knowledge around her but no skill in accessing it.” I would like to acknowledge the great assistance of my supervisor, Dr. Charles Trick, in helping me access my knowledge and present new ideas. He has presented me with both the most memorable learning experiences I could have ever dreamed of, and once-in-a-lifetime opportunities that I will never forget. Thank you for challenging my intellect and seeing my potential. The lessons I’ve learned and knowledge I’ve gained will follow me in all of my endeavors.

Ecological studies of this type are not done in a vacuum and I acknowledge the astronomic assistance of the Cochlan lab. This thesis would not have been possible without the guidance of Dr. William Cochlan, my co-supervisor, for his expertise and the opportunity to work in his lab at RTC. Even with the lack of windows, it truly was the highlight of my Masters. My personal and scientific growth would not have been realized without Julian Herndon who, unbeknownst, believed in my abilities. Your laboratory assistantship, knowledge and guidance were always exuded with patience with my never-ending questions. I must also thank my RTC lab-mate Chris Ikeda, not only for the laughs and lessons in pidgin, but for the deep scientific chats and comforting words of wisdom when I needed it most. Your wisdom and unconditional help never went unnoticed.

To my advisory committee: Dr. Mark Bernards and Dr. Denis Maxwell, I want to thank you for your ongoing insight throughout this process and for challenging my critical thinking skills. Your support and advice truly helped me push through the difficult times.

I would also like to thank Scott McCain, for working like a champion while helping me throughout many laboratory experiments. Thank you for being a wonderful little scientist in the making. I look forward to reading all of your fantastic publications one day.

Finally, to all of the members (past and present) of the Trick lab, the Creed lab, and the 4th-floor NCB’ers: You have all played an integral role in helping me through the past few years. For the knowledge I’ve gained and the friendships I’ve made, I will always hold this experience as one of the greatest in my life.

What is my job on the planet?

What is it on this planet that needs doing that I know something about, that probably won't happen unless I take responsibility for it?

Richard Buckminster Fuller

TABLE OF CONTENTS

Abstract	ii
Co-Authorship Statement.....	iii
Acknowledgements	v
Table of Contents	vii
List of Figures	xi
List of Tables	xv
List of Appendices.....	xvi
Acronyms and Abbreviations.....	xvii

1. CHAPTER 1: INTRODUCTION LINKING THE EFFECTS OF ANTHROPOGENICALLY-DERIVED GLOBAL CLIMATE CHANGE TO THE DYNAMICS OF OUR FUTURE OCEANS

1.1 Overview.....	1
1.2 The Future Ocean.....	2
1.2.1 Ocean acidification.....	3
1.2.2 Coastal upwelling systems.....	6
1.2.3 Eutrophication.....	8
1.2.4 Nitrogen.....	9
1.2.5 Iron.....	10
1.2.6 Water Mass Stability.....	12
1.2.7 Lipids.....	14
1.3 $p\text{CO}_2$ and pH manipulation.....	16
1.4 Growth and photosynthetic performance.....	18
1.5 Study Aims and Hypotheses.....	18
1.6 Thesis Outline.....	20
1.7 References.....	22

2. CHAPTER 2: GROWTH KINETICS OF *HETEROSIGMA AKASHIWO* UNDER COMBINATIONS OF TEMPERATURE AND SALINITY

2.1 Overview.....	28
2.2 Introduction.....	28
2.3 Materials and Methods.....	31
2.3.1 Experimental design.....	31
2.3.2 Methods of Analyses.....	33
2.3.2a Cell counts by flow cytometry.....	33
2.3.2b Growth rates.....	33
2.3.2c Measurement of cell permeability (SYTOX-Green).....	34
2.3.2d Dissolved Inorganic Carbon (DIC).....	35
2.3.2e Nutrients.....	35
2.4 Results and discussion.....	35

2.4.1 Growth under experimental salinity and temperature regimes.....	35
2.4.2 Dissolved inorganic carbon (DIC).....	41
2.4.3 SYTOX and cell membrane permeability.....	41
2.5 Conclusion.....	47
2.6 References.....	49

3. CHAPTER 3: GROWTH KINETICS, LIGHT UTILIZATION AND LIPID PRODUCTION OF MARINE PHYTOPLANKTON UNDER DIFFERENT PH EXPOSURES

3.1 Overview.....	52
3.2 Introduction.....	52
3.3 Materials and methods.....	56
3.3.1 Experimental design and rationale.....	56
3.3.2 Phytoplankton species selection.....	56
3.3.3 Culturing conditions.....	57
3.3.4 Seawater acidification and maintenance of culture pH.....	57
3.3.4a Adjustment and maintenance of culture pH.....	57
3.2.4b pH measurements.....	58
3.3.5 Iron replete and iron deplete experiments.....	58
3.3.5a Fe enrichment.....	59
3.3.5b NO ₃ ⁻ enrichment.....	59
3.3.6 Methods of analyses: growth measurements.....	59
3.3.6a Flow Cytometry counts.....	60
3.3.6b Haemocytometer.....	60
3.3.6c Spectrophotometer.....	60
3.3.7 Photosynthetic performance.....	61
3.3.7a Sample concentration.....	61
3.3.7b Pulse Amplitude Modulatory Fluorometry (PAM).....	62
3.3.7c Oxygen evolution.....	62
3.3.7d Chlorophyll- <i>a</i> isolation.....	63
3.3.8 Nile red lipid analyses.....	64
3.4 Results.....	64
3.4.1 Acidification.....	65
3.4.1a Examining acid/base titration pH changes in medium without cell culture.....	65
3.4.1b Examining pH changes in media with phytoplankton.....	67
3.4.1c Buffer selection.....	67
3.4.1d Fe selection.....	71
3.4.2 Algal growth.....	79
3.4.3 Cell density variation among iron and pH treatments.....	81
3.4.4 Chlorophyll.....	82

3.4.5 Oxygen evolution.....	88
3.4.6 Nitrogen enrichments on lipid production.....	96
3.4.7 Low N enrichment on growth and lipid production.....	99
3.4.7a Algal growth.....	99
3.4.7b Chlorophyll production.....	101
3.4.7c PAM.....	101
3.4.7d Oxygen evolution.....	101
3.4.7e Lipid production.....	105
3.4.8 Examining density changes in acid/base buffered cell cultures.....	105
3.5 Discussion.....	108
3.5.1 Acid/base buffering.....	108
3.5.2 Algal growth kinetics and photosynthetic changes to ocean acidification.....	109
3.5.3 Lipid production response to ocean acidification.....	115
3.6 References.....	118

4. CHAPTER 4: THE COMBINED EFFECTS OF PH AND PCO_2 ON THE GROWTH AND PHOTOSYNTHETIC CAPACITY OF *HETEROSIGMA* *AKASHIWO*

4.1 Introduction	122
4.2 Materials and methods.....	124
4.2.1 Phytoplankton species selection.....	124
4.2.2 <i>Heterosigma akashiwo</i> culturing conditions.....	125
4.2.3 Seawater acidification and carbonate chemistry measurements....	125
4.2.3a Monitoring pH and acidification using pCO ₂ bubbling...	125
4.2.3b Colorimetric pH measurements.....	127
4.2.3c Dissolved inorganic carbon (DIC) determination.....	127
4.2.4 Experimental design: iron replete and deplete experiment.....	128
4.2.5 Methods of analyses: growth measurements.....	130
4.2.5a Cell counts.....	130
4.2.5b Flow Cytometry.....	130
4.2.5c Chlorophyll Fluorescence.....	131
4.2.6 Photosynthetic performance.....	131
4.2.7 Nutrient analyses.....	132
4.2.7a Particulate Nitrogen (PN) and Phosphate.....	132
4.2.7b Particulate Carbon (PC)	132
4.2.8 Trace metal analyses.....	132
4.3 Results and discussion.....	133
4.3.1 Algal growth.....	134
4.3.2 Cell yield.....	139
4.3.3 PSII efficiency.....	145

4.4 Conclusion.....	147
4.5 References.....	148
5. CHAPTER 5: TYING IT ALTOGETHER.....	150
5.1 References.....	155
APPENDICES.....	156
CURRICULUM VITAE.....	172

LIST OF FIGURES

Figure 1.1 Diagram illustrating predicted nutrient partitioning and subsequent intracellular carbon storage among: a) a phytoplankton cell under nutrient-rich and b) a phytoplankton cell under nutrient-poor, acidic coastal water conditions.

Figure 2.4.1 Average specific growth rates for exponentially growing *H. akashiwo* cells, grown in medium adjusted to a range of salinity treatments and temperatures at a fixed photon flux.

Figure 2.4.2 Specific growth rates for acclimated *H. akashiwo* cells grown in medium adjusted to a range of salinity treatments and temperatures at a fixed photon flux.

Figure 2.4.3 Total DIC remaining in the media on the last day of sampling for the combinatorial experiments of temperature and salinity.

Figure 2.4.4 Cell permeability was determined using the nucleic acid stain SYTOX, with cells during the second day of exponential growth.

Figure 2.4.5 Cell membrane permeability was determined using the nucleic acid stain SYTOX with cells from the last day of exponential growth.

Figure 2.4.6 Cell permeability was determined using the nucleic acid stain SYTOX with cells from the fourth day of stationary growth.

Figure 3.1. pH readings over 5 days of ESAW medium adjusted to pH 7.4, 7.8 and 8.1 with HCl, in the absence of cells.

Figure 3.2. Non-buffered *Synechococcus* sp. CCMP 833 in ESAW medium adjusted to a pH of 7.4, 7.8, and 8.1 with 10% HCl.

Figure 3.3. pH changes in acid/base titrated cultures over a 5-day growth period for *Synechococcus* sp. CCMP 833 grown in ESAW medium with the addition of HEPES buffer.

Figure 3.4. Average growth rate ($\text{day}^{-1} \pm \text{SD}$) of *Synechococcus* sp. CCMP 833 grown in ESAW medium at varying iron concentrations and pH levels.

Figure 3.5. Growth curve of *Synechococcus* sp. CCMP 833 grown in ESAW medium (880 μM N) with altered Fe concentrations and pH levels.

Figure 3.6. Growth curve of *Synechococcus* sp. CCMP 833 grown in ESAW medium (880 μM N) with altered Fe concentrations and pH levels.

Figure 3.7. Growth curve of *Thalassiosira weissflogii* CCMP 1051 grown in ESAW medium with altered Fe concentrations and pH levels.

Figure 3.8. Growth curve of *H. akashiwo* NWFSC 503 grown in ESAW medium with altered Fe concentrations and pH levels.

Figure 3.9. Mean growth rate of *H. akashiwo* NWFSC 503 grown in ESAW medium at varying Fe concentrations and pH levels.

Figure 3.10 Mean growth rate of *Synechococcus* sp. CCMP 835 at grown in ESAW medium varying iron concentrations and pH levels.

Figure 3.11 Mean growth rate of *Synechococcus* sp. CCMP 833 grown in ESAW medium at varying iron concentrations and pH levels.

Figure 3.12 Mean growth rate of *T. weissflogii* CCMP 1051 grown in ESAW medium at varying iron concentrations and pH levels.

Figure 3.13 Cell density/pigment variation between pH treatments and Fe concentrations in A) *Synechococcus* sp. CCMP 833. B) *Synechococcus* sp. CCMP 835, C) *T. weissflogii* CCMP 1051 and D) *H. akashiwo* NWFSC 503 grown in ESAW medium.

Figure 3.14. Mean chlorophyll-*a* values on day 5 and day 9 of growth for *Synechococcus* sp. CCMP 835 grown in ESAW medium.

Figure 3.15. Mean chlorophyll-*a* values on day 5 and day 9 of growth for *Synechococcus* sp. CCMP 833 grown in ESAW medium.

Figure 3.16. Mean chlorophyll-*a* values on day 5 and day 9 of growth for *T. weissflogii* CCMP 1051 grown in ESAW medium.

Figure 3.17 Figure shows mean chlorophyll-*a* values on day 5 and day 9 of growth for *H. akashiwo* NWFSC 503 grown in ESAW medium.

Figure 3.18 Oxygen evolution of *Synechococcus* sp. CCMP 835 grown in ESAW medium (880 μ M) at varying Fe enrichments and pH levels during: A) exponential growth phase and B) stationary growth phase.

Figure 3.19 Oxygen evolution of *Synechococcus* sp. CCMP 833 grown in ESAW medium at varying Fe enrichments and pH levels during: A) exponential growth phase and B) stationary growth phase.

Figure 3.20 Oxygen evolution of *H. akashiwo* NWFSC 503 grown in ESAW medium at varying Fe enrichments and levels of pH during exponential growth.

Figure 3.21 Oxygen evolution curve of *T. weissflogii* CCMP 1051 grown in ESAW medium at varying Fe concentrations and levels of pH during: A) exponential growth phase and B) stationary growth phase.

Figure 3.22 Log normalized growth curve of *H. akashiwo* NWFSC 503 grown in ESAW medium + f/2 nutrients at varying N-concentrations.

Figure 3.23 Neutral lipid content (% of the Chemically Defined Lipid Concentrate, CDLC) over time in *H. akashiwo* 503 at varying N concentrations.

Figure 3.24 Growth curve of *Synechococcus* sp. CCMP 833, *Synechococcus* sp. CCMP 835, *T. weissflogii* CCMP 1051, and *H. akashiwo* NWFSC 503 over a 20 day time period at a low Fe concentration of 0.01 μ M, a high Fe concentration of 11.0 μ M and a pH of 7.4 and 8.1.

Figure 3.25 Total chlorophyll-*a* of *Synechococcus* sp. CCMP 833, *Synechococcus* sp. CCMP 835 and *T. weissflogii* CCMP 1051 was not different between the two Fe concentrations examined and between pH treatments.

Figure 3.26 PSII efficiency of *Synechococcus* sp. CCMP 833, *Synechococcus* sp. CCMP 835 and *T. weissflogii* CCMP 1051 was not different between the two Fe concentrations examined and between pH treatments.

Figure 3.27 Oxygen evolution curve of *T. weissflogii* CCMP 1051 grown in ESAW medium (80 μ M N) at varying Fe concentrations and levels of pH.

Figure 3.28 Neutral lipid production (as a % of the CDLC) over time in *Synechococcus* sp. CCMP 833, *Synechococcus* sp. CCMP 835, *T. weissflogii* CCMP 1051, and *H. akashiwo* NWFSC 503 over a 20 day time period at a low Fe concentration of 0.01 μ M, a high Fe concentration of 11.0 μ M and a pH of 7.4 and 8.1

Figure 3.29 Chlorophyll fluorescence was used to exemplify cell density changes in *Synechococcus* sp. CCMP 833 grown in ESAW acidified to a pH of 7.4, 7.8 and 8.1.

Figure 4.1 Nitrate and phosphate drawdown concentrations, with corresponding cell density increases in *H. akashiwo* NWFSC 503 at pH 7.4 and 8.1.

Figure 4.2 LN growth curve of *H. akashiwo* NWFSCS 503 grown in ESNW medium at a pH of 7.4 (\pm 0.5) and 8.1 (\pm 0.5), with the addition of 6.6 μ M Fe (+Fe) and without the addition of any Fe (-Fe).

Figure 4.3 Comparison of growth rates (divisions day⁻¹) of *H. akashiwo* NWFSC 503 grown in ESAW with 80 μ M N using an acid/base titrated system grown in ESNW with 220 μ M N using a CO₂(g) bubbling system and grown in ESAW with 880 μ M N using an acid/base titrated system.

Figure 4.4 Comparison of maximum cell yeild of *H. akashiwo* NWFSC 503 grown in: ESAW with 80 μ M N using an acid/base titrated system, grown in ESNW with 220 μ M N

using a CO₂(g) bubbling system and ESAW with 880 µM N using an acid/base titrated system.

Figure 4.5 Total cell density differences in *H. akashiwo* NWFSC 503 as a result of cell counting using the flow cytometer and direct microscope counts.

Figure 4.6 PSII efficiency was examined using a DCMU protocol with the alga, *H. akashiwo* NWFSC 513, grown in ESNW medium at a pH of 7.4 (± 0.5) and 8.1 (± 0.5), with the addition of 6.6 µM Fe (+Fe) and without the addition of any Fe (-Fe).

LIST OF TABLES

Table 3.1 Growth rates of *Synechococcus* spp. 833 grown in ESAW (+F/2 nutrients), supplemented with three different concentrations of HEPES buffer.

Table 3.2 Optical density as a proxy for cell yield of *Synechococcus* spp. 833 grown in ESAW (+f/2 nutrients), supplemented with three different concentrations of HEPES buffer.

Table 3.3 Photosynthetic efficiency, apparent and true photosynthetic capacity, and photorespiration of *Synechococcus* sp. CCMP 833, *Synechococcus* sp. CCMP 835, *T. weissflogii* CCMP 1051, and *H. akashiwo* NWFSC 503 at: A) low Fe and B) high Fe.

Table 3.4 Growth rate and cell yield of *H. akashiwo* NWFSC 503 grown in ESAW medium at various initial N concentrations.

Table 4.1 pH records after correcting for salinity and temperature.

LIST OF APPENDICES

Chapter 3 Appendices

Appendix I: Stable pH readings with buffered and acidified cultures

Appendix II: Selection of Fe enrichment

Appendix III: Oxygen evolution rationale

Appendix IV: Nile red plate reader organization

Chapter 4 Appendices

Appendix I: Enriched Seawater, Natural Water (ESNW)

Appendix II: Diagrammatic representation of QUBIT

Appendix III: Tris Buffer CRM Certificate

Appendix IV: Colour changes from the colorimetric pH measurement procedure

Appendix V: Comparison of *in vivo* fluorescence from *Heterosigma akashiwo* NWFSC 513, with different DFB concentrations

Appendix VI: Lab-ware cleaning protocol

Appendix VII: Care and maintenance of pH probe

Appendix VIII: DCMU protocol

ACRONYMS AND ABBREVIATIONS

ANOVA	analysis of variance
CRM	certified reference material
CCS	California Current System
DCMU	3-(3,4-dichlorophenyl)-1,1-dimethylurea
DFB	desferrioxamine B, Desferal ®
DHA	docosahexanoic acid
DI	deionized water
EBUS	eastern boundary upwelling system
EFA	essential fatty acids
EPA	eicosapentanoic acid
ESAW	enriched seawater artificial water
ESNW	enriched seawater natural water
F _m	maximal fluorescence
F _o	minimal fluorescence
F _v /F _m	maximal PSII photochemical efficiency
HEPES	4-(2-hydroxyethyl)-1-piperazineethanesulfonic acid
HSD	Tukey's Honestly Significant Difference
PAM	pulse amplitude modulatory fluorometry
PAR	photosynthetically active radiation
pH	-log [H ₃ O ⁺]
PSI and PSII	Photosystem one or photosystem two, respectively
psu	Practical salinity units
PUFA	polyunsaturated fatty acid
RCF	relative centrifugal force
RPM	rotations per minute
SOP	standard operating procedure
μ _{max}	maximal growth rate
yield _{max}	maximal yield

CHAPTER 1

1. Introduction: linking the effects of anthropogenically-derived global climate change to the dynamics of our oceans

1.1 Overview

Coastal oceans are fundamental to the economics, nutrition, recreation and aesthetics of a large portion of the human population. Over 3.2 billion people around the globe live within coastal areas, characterized by a 120-mile wide strip of the coastline, while over 4 billion people reside within 250 miles of the coast (Hinrichsen 1998). Marine and coastal resources and industries are valued at \$3 trillion (USD) per year, equating to about 5% of global GDP (United Nations), while fisheries contribute approximately \$274 billion (USD) to the total global GDP (World Bank 2009). The Fisheries and Aquaculture Department (FAO) of the United Nations estimates that fish are one of the most traded commodities, generating \$102 billion (USD) in export value (FAO 2010, FAO 2011). As the global human population exceeds 7 billion people, many of our wastes ultimately end up in an often-overlooked global ecosystem chain - the oceans. The first barrier that must be crossed before the anticipated dilution by the ocean is the coastal barrier water - a water system that is not only impacted by humans, but also used and often abused by humans.

Globally, 11 million tons of synthetic nitrogen fertilizer runoff in coastal waters each year (representing 40% of global anthropogenic nitrogen entering marine ecosystems), while 16 million tons of nitrogen per year enter coastal regions from the combined inputs of domestic and industrial sewage, animal wastes, growth of legume crops and atmospheric loads from the burning fossil fuels (collectively representing the remaining 60% of global anthropogenic nitrogen entering marine ecosystems) (Maranger

et al. 2008). Additionally, over 27 million metric tons of fish are removed each year through fisheries exploitation, which is around one-third of the estimated 77 million metric tons of catch that is retained each year (Alverson *et al.* 1994). The addition of nutrients via fertilizers, pesticides and sewage exerts a bottom-up control on the aquatic environment and the removal of predation via over-fishing exerts a top-down control on the aquatic environment. This change in marine predation dynamics will have a substantial effect on the phytoplankton species composition and, perhaps the quality of food at the base of the food chain (Cury *et al.* 2001).

1.2 The Future Ocean

Humans have had a strong impact on the chemistry, biology, and as an extension, the overall ecology of the globe. Often discussed as individual effects such as acid rain or issues of landscape use and form, the largest changes have altered the entire biogeochemistry of the earth. The scale of these changes has been so grand that many are referring to the present age as the Anthropocene - a period in the earth's history dominated by human induced changes in the quality of major ecosystems, the quality of different reservoirs (for example, the atmosphere or freshwater supplies), and the overall quality of ecological services on which human development and growth depends. These changes include the acceleration of the nitrogen cycle, the accumulation of inorganic carbon and water in the earth's atmosphere, the loss of UV-scavenging upper atmospheric products (ozone) and the overall accumulation of deep products from the earth's crust at the surface through exposure by human activities (exposure by copper, mercury and lead, to name a few). At larger scales, the products of these activities involve altered global and regional temperatures, modified patterns and magnitudes of rain events, and altered soil fertility (Zalasiewicz 2008). The Anthropocene is, to say the least, a period of

extensive and rapid change. The coastal ocean is at the forefront of the regions of change because most of the human population lives in close proximity to the coastlines.

The coastal waters are in the intersection of two dramatic environmental stresses - ocean acidification and coastal eutrophication. What will be referred to herein as the “future ocean” refers to a future coastal marine ecosystem that will certainly look different than the present coastal community. It has been posed that the future coastal ocean will, for some time, be richer in macronutrients, more acidic overall (but specifically in upwelling areas), as well as be warmer and thus, more stable (characterized by less vertical mixing to depths) (Snyder et al. 2003). Each one of these changes directly alters the base of the coastal food chain - the phytoplankton community. This thesis approaches our understanding of this problem using a model phytoplankton cell (*Heterosigma akashiwo*) that is normally stimulated by extra nutrients and is likely to be a substantial component of the phytoplankton community to exist in the eutrophic and acidic coastal waters predicted for the future.

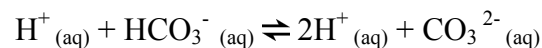
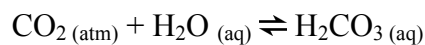
1.2.1 Ocean Acidification

One of the anticipated coastal alterations that will potentially change the composition of the phytoplankton community is ocean acidification. Over the past millennium, human activities have altered many ecosystems on Earth. Since the beginning of the Industrial Era, a dramatic increase in fossil fuel burning, either directly or indirectly due to human activities, has resulted in a flux of greenhouse gas emissions into the atmosphere including methane (CH₄), nitrous oxide (NO) and carbon dioxide (CO₂) (IPCC 2001; Caldeira and Wicket 2003). Notably, anthropogenic CO₂ emissions have greatly contributed to a rise in global temperatures, leading to extreme climatic events (IPCC 2001; The Royal Society 2005). Approximately three-quarters of all

atmospheric CO₂ emissions during the past 20 years are due to the rise in fossil fuel combustion activities, but the accumulation in the atmosphere is buffered as CO₂ partitions into the surface ocean.

Oceanic CO₂ sequestration accounts for nearly one third of anthropogenic sources added to the atmosphere since the beginning of the industrial era, which is roughly equal to 127 ± 18 billion metric tons of carbon as CO₂ (Sabine *et al.* 2004; Sabine and Feely 2007; Feely *et al.* 2008; Doney *et al.* 2009). The oceans will eventually take up the majority of CO₂ that is released in the atmosphere, as they cover over two-thirds of the Earth's surface, contain more primary production than any terrestrial ecosystem and have nutrient regimes under-saturated with regards to CO₂ (Caldeira and Wickett 2003; The Royal Society 2005). The consequence of oceanic uptake is regarded as the often-overlooked effect of global climate change, known as ocean acidification.

Ocean acidification is the lowering of oceanic hydrogen ion concentration (pH), that is, the measure of acidity that occurs when atmospheric CO₂ dissolves in the surface ocean according to the following series of reversible reactions:



This process is accompanied by predictable changes in ocean chemistry, including an increase in the partial pressure of carbon dioxide ($p\text{CO}_2$) and a reduction in the carbonate ion concentration [CO_3^{2-}]. Gas exchange between the air and sea equilibrates surface water CO₂ to atmospheric levels, within approximately a one-year timeframe (Doney *et al.* 2009).

Atmospheric CO₂ concentrations have dramatically increased from the pre-industrial level of approximately 280 parts per million (ppm) (The Royal Society 2005). Over the past few years alone, atmospheric CO₂ measurements taken at the Mauna Loa Observatory, Hawaii, indicated a rise from 389.68 ppm in December 2010, to 398.58 ppm in June 2013 (Tans and Keeling 2012). The corresponding average ocean surface water pH before industrial times has declined by approximately 0.1 units, from 8.21 to 8.10 and is predicted to drop a further 0.3-0.4 pH units if global emissions of CO₂ from human activities continue to climb (The Royal Society 2005; Doney *et al.* 2009). Adding CO₂ to the ocean increases aqueous CO₂, bicarbonate (HCO₃⁻) and hydrogen ion concentrations (H⁺). Since $\text{pH} = -\log_{10} [\text{H}_3\text{O}^+]$, the projected pH decline of 0.1 units is equivalent to a 150% increase in H⁺ ions (acidity), which underscores the urgency of the problem (Orr *et al.* 2005; Doney *et al.* 2009).

Studies have demonstrated the potential biological consequences, in particular, the effects of an increase in $p\text{CO}_2$ and a decrease in $[\text{CO}_3^{2-}]$ on marine organisms, but so far, the overall impact of decreasing pH is less well known. (Doney *et al.* 2009; Shi *et al.* 2010). Most biota resides near the surface ocean, where the greatest pH change is expected to occur, but deep-ocean biota may be more sensitive to pH changes (Seibel and Walsh 2001; Caldeira and Wickett 2003). In assessing the vulnerability of marine organisms to these changes, it is not sufficient to examine only global mean changes in pH. Global mean values may not properly highlight regional variability among pH and carbonate chemistry, which can mask the urgency of the acidification problem (Hauri *et al.* 2009).

Ocean acidification will result in changes that may exacerbate the effects of global climate change and therefore, requires innovative approaches to study. Currently, much of

the previous research on ocean acidification has involved examining changes in biomass and phytoplankton community structure, and has determined limited changes in community composition in coastal waters resulting from the lower pH environment (Kim *et al.* 2006; Riebesell *et al.* 2007; Suffrian *et al.* 2008; Aberle *et al.* 2012; Nielsen *et al.* 2012). Yet, unresolved is whether the quality of phytoplankton as a food source will remain unaltered and how eutrophication will fit into the dynamics of our coastal waters. There is an absolute need to assess whether a link exists between the nutritional value of phytoplankton as suitable prey to support highly productive food webs, and the altered chemistry of an acidifying ocean. Of particular ecological importance is the consequence of altered phytoplankton nutritional states, to the reproductive and developmental potential of higher trophic levels.

1.2.2 Coastal upwelling systems

Ocean acidity varies both spatially and temporally, with some areas of the ocean more vulnerable to pH fluctuations than others. Eastern boundary upwelling systems (EBUS) in temperate waters, such as in the upwelling occurring on the west coast of North America, is an example of an area that is especially vulnerable to future ocean acidification (Hauri *et al.* 2009). Although the corrosive character of these waters is the result of respiration as well as organic matter decomposition at depths below the euphotic zone, the added pressure of anthropogenic CO₂ dissolution exacerbates the impacts of ocean acidification within this current (Feely *et al.* 2008). Upwelled waters along the coast are already experiencing ocean acidification conditions as low as a pH of ~7.7, compared to the average ocean pH of ~8.1, which wasn't expected to occur for another 100 years (Feely *et al.* 2008).

The real problem arises from prevailing northeasterly winds causing extensive upwelling of cool sub-surface water, acting through the Ekman effect. Winds of the appropriate direction and strength to induce upwelling are more prevalent in eastern boundary currents than other areas. These winds drive water upwards to replace the surface water moving away from the coast in an event known as upwelling. As a result of this upwelling, waters along the western coastline of North America are rich in nutrients and make this area a key zone for fish production. These low pH regions are constrained near shore, because in the presence of high nutrients and light, photosynthetic removal of CO₂ draws down surface $p\text{CO}_2$ with a concomitant increase in surface water pH, as the upwelled surface water advects offshore through Ekman transport (Hauri *et al.* 2009). Given the economic and biogeochemical importance of these productive fishing areas, it is critical to assess the impacts of ocean acidification in regions occurring along the west coast of North America in a controlled laboratory setting (Chavex and Toggweiler 1995; Hauri *et al.* 2009).

The coastal upwelling system is one of the most productive marine regimes on Earth and is responsible for a disproportionate fraction of total global new productivity. The coastline is presently a mosaic of iron-limited phytoplankton, both regionally and seasonally. Iron-dependent shifts in community structure between large diatoms and a smaller picoplankton community may occur and consequently will have large implications for export fisheries production, as well as carbon cycling (Hutchins and Bruland 1998). Frequent inputs of nitrate (NO₃⁻) enable phytoplankton to synthesize polar lipids, essential fatty acids and proteins. Under iron-limitation, it is anticipated that phytoplankton will shift towards producing neutral lipids. This brings rise to the questions: Does an altered pH increase or decrease Fe availability? Will iron-limitation

in the CCS change the mosaic of Fe-limited phytoplankton? To answer these questions, it is important to mimic typical environmental conditions that would be expected *in situ*, throughout all laboratory experimentations.

1.2.3 Eutrophication

Over the last few decades, there has been a massive increase of nutrients entering the coastal waters, where the natural eutrophication process has been advanced due to human activities (Burkholder 2000). In many cases the result is simply an increase in the level of phytoplankton and the transfer of the new biomass through the food chain. In many other cases increases in nitrate, ammonia, and phosphorus has altered the phytoplankton community by switching to a resource-limited complex marine community with a single (or small number) of species that outcompete the majoring species and dominate the phytoplankton community at high biomass (Tilman 1997; Smayda 1990, 1997). While many of these species are just nuisance high-biomass species, many others are phytoplankton which show adverse health effects on organisms higher in the food chain- many of which are known to express toxins that adversely effect humans or fish (Anderson *et al.* 2002). The resulting communities are referred to as harmful algal blooms (HABs) (or as some jokingly point out - “algae with an attitude”) and these species no longer provide benefit to the food chain of the coastal resources. Overall, the release of macronutrients into the coastal ocean results in the propagation of a select and usually undesirable species to which the food chain must adapt.

Linked to the eutrophication of coastal waters in the future ocean is the availability of nitrogen. While in lake systems, the availability of phosphorus generally regulates the level of productivity (Schindler 1997), the level of productivity and the phytoplankton species composition in marine coastal systems is regulated by the mass

loading, as well as the form, of nitrogen present (Dugdale and Goering 1967; Gilbert 1998).

1.2.4 Nitrogen

While most attention on ocean acidification research has been put towards calcium carbonate production and dissolution in shelled organisms, much less consideration has been given to the impact of decreasing pH on the chemistry of macro- and micronutrients and their availability to the broader phytoplankton community (Hare *et al.* 2007; Tortell *et al.* 1998). There are several metabolic processes that are sensitive to the Iron supply available to phytoplankton, including nitrogen assimilation. Major nutrients such as carbon (C), nitrogen (N), and phosphorus (P) have essential structural, energy and information roles within phytoplankton cells. Micronutrients, such as Fe, play a large catalytic role as a cofactor of enzymes required for the assimilation of these major nutrients. Nutrient limitation can affect growth rates by impairing essential biochemical functions. Proteins that contain iron are directly involved in processes including, but not limited to nitrate (NO_3^-) and nitrite (NO_2^-) reduction (Geider and La Roche 1994; Wells *et al.* 1995). These essential metabolic pathways are known to require relatively large amounts of Iron (Raven 1988). Because of the diversity of the role of Fe, many cellular processes are likely to be affected by Fe-limitation.

In episodic upwelling regions, phytoplankton are frequently exposed to high concentrations of macronutrients. Given the critical role of iron in the bioenergetics of C and N metabolism, a reduction in the bioavailability of iron to phytoplankton (due to a decreased pH) would likely be reflected in their inability to effectively utilize abundant macronutrient reserves, in particular, NO_3^- (Raven 1988; Morel *et al.* 1991). A reduction in iron availability due to increased acidity can impact phytoplankton nitrogen uptake in a

number of ways: by either slowing NO_3^- uptake by resident cells, forcing cells to use ammonium (NH_4^+) and urea ($\text{CO}(\text{NH}_2)_2$) which use less iron for assimilation and are energetically less expensive to assimilate, or shifting to a smaller cell-sized community which can better utilize these reduced but less available forms for N (Raven 1988; Price *et al.* 1991). Under any of the proposed scenarios, cells become increasingly N-stressed despite the abundance of ambient NO_3^- in the water column. Each phytoplankton species has their own mechanism for nitrogen-uptake that is dependent on the nutrients available within the water column. With excess cultural eutrophication, will our future acidic ocean consist of an abundance of NO_3^- , NH_4^+ or $\text{CO}(\text{NH}_2)_2$, and what species will the resulting future ocean be able to support?

1.2.5 Iron

There is a large degree of conflicting evidence regarding how ocean acidification will impact the chemical speciation of essential trace metals and nutrient availability with anticipated corresponding consequences on phytoplankton growth and metabolism (Doney *et al.* 2009). Our present state of knowledge cannot predict if Fe-limitation will be alleviated or enhanced at a more neutral pH (Shi *et al.* 2010).

Ironsolubility in seawater is strongly affected by pH and will undergo speciation shifts as a response to ocean acidification. Iron must be dissolved for phytoplankton to acquire it, making the bioavailability of iron a function of its solubility (Rich and Morel 1990; Millero *et al.* 2009). Under normal pH (~8.1) conditions, hydroxide (OH^-) and carbonate (CO_3^{2-}) ions can form strong complexes in seawater with trivalent metals, including trivalent iron (Fe^{3+}), but under low pH conditions these ion concentrations are reduced (Millero *et al.* 2009; Shi *et al.* 2010). As ocean waters acidify, decreasing OH^- ion concentrations, iron speciation is altered and iron (III) solubility will increase (Shi *et*

al. 2010). For example, a decrease in pH by 0.3 units slightly increases iron solubility, as most dissolved iron in the ocean is highly insoluble due to OH⁻ ion binding or chelation to natural ligands by organic compounds (Breitbarth 2009; Shi *et al.* 2010). These Fe-chelating ligands work in two ways to increase iron availability to the cell: by solubilizing surrounding Fe³⁺ and by assimilating Fe³⁺ in waters where the availability limits growth (Wilhelm *et al.* 1996).

As iron is an important micronutrient, it has been suggested that the outcome of increasing iron solubility under acidic conditions will increase iron availability to phytoplankton and microbes, leading to an increase in primary production (Martin 1990; Brand 1991). Additionally, in certain coastal isolates at low iron concentrations, high-affinity siderophore-mediated iron uptake systems can be induced (Wilhelm and Trick 1994). Any competition to bind with iron would lessen the biological availability of this metal to microbes and could influence primary productivity in some marine environments (Wilhelm *et al.* 1996; Shi *et al.* 2010). Shi *et al.* (2010) suggested that a decrease in pH and OH⁻ ion will alter the capabilities of iron chelation to certain natural organic ligands, and therefore shift the level of iron acquired by marine organisms. In the same study, it was shown that the availability of iron to phytoplankton in surface seawater should decrease with pH as a result of the acid-base chemistry of the specific chelating ligand (Shi *et al.* 2010). With the pH of average seawater decreasing from 8.1 to 7.4, as anticipated for the year 2100, the solubility of Fe (III) will increase by roughly 40% (Brand 1991; Millero *et al.* 2009).

Considerable research has been conducted to determine the role iron plays in influencing primary productivity under optimal conditions. Less research has questioned iron acquisition in Fe-limited, non-optimal conditions. Hutchins and Bruland (1998)

demonstrated that Fe-poor waters limit primary producers in some upwelling areas. Additions of iron along the coast of Big Sur, California, were shown to increase phytoplankton growth rates, biomass, nitrate uptake, and resulted in dominant taxa to change from nano- and pico-plankton to large diatoms (Hutchins and Bruland 1998; Hutchins *et al.* 1998). Although our understandings of the effects on iron uptake by phytoplankton have been extensively examined, the impacts on other metabolic pathways, such as the synthesis of essential fatty acids, are less understood. Since a decrease in pH alters biogeochemical conditions of seawater and micronutrient availability, it poses the question: how do alterations in seawater chemistry affect physiological responses of phytoplankton under Fe-stressed conditions?

1.2.6 Water Mass Stability

The future ocean is predicted to have a warmer surface layer due to three factors, collectively referred to as water mass stability: the warmer terrestrially fed surface water (itself predicted to be warmed due to the heating of land masses), the increased levels of direct heating of the surface water due to irradiance, and the lesser degree of water mixing between the warm surface water and the cooler, denser seawater below. The result of this prediction is that the surface water is more stable and more separate from the cooler, nutrient-rich water below (Sprintall and Cronin, 2001). In this situation, the surface water is in equilibrium with atmospheric CO₂ and generally will not contain excess CO₂ that would result in acidic waters. The potential for acidity is further reduced, as cells in the upper waters are most likely to photosynthesize, a base-generating process.

One physical regime that obliterates the water mass layering is the coastal upwelling system. As discussed, upwelling areas are regions where the physical movement of the earth forces the deeper water (down to 100 m) to shift to the surface

where it either mixes with the warmer water or pushes the warmer water away from the coast. Since the water that is forced to the surface is higher in acidity due to the dissolution of carbonates in the cold-water depth, these upwelling regions can be referred to as the lost acidic areas of coastal waters. Consequences from these acidic waters arise within the structure of the phytoplankton community, where species are likely to change based on the availability of nutrients (through eutrophication), light (thinner ozone layer), salinity (density) and temperature (global warming). These factors bring rise to the questions: will the current oceanic phytoplankton species composition remain stable? Or will there be a shift in the current phytoplankton community that dominates our coastal water because of the water mass stability factor?

Presently, in coastal regions that are abundant in nutrients, diatoms tend to be the most prevalent species. This is the result of a large amount of kinetic energy (driven by convection) that overturns to vertically displace water mass, enabling diatoms to outcompete other groups when nutrients and light are available. However, their sinking rates prevent them from sustaining their populations near the surface (Gregg *et al.* 2003). Cyanobacteria are opposite to diatoms in that they cannot outcompete diatoms under favourable nutrient rich waters. However, they have a competitive advantage in low nitrogen areas because of their nutrient uptake efficiency, low sinking rates and ability to fix molecular nitrogen- enabling them to predominate areas such as mid-ocean gyres where circulation is weak, mixed layers are deep and nutrients are rarely added into the mixed layer (Glover 1985; Itturiaga and Mitchell 1986; Gregg *et al.* 2003). On the other hand, flagellates tend to be predominant where severe iron limitation limits diatom abundances, and have been characterized as occupying transitional regions (Ondrusek *et al.* 1991; Obayashi *et al.* 2001). Transitional regions are areas where nutrient and light

availability are insufficient to allow diatoms to predominate, but where nutrients are not so low as to prevent sinking losses in an effort to compensate growth. These areas are a function of a flagellate's intermediate growth, sinking (swimming) and nutrient uptake efficiency relative to diatoms and cyanobacteria, where the largest flagellate concentrations tend to occur during the transition between diatoms and cyanobacteria (Gregg *et al.* 2003). Lastly, in areas with oligotrophic waters, picoplankton are always found to be most dominant.

In the future ocean, upwelling is expected to intensify, meaning that the duration of acidic waters exposed to surface light and nutrients will be longer than present conditions. There will also be changes on the seasonality of the upwelling, suggesting that not only will the periods of upwelling be long, there will also be more yearly upwelling periods. This intensification may lead to enhanced productivity (Snyder *et al.* 2003). The shift in water mass stability may result in unrecognized consequences within the oceanic food-web dynamics where our current diatom-dominated waters might be replaced by new conditions of flagellate-dominated waters. The real consequence lies within the specific Essential Fatty Acid (EFA) profile of phytoplankton, and whether the species with the competitive advantage will be met with conditions facilitating specific EFA production required by higher marine organisms. This future situation forms the experimental model of this thesis - nitrogen-rich, iron-variable acidified waters in the photic zone.

1.2.7 Lipids

Essential fatty acid production in phytoplankton has the unique potential to exert bottom-up control on animal populations in aquatic systems. Quantifying the link among phytoplankton EFA production, nutrient availability and ocean acidification is crucial because EFAs are the only lipid constituents that cannot be synthesized by animals and

must be obtained through diet (Igarashi *et al.* 2007). Nutrient availability, with current and future ocean acidity changes, will either enhance or reduce the lipid quality of coastal phytoplankton as a food resource for secondary consumers. Uncertainty lies with whether the key to success is the shift from waters that are NO_3^- replete and iron deplete to waters that are NO_3^- replete and iron replete. Results will have drastic implications for improvements in the productivity and quality of marine fisheries, economies, as well as for the health of communities around the globe that rely on fish for sustenance.

Fatty acid desaturases are members of a large group of membrane-bound, iron containing enzymes (Shanklin and Cahoon 1998; Sasata *et al.* 2004). These iron containing enzymes remove two hydrogen atoms from an existing saturated fatty acid creating a carbon-carbon double bond, forming an unsaturated fatty acid. Iron deficiency is known to affect lipid metabolism in higher organisms, beginning with primary producers and cascading up the marine food web to higher fish (Stangl *et al.* 2008). Fatty acid desaturases are necessary for algal species to uptake essential nutrients from the water column, allowing them to fulfill their intracellular lipid, carbohydrate or protein needs. It is reasonable to expect that decreasing the availability of Fe, accompanied by metal speciation shifts from ocean acidification, will have an indirect impact on the composition and metabolism of lipids, carbohydrates and/or proteins in marine phytoplankton.

Phytoplankton lipids are synthesized from free fatty acids and divided into two primary classes: the structural polar lipids that play a key role in maintaining the integrity of the cell and chloroplast membranes, and neutral lipids that primarily serve as an energy storage reserve (Geider and La Roche 2002). Under optimal nutrient-rich conditions, when cells are experiencing exponential growth, as in what one would expect to see in

upwelling areas, phytoplankton are able to synthesize fatty acids principally for polar or membrane lipids (Brown *et al.* 1996; Hu *et al.* 2008). Under nutrient limitation, however, the overall cellular lipid content increases and phytoplankton shift their lipid biosynthetic pathways from polar lipids toward the formation and accumulation of neutral lipids that do not perform a structural role but serve as a storage form of carbon energy (Fig. 1.1). Although many environmental factors can alter cellular lipid production, the most common trigger of neutral lipid formation, is macronutrient limitation (Spoehr and Milner 1948). There have been no studies specifically investigating the degree to which ocean acidification affects the competitive success of eicosapentanoic acid (EPA)-rich diatoms versus docosahexanoic acid (DHA)-rich dinoflagellates in productive ecosystems, and consequently how this will alter the food quality of primary production available for higher fish. Changing the diversity or concentration of diets rich in algae (between either diatoms or dinoflagellates), may affect the reproductive responses of higher trophic levels. Very few phytoplankton studies have reported on fatty acid profiles as a function of nutrient sufficiency.

1.3 $p\text{CO}_2$ and pH manipulation

There is currently no consensus on the optimal method for manipulating ocean acidification events within a laboratory setting. There is considerable debate regarding the various methods of $p\text{CO}_2$ /pH adjustment- acid/base addition with the use of buffers or bubbling CO_2 gas- and which method is best to apply. Notably, methods would differ depending on the objective of the study and the organism in question. With the two most commonly used methods, there is considerable evidence supporting that a $p\text{CO}_2$ type of system is most representative of a natural environmental acidification scenario, while

other studies report that an acid/base manipulation type of system would suffice (Gattuso and Lavigne 2009; Shi *et al.* 2009). Both methods can have different effects on the

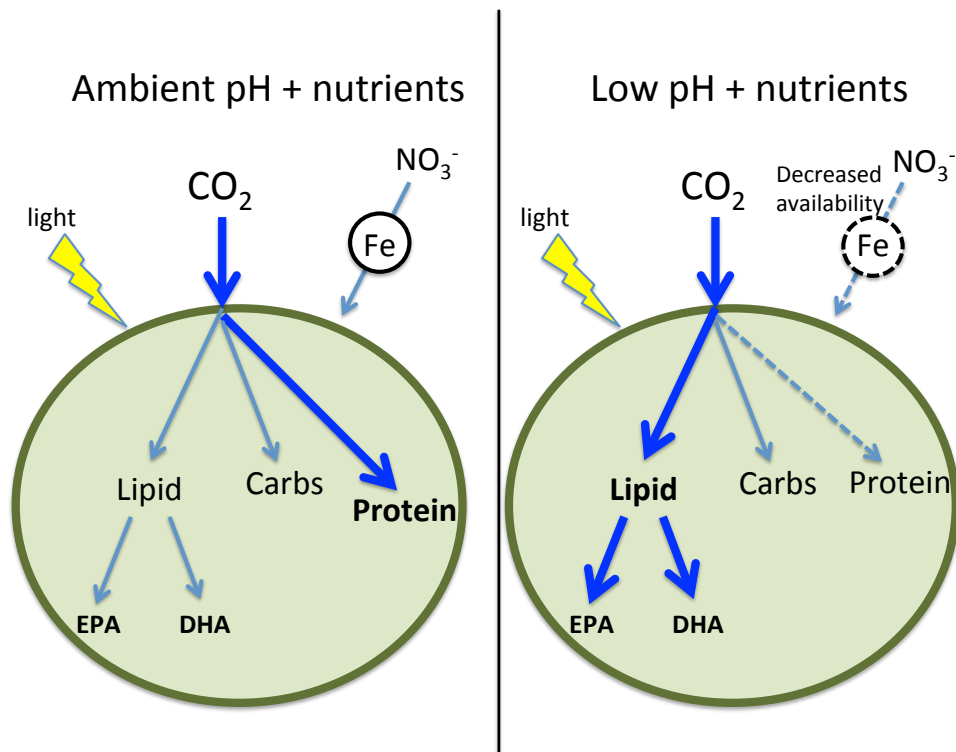


Figure 1.1 Diagram illustrating predicted nutrient partitioning and subsequent intracellular carbon storage among: a) a phytoplankton cell under nutrient-rich and b) a phytoplankton cell under nutrient-poor, acidic coastal water conditions. The solid blue lines represent a normal physiological pathway, with thick blue lines representing the more dominant fate of carbon partitioning, and the dotted lines represent a compromised metabolic pathway.

carbonate system of seawater, which could result in contradictory results. For instance, adding a biologically benign buffer to an acid (or base)-adjusted culture would control pH and is advantageous as it would leave the amount of DIC constant by continually adjusting DIC when it becomes depleted during culture growth. However, bubbling $p\text{CO}_2$ gas would change the DIC, but has the advantage of maintaining culture alkalinity (Shi *et al.* 2009). There are also other issues concerning the potential mechanical damage that could be imposed on the culture through bubbling gases in the medium. In this study, both methods were examined to tease apart the physiological differences that could arise intracellularly when using either ocean acidification technique.

1.4 Growth and photosynthetic performance

Current research suggests that ocean acidification can either stimulate or reduce primary production, depending on the organism in study. Readily available dissolved oceanic CO_2 concentrations are currently at limiting levels for RuBisCo, the enzyme responsible for the first step in photosynthesis. Increasing $p\text{CO}_2$ concentrations from the effect of ocean acidification could alleviate RuBisCo driven $p\text{CO}_2$ limitation, thereby enhancing phytoplankton primary production unless the species already contains an effective carbon-concentrating mechanism (Beardall and Raven, 2004; Riebesell *et al.*, 2007).

1.5 Study Aims and Hypotheses

The overall aim of this study is to examine the effects of our future ocean (namely, a reduced seawater pH and modified nitrogen supplies), on the growth, photosynthesis and fatty acid composition of three examples of marine phytoplankton. Using the marine phytoflagellate, *Heterosigma akashiwo*, the marine diatom *Thalassiosira weissflogii* and two phenotypes of the marine cyanobacterium, *Synechococcus* sp. Three experimental pH

levels were considered for this research, and included levels that reflect ambient seawater (pH 8.1 or pH 8.2), and two ecologically relevant pH levels predicted for the year 2050 and 2100 (pH 7.4 and pH 7.8, respectively).

There are three main objectives to this thesis. First, a growth characterization study was completed for *H. akashiwo*. As a key harmful algal species *H. akashiwo* is likely to be found as an important constituent for the future ocean (Smayda 1990). The ranges of maximal tolerance and growth under different combinations of temperature and salinity were ascertained.

For the second objective, the differential rates of growth, neutral lipid production and photosynthetic activity for *H. akashiwo* were examined in comparison to a common diatom, *T. weissflogii* and the photosynthetic prokaryote, *Synechococcus* sp. under different pH media where the pH was adjusted to a buffered medium.

In the third objective, growth rates and nutrient yields of *H. akashiwo* under different $p\text{CO}_2$ levels, corresponding directly to a CO_2 induced pH change, were examined. In these later experiments, pH levels were changed through supplementation with $p\text{CO}_2$ gas. The experiments were performed under two environmental conditions that reflect the predicted coastal ocean: nitrate-rich seawater with high levels of iron and nitrate-rich seawater with low levels of iron.

It is understood that there will be less diatoms in the future ocean, and the species composition will likely shift to one dominated by flagellates due to their ability to migrate and utilize nutrients in eutrophic waters. As a flagellate, *H. akashiwo* is used in this thesis as a model organism for a species that is likely to be abundant in the conditions that are pertinent to future ocean studies, particularly because there is a recognition that flagellates will predominate in the future eutrophic, warm and acidic ocean.

1.6 Thesis Outline

Chapter 1 outlined the background for the study of *H. akashiwo* in the future ocean. Specifically Chapter 1 logically offered information leading to the hypothesis: *Heterosigma akashiwo* will be a successful member of the phytoplankton community under the future ocean.

Chapter 2 investigates and provides basic information regarding the optimal laboratory conditions for culturing *H. akashiwo* (strain NWFSC 513). Primary environmental parameters include salinity and temperature, with growth recorded under a fixed photon flux.

Chapter 3 establishes the growth characteristics (growth rate and yield), neutral lipid production and the photosynthetic capacities of three marine phytoplankton isolates: *H. akashiwo* strain NWFSC 513 (isolated from Clam Bay, Washington, USA on June 16, 2010), *T. weissflogii* (isolated from the North Pacific, Kahaluu, Hawaii, USA on May 13, 1985) and *Synechococcus* sp. CCMP 833 and 835 (isolated from the North Atlantic in 1982 and 1985, respectively) under buffered pH environments that represent the future coastal ocean: pH 7.8 for the year 2050 and pH 7.4 for the year 2100.

Chapter 4 provides an examination of the combined effect of pH and $p\text{CO}_2$ changes on the growth and photosynthetic capacity of *H. akashiwo*.

While no single species can represent the entire phytoplankton community, research on *H. akashiwo* closes the gaps in our current understanding of the effects that ocean acidification might pose on the growth and intracellular nutrient composition in phytoplankton. As there are three variables that are essential to control: the change in $p\text{CO}_2$ of our ocean, the change in pH of our ocean and the change in the availability of

nutrients, the use of a modern HABs species served as an excellent model for the study of anthropogenically altered coastal waters.

1.7 References

- Aberle, N., Schulz, K. G., Stühr, A., Ludwig, A., and Riebesell, U. 2012. High tolerance of protozooplankton to ocean acidification in an Arctic coastal plankton community. *Biogeosci. Discuss.* **9**: 13031-13051.
- Anderson, D.M., Gilbert, P.M. and Burkholder, J.M. 2002. Harmful algal blooms and eutrophication: nutrient sources, composition and consequences. *Estuaries*. **25**: 704-726.
- Bell, J.G., Preston, T., Henderson, R.J., Strachan, F., Bron, J.E., Cooper, K. and Morrison, D.J. 2007. Discrimination of wild and cultured European sea bass (*Dicentrarchus labrax*) using chemical and isotopic analyses. *J. Agricult. Food Chem.* **55**: 5934-5941.
- Berges, J.A., Franklin, D.J. and Harrison, P.J. 2001. Evolution of an artificial seawater medium: Improvements in enriched seawater, artificial water over the last two decades. *J. Phycol.* **37**: 1138-1145.
- Bjornsson, W. 2009. Semi-quantitative estimate of intracellular lipid content using the plate reader and Nile Red. Standard Operating Procedure (SOP), Cellana Biofuels, Kona, Hawaii.
- Brand, L.E. 1991. Minimum iron requirements of marine-phytoplankton and the implications for the biogeochemical control of new production. *Limnol. Oceanogr.* **36**: 1756-1771.
- Breitbarth, E., Gelting, J., Walve, J., Hoffmann, L.J., Turner, D.R., Hasselov, M. and Ingri, J. 2009. Dissolved iron (II) in the Baltic Sea surface water and implications for cyanobacterial bloom development. *Biogeosci.* **6**: 2397-2420.
- Brown, M.R., Barrett, S.M., Volkman, J.K., Nearhos, S.P., Nell, J.A. and Allan, G.L. 1996. Biochemical composition of new yeasts and bacteria evaluated as food for bivalve aquaculture. *Aquacult.* **143**: 341-360.
- Burkholder, J. M. 2000. Eutrophication and oligotrophication, p. 649–670. In S. Levin [eds.], *Encyclopedia of Biodiversity*, Volume 2. Academic Press, New York.
- Caldeira, K. and Wickett, M.E. 2003. Anthropogenic carbon and ocean pH. *Nature* **425**: 365-365.
- Cury, P., Shannon, L. and Yunn-Jai, S. 2001. The functioning of marine ecosystems. *Reykjavik Conference on Responsible Fisheries in the Marine Ecosystem*. Iceland: 121.
- Dickson, A.G., Sabine, C.L. and Christian, J.R. 2007. Guide to best practices for ocean CO₂ measurements, p.1991. In PICES [eds.] Special Publication.

- Doney, S.C., Fabry, V.J., Feely, R.A. and Kleypas, J.A. 2009. Ocean acidification: the other CO₂ problem. *Ann. Rev. Mar. Sci.* **1**: 169-192.
- Dugdale, R.C. and Goering, J.J. 1967. Uptake of new and regenerated forms of nitrogen in primary productivity. *Limnol. Oceanogr.* **12**: 196-7.
- Feely, R.A., Sabine, C.L., Hernandez-Ayon, J.M., Ianson, D. and Hales, B. 2008. Evidence for upwelling of corrosive "acidified" water onto the continental shelf. *Science* **320**: 1490-1492.
- Geider, R.J. and La Roche, J. 2002. Redfield revisited: variability of C:N:P in marine microalgae and its biochemical basis. *Eur. J. Phycol.* **37**: 1-17.
- Geider, R.J. and Laroche, J. 1994. The role of iron in phytoplankton photosynthesis, and the potential for iron-limitation of primary productivity in the sea. *Photosyn. Res.* **39**: 275-301.
- Glibert, P. M. 1998. Interactions of top-down and bottom-up control in planktonic nitrogen cycling. *Hydrobiol.* **363**: 1-12.
- Glover, H.E., 1985. The physiology and ecology of the marine cyanobacterial genus *Synechococcus*. *Adv. Microbiol.* **3**: 49-107.
- Gregg, W.W., Ginoux, P., Schopf, P.S. and Casey, N.W. 2003. Phytoplankton and iron: validation of a global three-dimensional ocean biogeochemical model. *Deep-Sea Res.* **11**: 3143-3169.
- Guillard, R.R.L. 1973. Division rates, p. 289-312. In Stein, J.R. Handbook of Phycological Methods: Culture Methods and Growth Measurements [eds.], Cambridge University Press, Cambridge.
- Hare, C.E., DiTullio, G.R., Riseman, S.F., Crossley, A.C., Popels, L.C., Sedwick, P.N. and Hutchins, D.A. 2007. Effects of changing continuous iron input rates on a Southern Ocean algal assemblage. *Deep-Sea Res.* **54**: 732-746.
- Harrison, P.J., Waters, R.E. and Taylor, F.J.R. 1980. A broad-spectrum artificial seawater medium for coastal and open ocean phytoplankton. *J. Phycol.* **16**: 28-35
- Hauri, C., Gruber, N., Plattner, G.K., Alin, S., Feely, R.A., Hales, B. and Wheeler, P.A. 2009. Ocean acidification in the California Current System. *Oceanogr.* **22**: 60-71.
- Held, P. and Raymond, K. 2011. Determination of algal cell lipids using Nile Red. Winooski, Vermont, USA: BioTek Instruments, Inc. 2010-2018.
- Hu, J.F., Zhang, G., Li, K.C., Peng, P.A. and Chivas, A.R. 2008. Increased eutrophication offshore Hong Kong, China during the past 75 years: Evidence from high-resolution sedimentary records. *Mar. Chem.* **110**: 7-17.

- Hutchins, D.A. and Bruland, K.W. 1998. Iron-limited diatom growth and Si:N uptake ratios in a coastal upwelling regime. *Nature* **393**: 561-564.
- Hutchins, D.A., Ditullio, G.R., Zhang, Y. and Bruland, K.W. 1998. An iron limitation mosaic in the California upwelling regime. *Limnol. Oceanogr.* **43**: 1037-1054.
- Igarashi, M., Demar, J.C., Ma, K.Z., Chang, L., Bell, J.M. and Rapoport, S.I. 2007. Docosaehaenoic acid synthesis from alpha-linolenic acid by rat brain is unaffected by dietary n-3 PUFA deprivation. *J. Lipid Res.* **48**: 1150-1158.
- IPCC, Climate Change 2001: The Scientific Basis. Contribution of Working Group I to the Third Assessment Report of the Intergovernmental Panel on Climate Change [Houghton, J.T., Y. Ding, D.J. Griggs, M. Noguer, P.J. van der Linden, X. Dai, K.] 34p.
- Itturiaga, R. and Mitchell, B.G., 1986. Chroococcoid cyanobacteria: a significant component in the food web dynamics of the open ocean. *Mar. Ecol. Prog. Ser.* **28**: 291–297.
- Maranger, R., N. Caraco, J. Duhamel, and M. Amyot. 2008. Nitrogen transfer from sea to land via commercial fisheries. *Nature Geosci.* **1**:111-113.
- Martin, J.H., Broenkow, W.W., Fitzwater, S.E. and Gordon, R.M. 1990. Does iron really limit phytoplankton production in the offshore sub-arctic pacific- yes, it does- a reply. *Limnol. Oceanogr.* **35**: 775-777.
- Millero, F.J., Woosley, R., Ditrolio, B. and Waters, J. 2009. Effect of ocean acidification on the speciation of metals in seawater. *Oceanogr.* **22**: 72-85.
- Morel, F.M.M., Hudson, R.J.M. and Price, N.M. 1991. Limitation of productivity by trace-metals in the sea. *Limnol. Oceanogr.* **36**: 1742-1755.
- Nielsen, L.T., Hallegraeff, G.M., Wright, S.W. and Hansen, P.J. 2012. Effects of experimental seawater acidification on an estuarine plankton community. *Aquat. Microb. Ecol.* **65**: 271-285.
- NOAA- National Oceanic Atmospheric Administration. noaa.gov. Retrieved 7-28-2012.
- Ocean Pollution - MarineBio.org. MarineBio Conservation Society. Web. 2013. <<http://marinebio.org/oceans/ocean-dumping.asp>>.
- Obayashi, Y., Tanoue, E., Suzuki, K., Handa, N., Nojiri, Y., and Wong, C.S. 2001. Spatial and temporal variability of phytoplankton community structure in the northern North Pacific as determined by phytoplankton pigments. *Deep-Sea Res.* **48**: 439–469.

- Ondrusek, M.E., Bidigare, R.R., Sweet, S.T., Defreitas, D.A., and Brooks, J.M. 1991. Distribution of phytoplankton pigments in the North Pacific Ocean in relation to physical and optical variability. *Deep-Sea Res.* **38**: 243–266.
- Orr, J.C., Fabry, V.J., Aumont, O., Bopp, L., Doney, S.C., Feely, R.A., Gnanadesikan, A., Gruber, N., Ishida, A., Joos, F., Key, R.M., Lindsay, K., Maier-Reimer, E., Matear, R., Monfray, P., Mouchet, A., Najjar, R.G., Plattner, G.K., Rodgers, K.B., Sabine, C.L., Sarmiento, J.L., Schlitzer, R., Slater, R.D., Totterdell, I.J., Weirig, M.F., Yamanaka, Y. and Yool, A. 2005. Anthropogenic ocean acidification over the twenty-first century and its impact on calcifying organisms. *Nature*. **437**: 681-686.
- Parsons, T. R., Y. Maita and Lalli C. M. 1984. A Manual of Chemical and Biological Methods for Seawater Analysis, Pergamon Press, Oxford. 173p.
- Price, N.M., Andersen, L.F. and Morel, F.M.M. 1991. Iron and nitrogen nutrition of equatorial Pacific plankton. *Deep-Sea Res.* **38**: 1361-1378.
- Raven, J.A. 1988. The iron and molybdenum use efficiencies of plant-growth with different energy, carbon and nitrogen-sources. *New Phytol.* **109**: 279-287.
- Rich, H.W. and Morel, F.M.M. 1990. Availability of well-defined iron colloids to the marine diatom *Thalassiosira weissflogii*. *Limnol. Oceanogr.* **35**: 652-662.
- Rost, B., Zondervan, I. and Wolf-Gladrow, D. 2008. Sensitivity of phytoplankton to future changes in ocean carbonate chemistry: current knowledge, contradictions and research directions. *Mar. Ecol.-Progr. Ser.* **373**: 227-237.
- Sabine, C.L. and Feely, R.A. 2007. The oceanic sink for carbon dioxide. *Greenhouse Gas Sinks*. **1**: 31-49.
- Sabine, C.L., Feely, R.A., Gruber, N., Key, R.M., Lee, K., Bullister, J.L., Wanninkhof, R., Wong, C.S., Wallace, D.W.R., Tilbrook, B., Millero, F.J., Peng, T.H., Kozyr, A., Ono, T. and Rios, A.F. 2004. The oceanic sink for anthropogenic CO₂. *Science*. **305**: 367-371.
- Sasata, R.J., Reed, D.W., Loewen, M.C. and Covello, P.S. 2004. Domain swapping localizes the structural determinants of regioselectivity in membrane-bound fatty acid desaturases of *Caenorhabditis elegans*. *J. Biol. Chem.* **279**: 39296-39302.
- Schindler, D.W. 1977. Evolution of phosphorus limitation in lakes. *Science* **196**: 260–262.
- Seibel, B.A. and Walsh, P.J. 2001. Carbon cycle - potential, impacts of CO₂ injection on deep-sea biota. *Science* **294**: 319-320.
- Shanklin, J. and Cahoon, E.B. 1998. Desaturation and related modifications of fatty acids. *Ann. Rev. Plant Physiol. Plant Molecul. Biol.* **49**: 611-641.

- Shi, D.L., Xu, Y., Hopkinson, B.M. and Morel, F.M.M. 2010. Effect of ocean acidification on iron availability to marine phytoplankton. *Science* **327**: 676-679.
- Smayda, T. 1990. Novel and nuisance phytoplankton blooms in the sea: evidence for a global epidemic, p. 29–40. In E. Graneli, B. Sundstrom, L. Edler, and D. M. Anderson [eds.], *Toxic Marine Phytoplankton*. Elsevier, New York.
- Smayda, T. J. 1997. Harmful algal blooms: Their ecophysiology and general relevance to phytoplankton blooms in the sea. *Limnol. Oceanogr.* **42**: 1137–1153.
- Snyder, M. A., L. C., Sloan, N. S. Diffenbaugh, and Bell J. L. 2003. Future climate change and upwelling in the California Current. *Geophys. Res. Lett.*, **30**: 1823.
- Sprintall, J. and Cronin, M.F. 2001. Upper ocean vertical structure. In J. Steele, S. Thorpe, and K. Turekian [eds.] *Encyclopedia of Ocean Sciences*, **6**: 3120-3129, Academic Press, London, UK.
- St. John, M.A., Clemmesen, C., Lund, T. and Koester, T. 2001. Diatom production in the marine environment: Implications for larval fish growth and condition. *PICES J. Mar. Sci.* **58**: 1106-1113.
- Stangl, G.I. and Kirchgessner, M. 1998. Different degrees of moderate iron deficiency modulate lipid metabolism of rats. *Lipids* **33**: 889-895.
- Tans, P. and Keeling, R. 2012. NOAA/ESRL (www.esrl.noaa.gov/gmd/ccgg/trends/) and Scripps Institution of Oceanography (scrippsco2.ucsd.edu/).
- The Royal Society. 2005. Ocean acidification due to increasing atmospheric carbon dioxide. The Clyvedon Press Ltd.: Cardiff, United Kingdom.
- Tilman, D. 1977. Resource competition between planktonic algae: an experimental and theoretical approach. *Ecol.* **58**: 338–348.
- Tortell, P.D., Reinfelder, J.R. and Morel F.M.M. 1997. Active uptake of bicarbonate by diatoms. *Nature*. **390**: 243-244.
- Spoehr, H.A. and Milner, H.W. 1948. *Chlorella* as a source of food. Carnegie Institute of Washington Year Book. **47**: 100-103.
- Wells, M.L., Price, N.M. and Bruland, K.W. 1995. Iron chemistry in seawater and its relationship to phytoplankton- a workshop report. *Mar. Chem.* **48**: 157-182.
- Wilhelm, S.W., Maxwell, D.P. and Trick, C.G. 1996. Growth, iron requirements, and siderophore production in iron-limited *Synechococcus* PCC 7002. *Limnol. Oceanogr.* **41**: 89-97.

Wilhelm, S.W. and Trick, C.G. 1994. Iron-limited growth of cyanobacteria- multiple siderophore production is a common response. *Limnol. Oceanogr.* **39**: 1979-1984

Zalasiewicz, J. 2008. Are we now living in the Anthropocene? *GSA Today*. **18**: 4-8.

CHAPTER 2

2. Growth kinetics of *Heterosigma akashiwo* under combinations of temperature and salinity

2.1 Overview

This chapter focuses on providing information for the optimal laboratory culturing conditions of *H. akashiwo* (NWFSC 513), and aims at determining whether there was a combinatorial effect between the environmental parameters of salinity and temperature on the growth rate and cell membrane integrity of this Harmful Algal Bloom (HAB) species, under a fixed photon flux. The chapter additionally outlines the conditions causing cell membrane permeability from *H. akashiwo* under the interaction conditions of temperature and salinity.

2.2 Introduction

The most critical environmental parameter studied in phytoplankton ecophysiology research is the effect of temperature on growth and metabolism. As industrial and human activities continue exacerbating global climatic changes, if all greenhouse gas emissions were ended today, global atmospheric temperatures are still expected to rise between 1.1 to 6.4 °C by the year 2100, with corresponding increases in sea-surface temperatures (IPCC, 2007). While microalgae reside in extremely variable environments, increased temperature does not always result in faster growth or up-regulation of critical cellular processes. It is well established that each specific phytoplankton species has their own optimal temperature range for maximal growth, exhibiting a bell-shaped curve with peak metabolic rates (Falkowski and Raven 2007). Presently, it remains controversial whether the proposed rise in sea-surface temperatures will enhance or hinder the growth and photosynthesis of present algal communities. At

elevated temperatures alternative species may replace the less competitive species. Thus, the predicted future global climatic shift will undoubtedly be species specific.

Temperature changes over the next decade may pose profound effects not only at the species level, but also on the entire phytoplankton community and ocean ecosystem, especially in the context of Harmful Algal Blooms (HABs) – a taxonomically unrelated group of ecologically exploitive species. HABs are a national concern as outbreaks can grow explosively resulting in the production of either toxic or noxious compounds that can adversely affect not only the health of marine organisms, but can also affect the health of humans directly or indirectly through illness from seafood consumption (Taylor and Haigh, 1993; Connell *et al.*, 1997). The HAB species of interest in this study was the raphidophyte, *Heterosigma akashiwo*, isolated from Puget Sound (Washington, USA), which has been known to cause massive aquaculture fish kills. The frequency of reports of *H. akashiwo* HABs have increased over the past decade. The increased incidence of bloom outbreaks has become problematic not only to fish farmers but also natural fish communities migrating through extensive blooms (Rensel *et al.* 2010). With inevitable changing climatic events, it is anticipated that our existing coastal phytoplankton community will shift to be comprised of a community that can withstand the new oceanic conditions. Flagellated raphidophytes such as *H. akashiwo* are expected to be at the forefront of this shift due to their distinctive physiological characteristics: euryhaline, 10-30 chloroplasts, flagellated with strong vertical migration and lack of a rigid cell-wall (Montagnes 2006, Rensel *et al.* 2010). For this reason, *H. akashiwo* was used as the model species in this experiment, as it is proposed to thrive in our future ocean.

Future climatic changes are anticipated to result in new ocean conditions, including higher sea-surface temperatures with corresponding changes to a more robust

phytoplankton community having unique photoprotective abilities (Warner and Madden, 2007). With consummate mechanisms of photoprotection during sub-optimal temperature and irradiance conditions, raphidophytes have an innate ability to avoid stressors and continue photosynthesis. Warner and Madden (2007) found that to maintain photosynthesis during elevated irradiance, raphidophytes down-regulate the total number of PSII reaction centres in their chloroplasts (the first step in acquiring light energy for photosynthesis), and lower the rate of electron transport to avoid photoinhibitory effects. Raphidophytes also are exposed to photodamage by rising to the surface of the water column during light hours after settling to the bottom during dark hours (Handy *et al.* 2005). In particular, *H. akashiwo* have a unique ability to sense and react to light, remaining at bottom depths during continuous light exposure, giving this species a competitive advantage in the anticipated future ocean. However, if an imbalance between light acquisition and utilization happens to occur, photoinhibitory damage is likely to result in the main protein of the PSII reaction center (D1), leading to lower PSII efficiency (Hüner *et al.* 1998). Compared to the physiologic changes of reduced PSII efficiency in an attempt to acclimate to light stress, there have been several studies describing similar responses to other environmental stresses, including cold temperature (Maxwell *et al.* 1994; Hüner *et al.* 1998), salinity (Neale and Melis, 1989), nutrient deprivation (Davies and Grossman, 1998) and CO₂ deprivation (Miyachi *et al.* 2003).

Although physical mobility and physiologic changes in PSII proteins are proposed as responses to temperature, light and salinity stress, *H. akashiwo* toxin production might be the most critical consequence to these future environmental changes. Mechanisms for toxin production in *H. akashiwo* are currently not fully understood. In contrast to most phytoplankton, this genus lacks a rigid cell wall and can be easily lysed with physical

movement or agitation. This cellular fragility is often implicated in the toxicity of this genus – either in a direct means (causing fish gills to be clogged with broken cells) or by releasing toxins on cell lysis, affecting water quality (Smayda 1998). Thus researchers have focused on the physical state of the cell wall, specifically relating morphological changes with nutrient limitation wall, in correlational studies between lowered cellular growth rates, chlorophyll loss per cell, and elevated membrane permeability and the putative level of toxicity (Veldhuis *et al.* 1997, 2001).

The present experiment focused on assessing the growth and membrane integrity of temperature and salinity-acclimated *H. akashiwo* cells.

2.3 Materials and Methods

2.3.1 Experimental design

A non-axenic isolate of *H. akashiwo* (NWFSC 513) was collected from Clam Bay, WA, USA, in 2010 and maintained in batch culture conditions at the National Oceanic Atmospheric Administration (NOAA) Northwest Fisheries Science Center (NWFSC). The pre-experimental inoculum cells were grown for four days, equating to ca. 4.5 generations, at three salinity (31.5, 20, 10 psu) and five temperature (13.5, 16.5, 19.5, 22.5 and 25.5 °C) conditions. These cultures to be used as the inoculum for the experiment were grown in 50 mL borosilicate tubes that contained 40 mL of culture, and kept inside a temperature controlled light box (NOAA NWFCS) that created a temperature gradient through an aluminum block. Cells were exposed to a saturating average photosynthetic photon flux density (PPFD) of ca. $350 \mu\text{mol photon} \cdot \text{m}^{-2} \cdot \text{s}^{-1}$ under a 14 hr light : 10 hr dark cycle. PPFD was measured with a 4π scalar collector (QSL-100; Biospherical Instruments). For the pre-experimental inoculum cultures, daily *in vivo* fluorescence (10-AU, Turner Designs) was collected to measure cellular growth.

After the cultures had grown for four days at the respected experimental conditions, the cultures were used to inoculate four 50 mL borosilicate tubes (40 mL of culture per tube) containing fresh media for the experiment. All freshly inoculated cultures were grown under the same conditions as the initial experimental inoculum culture. All culture manipulations were performed using glassware, plastic-ware and equipment cleaned with 10% HCl (v/v) followed by three rinses in ultra-pure water.

Cultures were grown in 0.2 μ M filtered (Polycap 150 TC; Whatman) seawater collected from East Sound, Puget Sound, WA, USA. Seawater was enriched using a modified enriched seawater natural water (ESNW) medium (Harrison *et al.*, 1980; Berges *et al.*, 2001), which had reduced concentrations for N and P (50 and 5 μ M, respectively), to prevent inorganic carbon limitation due to biological activity (e.g., Howard *et al.*, 2007). Additionally, $\text{CuSO}_4 \cdot 5\text{H}_2\text{O}$, $\text{MnSO}_4 \cdot \text{H}_2\text{O}$ and Na_2SeO_3 were added to a final concentration of 3.93×10^{-9} M, 2.42×10^{-3} M and 1.27×10^{-5} M, respectively. All other nutrient enrichments followed the protocol established by Harrison *et al.* (1980) and modified by Berges *et al.* (2001). To achieve the desired salinity conditions, 0.2 μ M filtered seawater from East Sound (31.5 psu) was diluted to 20 and 10 psu with ultra-pure water (18.2 M Ω .cm). Additional NaHCO_3 was added to the 20 and 10 psu treatments to achieve a final concentration of 2.07×10^{-3} M in order to adjust for the change in DIC concentration during the dilution process.

Samples were collected daily for cell permeability using the nucleic acid stain SYTOX-green (S7020; Invitrogen Molecular Probes), cell counts by flow cytometer (C6 Flow Cytometer, BD AccuriTM) and *in vivo* fluorescence until the fourth day of stationary growth from all quadruplicates. On the final day of sampling, samples were collected from two of the quadruplicates for pH, nutrients (NO_3^- and H_3PO_4) and dissolve inorganic

carbon (DIC). The remaining volume was combined to produce two samples per quadruplicate for cellular toxicity analysis.

2.3.2 Methods of Analyses

2.3.2a Cell counts by flow cytometry

Subsamples (0.5 mL) from each quadruplicate were pipetted into 12 x 75 mm borosilicate test tubes (14-961-26, Fisher Scientific). Samples were fixed with a 0.5% (final concentration) Lugol's solution prior to counting cells. Quadruplicates were averaged to obtain daily cell density measurement (cells mL⁻¹). A total of 50 µL was used to characterize the cell density for each sample, and then averaged over the quadruplicate samples. To calculate the cell density, the C6 Analysis Software (BD AccuriTM) was used to create histogram plots of the sample population with high chlorophyll α fluorescence (i.e. > 10⁶). Due to the high number of chloroplast within *H. akashiwo*, a 90% attenuation filter was used to reduce the fluorescence response of individual cells.

2.3.2b Growth rates

Cellular growth rates were determined using data from both flow cytometer cell counts with and *in vivo* fluorescence. Specific growth rates were calculated from a least-square linear regression analysis for the exponential growth phase using natural log transformed data of either cell counts performed by flow cytometry or *in vivo* fluorescence using the following equation:

$$K_e = \frac{\ln \left(\frac{N_1}{N_0} \right)}{t_1 - t_0}$$

Where K_e is the growth constant (in units of d^{-1}) and N_1 and N_0 is either the cell counts or *in vivo* fluorescence at time 1 (t_1) and time 0 (t_0), respectively (Guillard, 1973).

2.3.2c Measurement of cell permeability (SYTOX- Green)

SYTOX-Green is a fluorescent dye that indicates cell viability by binding to DNA of cells with compromised cell membrane (Veldhuis *et al.*, 2001). SYTOX-Green was used to measure the amount of dye that entered viable cells in order to gauge changes in cell permeability as a function of salinity. A 50 μ M SYTOX-Green (S-34860, Invitrogen) working solution was prepared in ultra-pure water, and kept at -20 °C until use. Before staining cells with SYTOX-Green, the background fluorescence was measured using 50 μ L of unpreserved cells at the excitation and emission wavelength for SYTOX-Green (488/523 nm, respectively). After the background fluorescence was measured, 5 μ L of the SYTOX-Green working solution was added to the unstained cells for a final concentration of 0.6 μ M. Samples were then inverted 4 times before incubating at room temperature (~20 °C) for 15 minutes in the dark. A 50 μ L subsample of SYTOX-Green stained cells was then measured with a C6 Flow Cytometer using the following excitation/emission wavelength, 488/523 nm, respectively.

A histogram plot was used to gate compromised cells (i.e. SYTOX-Green stained cells), by first plotting non-SYTOX stained cells with high chlorophyll α fluorescence (i.e. $> 10^6$). A density scatter plot was then created that only showed the gated population with high chlorophyll α fluorescence, which was then separated into four quadrants. The line separating the lower right quadrant from the upper right quadrant was placed directly above the unstained cell population. SYTOX stained cells were then applied to the density scatter plot, with positively stained cells showing fluorescence in the upper right

quadrant. The portion of the cellular population in this upper right quadrant indicated viable cells with compromised cell membranes.

2.3.2d Dissolved Inorganic Carbon (DIC)

Unfiltered water samples for DIC determination were injected by syringe into an acid-washed 20 mL combusted (450 °C for 6 hours) glass scintillation vial. The inverted poly-cone caps for the glass scintillation vial were only acid-washed. To prevent bubbles from forming while the samples were injected into the scintillation vial, silicon tubing was attached to the end of the syringe in order to gently inject the sample into the container. DIC samples were then immediately preserved with 300 µL of 5% w/v mercuric chloride (HgCl₂) and sealed with an inverted poly-cone cap to ensure no headspace in the sample vial. Samples were kept in the dark until analysis with an acid-sparging non-dispersive infrared (NDIR) gas analyzer (Friederich *et al.*, 2002).

2.3.2e Nutrients

Nutrient samples for NO₃⁻ and H₃PO₄ were collected in polypropylene conical tubes (352097, Fisher Scientific) pre-soaked in ultra-pure water. A total of 12 mL was collected from two of the quadruplicate borosilicate tubes from each treatment. Unfiltered nutrient samples were stored at -20 °C until analysis. Prior to analysis with a flow injection auto analyzer (QuickChem 8000 Series, Lachat Instruments), samples were thawed over night at room temperature (~20 °C) before analysis using protocols developed by Smith and Bogren (2001) and Knepel and Borgen (2002).

2.4 Results and discussion

2.4.1 Growth under experimental salinity and temperature regimes

As a flagellate from temperate coastal waters, *H. akashiwo* was able to grow with relatively high growth rates at all salinity (32, 20 and 10 psu) and temperature (14.7, 18.4,

21.4, 24.4, 27.8 °C) conditions tested (Figure 2.4.1). Maximal growth rates were attained at 20 psu, which increased with temperature from 14.7 °C to 24.4 °C ($\mu=0.96 \pm 0.08$ to $1.48 \pm 0.05 \text{ d}^{-1}$), followed by 10 psu ($\mu=0.78 \pm 0.028$ to $1.69 \pm 0.021 \text{ d}^{-1}$) and 32 psu ($\mu=0.67 \pm 0.02$ to $1.16 \pm 0.12 \text{ d}^{-1}$). A one-way ANOVA followed by a Tukey's HSD test indicated that cells grown at 20 psu grew significantly faster ($P < 0.05$) than either the 32 or 10 PSU treatment, except at 18.4 °C and 24.4 °C where no significant difference was seen. It should be noted that at 24.4 °C, the 20 psu treatment was only marginally non-significant compared to the 32 psu treatment ($P = 0.0587$). Salinity treatments grown at 27.8°C was not included in Figure 2.4.1, as only two time points were collected during the exponential growth phase.

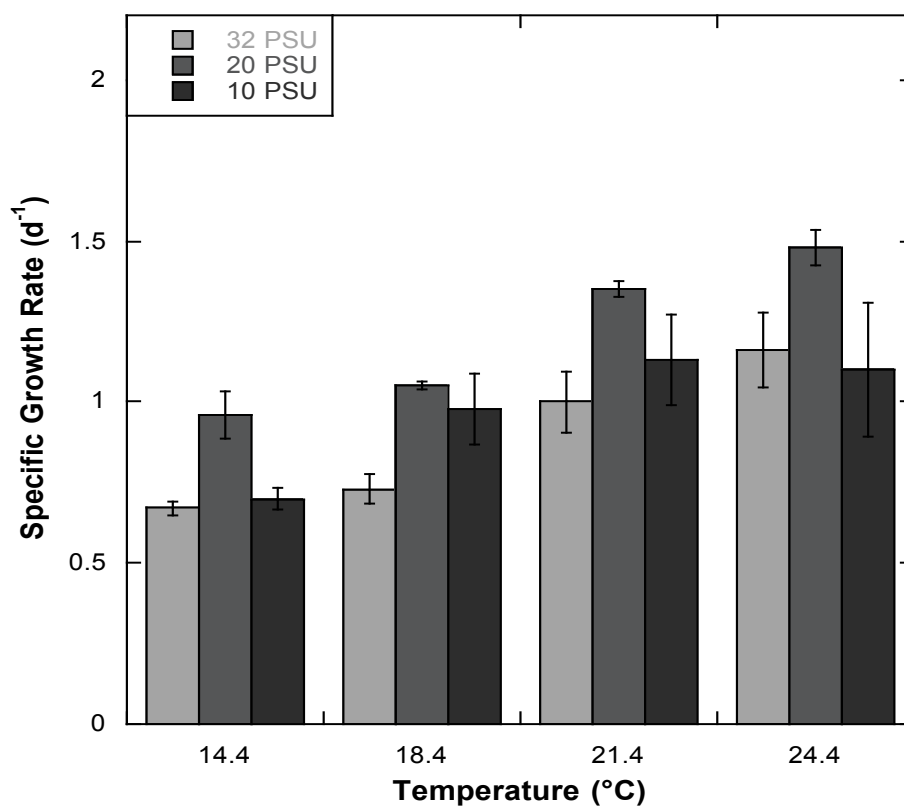


Figure 2.4.1 Average specific growth rates for exponentially growing *H. akashiwo* cells, grown in medium adjusted to a range of salinity treatments (32, 20 and 10 psu), and temperatures (14.4, 18.4, 21.4, 24.4 and 27.8 °C) at a fixed photon flux. Values indicate the average of quadruplicate samples, with error bars indicating one standard deviation.

The first factor influencing *H. akashiwo* growth was salinity, where a lowering of salinity has been suggested to trigger the germination and growth of *Heterosigma* cells that grow optimally at salinities around 20 - 25 psu (Haque and Onoue 2002; Kempton *et al.* 2008). The optimum salinity range for non-adapted *H. akashiwo* cell growth, established by Honjo (1993), was at a very broad range between 20 and 35 psu. As demonstrated from the specific growth rates (Figure 2.4.1), *H. akashiwo* maximal growth occurred at a temperature of 24.4 °C and a salinity of 20 psu. At 24.4 °C, *H. akashiwo* growth rates decreased from 20 > 10 > 32 psu, suggesting that this alga may show a competitive dominance through its ability to acclimate to lower salinity conditions. Even growth at 5 psu has been reported by Tomas (1978), however, other investigations reported lack of growth below 10 psu (Haque and Onoue 2002). In a study on an *H. akashiwo* isolate from the Nervion River, Spain (Orive *et al.* 2004), the alga was found to grow at a range of salinities from above 5 to 35 psu, where growth was higher at 21 °C than 17 °C. It is clear that across-strain differences arise from *H. akashiwo* cells isolated from different geographic areas, indicating that the species isolates may be genetically different and may differ in salinity tolerance, carotenoid production and growth rate (Smayda 1998; Han *et al.* 2002). Most studies demonstrate that as cells are given a longer time for salinity acclimation- that is, physiologically adjusting to a change in salinity without compromising growth or metabolism- growth rates among strains isolated from different geographic locations become similar (Martinez *et al.* 2010), highlighting the robustness of this alga.

As documented by Fig. 2.4.2, when temperature was increased to 27.8 °C, a salinity of 32 psu resulted in the highest growth rate for this alga, followed by 10 psu, then 20 psu. These findings can be important, considering the warmer conditions

predicted by the future ocean, indicating that *H. akashiwo* would not be excluded from the community at the lower (10 psu) or higher salinities (32 psu). Similarly, in a study by Zhang *et al.* (2006), an *H. akashiwo* isolate from Delaware Inland Bays was found to be more phenotypically plastic than other HAB species in that it had a higher range and tolerance to salinity and temperature, and a maximal growth at 30 °C. In contrast, the origin of the isolate used in this study (Puget Sound) is reported to have average winter temperatures of 7.2 and 12.8 °C in the summer and would rarely (if ever) reach temperatures greater than 25 °C. The optimal temperature growth range of an *H. akashiwo* isolate from this area was previously noted to be from 11-16 °C (Staubitz *et al.* 1997). With all studies considered, it is clear that *H. akashiwo* demonstrates a resilient ability to survive in many temperature and salinity conditions, indicating that this species is likely to be a competitive member of the phytoplankton species assemblage predicted for the future. Additionally, considering the effects of elevated CO₂ anticipated in the future, growth rates for *H. akashiwo* (from the DIB isolate) grown at 30 °C were faster than those reported in earlier work with or without CO₂ supplementation at a lower temperature of 25 °C, indicating that temperature may play a larger role in growth than CO₂ supplementation (Zhang *et al.* 2006; Fu *et al.* 2008). With this factor in mind, CO₂ enrichment at 20°C was explored in Chapter 4.

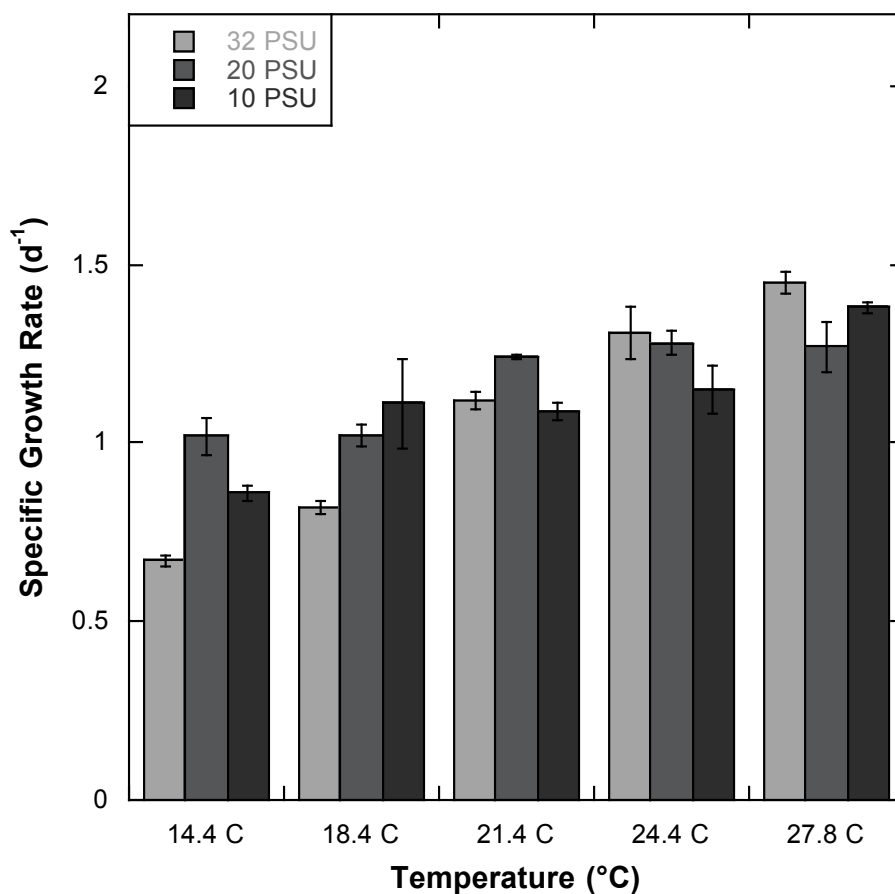


Figure 2.4.2 Specific growth rates for acclimated *H. akashiwo* cells grown in medium adjusted to a range of salinity treatments (32, 20 and 10 psu), and temperatures (14.4, 18.4, 21.4, 24.4 and 27.8 °C) at a fixed photon flux. Values were determined by *in vivo* fluorescence during the exponential growth phase, and indicate the average of quadruplicate samples (n = 4), with error bars indicating one standard deviation.

2.4.2 Dissolved inorganic carbon (DIC)

After diluting the seawater with ultra-pure Milli-Q® water to achieve the desired salinity concentrations of 20 and 10 psu, NaHCO_3 was added in a 2.07×10^{-3} M concentration to the 20 and 10 psu treatments. NaHCO_3 was added to adjust for changes in the DIC in the 20 and 10 psu as a result of the increased DIC from the background concentration of $1,994 \mu\text{M C}$ (32 psu) to $2,112 \mu\text{M C}$ (20 psu) and $2,046 \mu\text{M C}$ (10 P psu). The increased DIC for both the 20 and 10 psu treatment compared to the 32 psu treatment is due to the unaccounted DIC in the seawater being added to the extra NaHCO_3 that was injected after diluting with ultra-pure water. Figure 2.4.3 shows the starting DIC ($T=0$) for all three salinity conditions as well as the final DIC values on the last day of sampling for each treatment. For all salinity treatments, a downward trend is observed, where the availability of DIC in the media is inversely proportional to increasing temperature. Due to the low sample size for the DIC measurements ($n = 2$), it is unclear if DIC values are significantly different from each other.

2.4.3 SYTOX and cell membrane permeability

Cell permeability, measured with SYTOX-green, indicated that cells grown at 20 psu (5741 ± 724 RFU/cell) and 10 psu (5467 ± 828 RFU cell⁻¹) had higher SYTOX fluorescence than 32 psu -grown cells (763 ± 83 RFU cell⁻¹) at 14.4°C , which decreased to 899 ± 275 , 611 ± 138 and 414 ± 84 RFU cell⁻¹, respectively, at 24.4°C . This suggests that cells become more permeable adjusting to osmotic pressure at low temperature.

During exponential phase of growth, results from SYTOX-Green demonstrate that the cell membranes of *H. akashiwo* are more permeable at $10 > 20 > 32$ psu, supporting the concept that cells are changing the composition of their membranes as a method to

acclimate to lower salinity conditions. These findings have not been demonstrated previously with this raphidophyte. Phytoplankton express very different biochemical responses to growth limitation. There were no obvious changes in cell morphology, but there was likely a process of intracellular protein degradation brought about by nitrogen deprivation, as photochemical efficiency declined. Such internal degradation leads to the dismantling of the photosynthetic apparatus and the loss of photosynthetic pigment fluorescence. The loss of pigment fluorescence (“chlorosis”, Geider *et al.* 1993) correlates with decreased enzyme activity and increased membrane permeability (Franklin *et al.* 2012).

There was a change in relative SYTOX fluorescence per cell in relation to both salinity and temperature. Figure 2.4.4 shows the relative SYTOX fluorescence for cells on the second day of exponential growth. At low temperatures (14.4 and 18.4 °C), cellular permeability was highest at 10 psu and decreased with increasing salinity. Higher temperatures (21.4, 24.4, 27.8 °C) resulted in the cellular permeability generally being the highest at the 20 psu. For all temperatures, except 24.4 °C, the 32 psu had the lowest relative SYTOX fluorescence per cell compared to the 20 and 10 psu treatment. By the last day of exponential growth (Figure 2.4.5) the relative SYTOX fluorescence per cell had decreased by 1-2 orders of magnitude for all treatments. A downward trend is observed for all salinity treatments as temperature increased, with the lowest relative SYTOX fluorescence per cell occurring at 27.8 °C. By the fourth day of stationary growth (Figure 2.4.6), there was little change in the relative SYTOX fluorescence per cell when compared to the last day of exponential growth for each treatment.

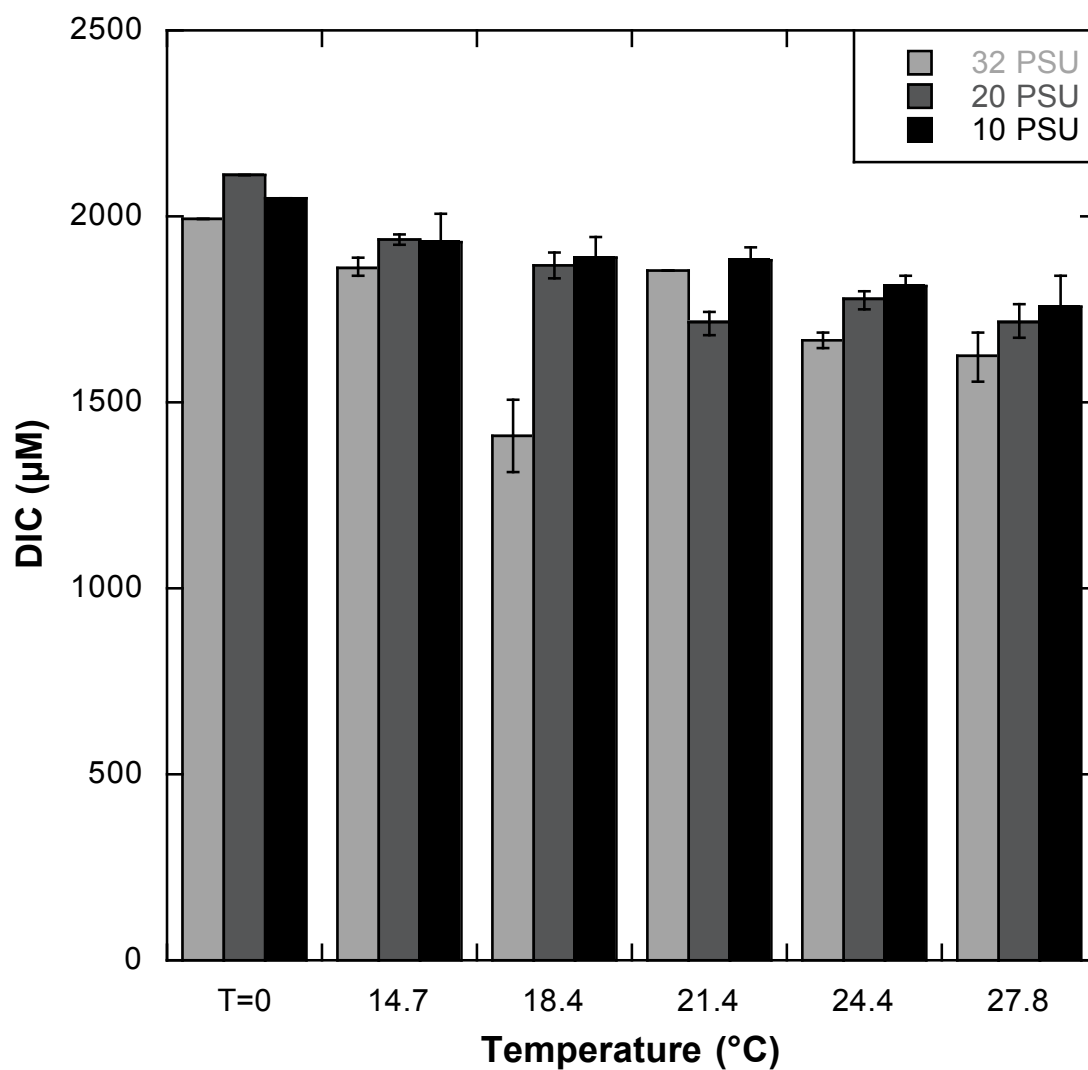


Figure 2.4.3 Total DIC remaining in the media on the last day of sampling for all temperatures and salinities tested. T=0 is the initial DIC concentration after NaHCO_3 was added. Error bars indicate the range of duplicate (n=2) samples, except for T=0 and 21.4 °C, where n=1.

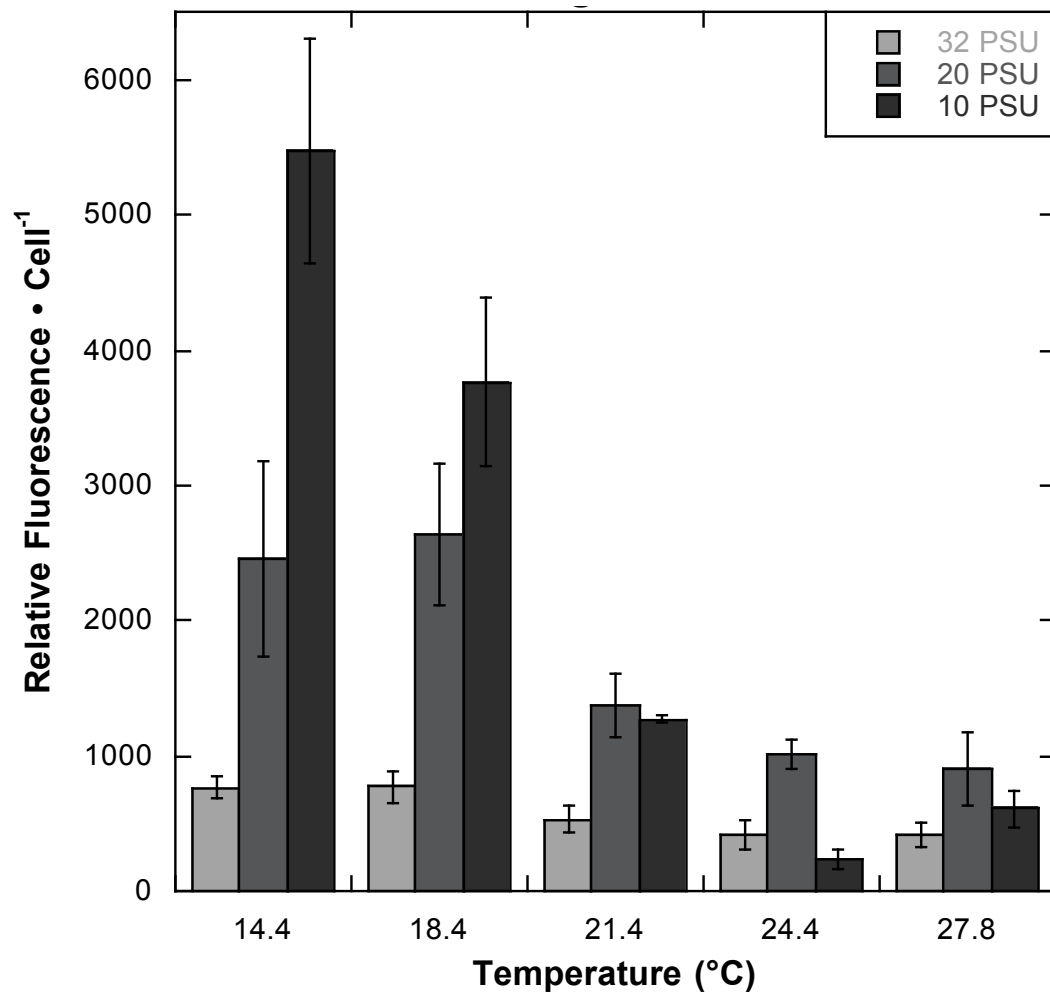


Figure 2.4.4 Cell permeability after two days of exponential growth. Cell permeability was determined using the nucleic acid stain SYTOX, with cells during the second day of exponential growth. Bars represent the average of quadruplicate (n=4) samples, with error bars indicating one standard deviation.

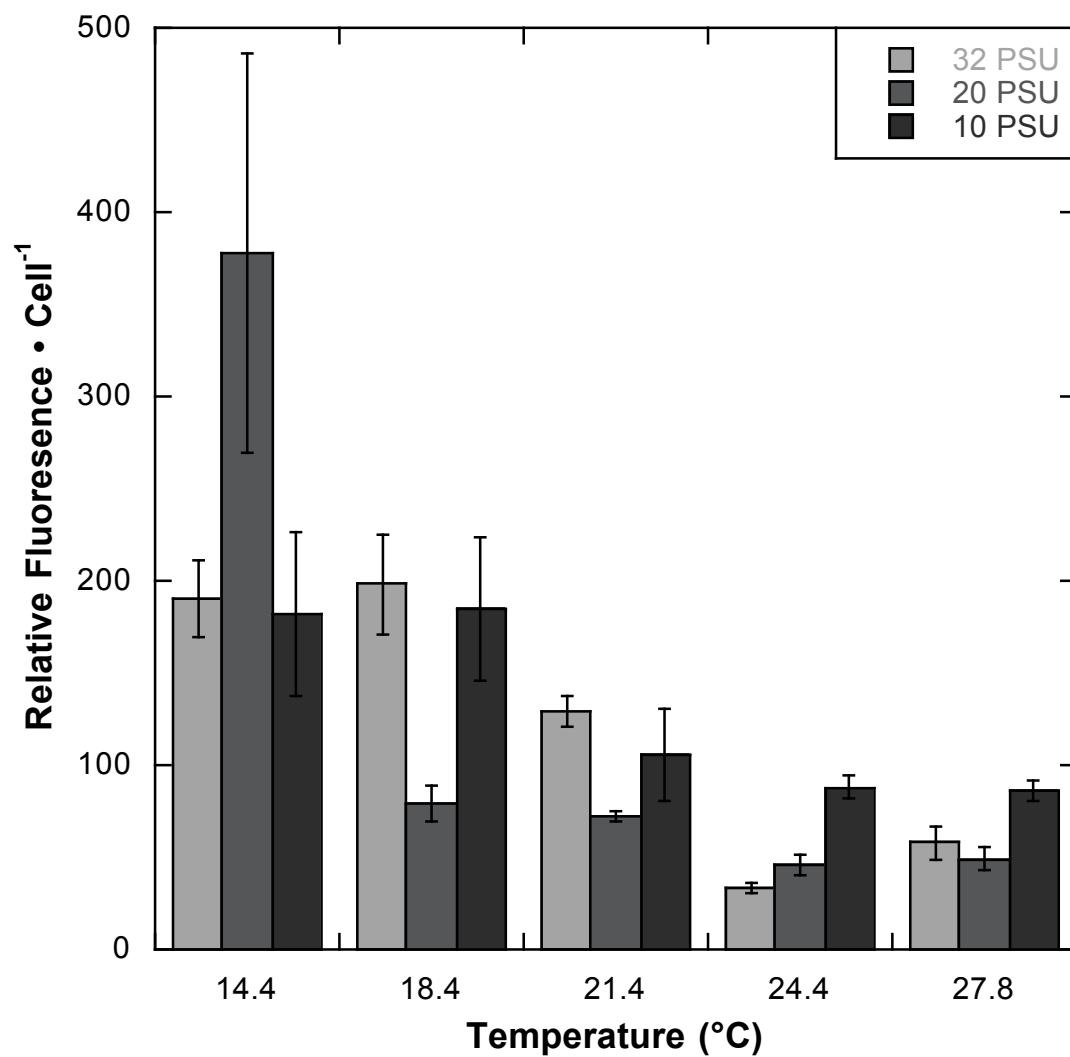


Figure 2.4.5 Cell Permeability on the last day of exponential growth. Cell membrane permeability was determined using the nucleic acid stain SYTOX with cells from the last day of exponential growth. Bars represent the average of quadruplicate (n=4) samples, with error bars indicating one standard deviation.

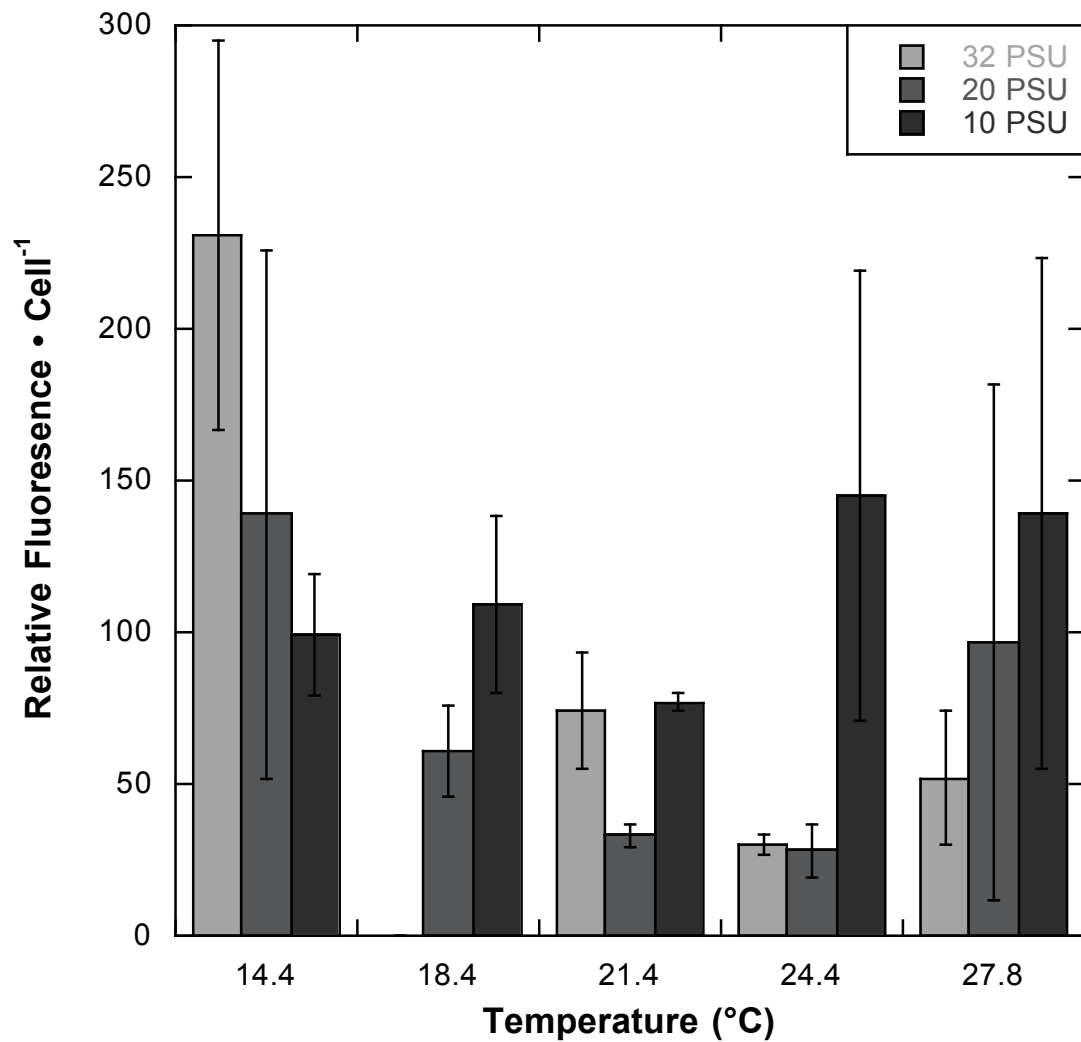


Figure 2.4.6 Cell permeability after four days of stationary growth. Cell permeability was determined using the nucleic acid stain SYTOX with cells from the fourth day of stationary growth. The treatment at 32 psu and 18.4 °C was not included due to contamination, which resulted in a high relative fluorescence per cell. Bars represent the average of quadruplicate (n=4) samples, with error bars indicating one standard deviation.

It is important to note that the dates chosen for the last day of exponential growth is specific to the stage of growth for each culture and not the duration all treatments had been in culture. Likewise, the last sample collected for each temperature depended on reaching the fourth day of stationary growth. Only Figure 2.4.4 represents cultures at different stages of physiological growth as the collected data are from the second day of the experiment and do not take into account the rate of growth for each culture.

2.5 Conclusion

The euryhaline nature of the raphidophyte, *Heterosigma akashiwo*, is a documented adaptive characteristic but the mechanism that allows for rapid adaptation to salinity, and the potential increase in ichthyotoxicity to brackish waters is poorly understood. Considering the increased temperatures predicted in the future and corresponding changes in oceanic salinity, it was alarming to note that maximal growth rates were attained at 20 psu, which increased with temperature from 14.7 °C to 24.4 °C ($\mu = 0.96 \pm 0.08$ to 1.48 ± 0.05 d⁻¹), followed by 10 psu (0.70 ± 0.04 to 1.10 ± 0.21 d⁻¹) and 32 psu ($\mu = 0.67 \pm 0.02$ to 1.16 ± 0.12 d⁻¹).

Cell permeability, as measured with SYTOX-green that is commonly used to measure cell viability, indicated that cells grown at 20 psu and 10 psu had higher SYTOX fluorescence than 32 psu, possibly accounting for the cell's process of osmotic regulation at low salinities. Additionally, cell permeability decreased with increasing temperatures, indicating that the cell's enzymes are more functional at warmer temperatures and are better at utilizing and metabolizing nutrients to support the structure of their cell membranes. This finding can be supported from the DIC results that showed less DIC (indicating more intracellular particulate carbon concentrations) in cooler temperatures

compared to warmer temperatures. Cells are better able to acquire key nutrients as temperatures increase, due to the efficiency of their enzyme kinetics.

Using SYTOX as a metric for assessing cell membrane permeability is a novel use of this fluorescent probe. The most interesting result indicated that *H. akashiwo* cells are more permeable during their exponential phase of growth compared to their stationary growth. This finding was surprising because it contradicts the prediction that cells are more fragile during the stationary phase of their growth cycle, when nutrients are depleted. The result can be explained by understanding the growth cycle of *H. akashiwo* and the cell's unique ability at producing cysts when the alga enters stationary growth. When *H. akashiwo* can sense a time of nutrient limitation, in order to preserve the species, cells begin producing cysts that are better able at surviving low nutrient environments because of their decreased cell size, decreased nutrient demands, and increased cell membrane rigidity. By forming cysts, this strengthens their cell membranes, which may be why lowered SYTOX fluorescence was observed during stationary growth.

Given the potential for harmful algal bloom outbreaks and favourable oceanic conditions anticipated for the future, *H. akashiwo* is a species likely to dominate and pose a threat in the marine ecosystem of the future ocean.

2.6 References

- Berges, J.A., Franklin, D.J., and Harrison, P.J. 2001. Evolution of an artificial seawater medium: improvements in enriched seawater, artificial water over the last two decades. *J. Phycol.* **37**: 1138-1145.
- Davies, J. and Grossman, A. 1998. Nutrient stress. In *The Molecular Biology of Chloroplasts and Mitochondria in Chlamydomonas*, [eds.] Rochaix JD, Goldschmidt-Clermont M and Merchant S. Kluwer Academic. Publishers, Dordrecht, Netherlands.
- Franklin, D.J., Airs, R.L., Fernandes, M., Bell, T.G., Bongaerts, R. J., Berges, J.A. and Malin, G. 2012. Identification of senescence and death in *Emiliania huxleyi* and *Thalassiosira pseudonana*: cell staining, chlorophyll alterations, and dimethylsulfoniopropionate (DMSP) metabolism. *Limnol. Oceanogr.* **57**: 205-317.
- Friederich, G. E., Walz, P.M., Burczynski, M.G. and Chavez. F.P. 2002. Inorganic carbon in the central California upwelling system during the 1997-1999 El Niño-La Niña event. *Progr. Oceanogr.* **54**: 185-203.
- Geider, R.J., J. Laroche, R.M. Greene, and M. Olaizola.. 1993. Response of the photosynthetic apparatus of *Phaeodactylum tricornutum* (Bacillariophyceae) to nitrate, phosphate, or iron starvation. *J. Phycol.* **29**: 755–766.
- Guillard, R.R.L. 1973. Division rates, p. 289-311. In Stein, J.R. [eds.], *Handbook of Phycological Methods—Culture Methods and Growth Measurements*. Cambridge University Press.
- Haque, S. M. and Onoue, Y. 2002. Effects of salinity on growth and toxin production of a noxious phytoflagellate, *Heterosigma akashiwo* (Raphidophyceae). *Bot. Mar.* **45**: 356–363.
- Han, M. S., Kim, Y. P. and Cattolico, R. A. 2002. *Heterosigma akashiwo* (Raphidophyceae) resting cell formation in batch culture: strain identity versus physiological response. *J. Phycol.* **38**: 304–317.
- Harrison, P.J., Waters, R.E., and Taylor, F.J.R. 1980. A broad spectrum artificial seawater medium for coastal and open ocean phytoplankton. *J. Phycol.* **16**: 28-35.
- Honjo, T. 1993. Overview on bloom dynamics and physiological ecology of *Heterosigma akashiwo*. p.33-41. In Smayda, T. J. and Shimizu, Y. Y. [eds.], *Toxic Phytoplankton Blooms in the Sea*. Elsevier, Amsterdam.
- Howard M.D.A., Cochlan. W.P., Ladizinsky, N., Kudela, R.M. 2007. Nitrogenous preference of toxigenic *Pseudo-nitzschia australis* (Bacillariophyceae) from field and laboratory experiments. *Harmful Algae* **6**: 206-217.

- Hüner NPA, Oquist G and Sarhan F. 1998. Energy balance and acclimation to light and cold. *Trends Plant Sci.* **3**: 224–230.
- Kempton, J., Kepler, C. J., Levitus, A. 2008. A novel *Heterosigma akashiwo* bloom extending from a South Carolina bay to offshore waters. *Harmful Algae* **7**: 235–240.
- Knepel, K. and Bogren, K. 2001. Determination of orthophosphorous by flow injection analysis in seawaters. *In* Saline Methods of Analysis. Lachat Instruments, Milwaukee, WI. 14p.
- Maxwell, D.P., Falk, S., Trick C.G. and Hüner, N.P.A. 1994. Growth at low temperature mimics high-light acclimation in *Chlorella vulgaris*. *Plant Physiol.* **105**: 535–543.
- Martinez, R., Orive, E., Laza-Martinez, A. and Seoane, S. 2010. Growth response of six strains of *Heterosigma akashiwo* to varying temperature, salinity and irradiance conditions. *J. Plankton Res.* **4**: 529–538.
- Miyachi, S., Iwasaki, I. and Shiraiwa Y. 2003. Historical perspective on microalgal and cyanobacterial acclimation to low- and extremely high-CO₂ conditions. *Photosynth. Res.* **77**: 139–153.
- Montagnes, D. 2006. Guide to Harmful Phytoplankton. University of Liverpool. UK. http://www.liv.ac.uk/hab/Data%20sheets/h_akas.htm. Accessed 16 Jan 2012.
- Neale, P.J. and Melis, A. 1989. Salinity-stress enhances photoinhibition of photosystem II in *Chlamydomonas reinhardtii*. *J. Plant Physiol.* **134**: 619–622.
- Orive, E., Franco, J., and Madariaga, I. 2004. Bacterioplankton and phytoplankton communities, p. 367–393. *In* Borja, A. and Collins, M. [eds.] Oceanography and Marine Environment of the Basque Country. Elsevier, Amsterdam.
- Rensel, J. E., Haigh, N. and Tynan, T. J. 2010. Fraser river sockeye salmon marine survival decline and harmful blooms of *Heterosigma akashiwo*. *Harmful Algae.* **10**: 98–115.
- Smayda, T. J. 1998. Ecophysiology and bloom dynamics of *Heterosigma akashiwo* (Raphidophyceae), p. 113–131. *In* Anderson, D. M., Cembella, A. and Haellegraeff, G. M. [eds.], Physiological Ecology of Harmful Algal Blooms. NATO ASI Series 41. Springer-Verlag, Berlin.
- Smith, P., Bogren, K. 2001. Determination of nitrate and/or nitrite in brackish or seawater by flow injection analysis colorimeter: QuickChem Method, *In* Saline Methods of Analysis. Lachat Instruments, Milwaukee, WI. 31p.
- Staubitz, W.W., Bortleson, G.C., Semans, S.D., Tesoriero, A.J. and Black, R.W. 1997. Water-Quality Assessment of the Puget Sound Basin, Washington, Environmental Setting

and Its Implications for Water Quality and Aquatic Biota. US Geological Survey Water Res. Invest. Report. 97-4013.

Veldhuis, M.J.W., Cucci, T. L., and Sieracki, M. E. 1997. Cellular DNA content of marine phytoplankton using two new fluorochromes: Taxonomic and ecological implications. *J. Phycol.* **33**: 527–541.

Veldhuis, M.J.W., Kraay, G.W., Timmermans, K.R. 2001. Cell death in phytoplankton: correlation between changes in membrane permeability, photosynthetic activity, pigmentation and growth. *Euro. J. Phycol.* **36**: 167-177.

Zhang, Y.H., Fu, F.X., Whereat, E., Coyne, K.J. and Hutchins, D.A. 2006. Bottom-up controls on a mixed-species HAB assemblage: A comparison of sympatric *Chattonella subsalsa* and *Heterosigma akashiwo* (Raphidophyceae) isolates from the Delaware Inland Bays, USA. *Harmful Algae.* **5**: 310-320.

CHAPTER 3

3. Growth kinetics, light utilization and lipid production of marine phytoplankton under different pH exposures

3.1 Overview

This chapter establishes the relationship between growth (cell growth rate and yield), photosynthetic competences and neutral lipid composition of *Heterosigma akashiwo* strain NWMFS 503 under buffered pH environments that represent the future coastal ocean: ambient average oceanic pH 8.1, pH 7.8 (for the year 2050) and pH 7.4 (for the year 2100).

The findings for *H. akashiwo* strain NWMFS 503 are placed in comparison with the responses of three isolates (2 genera) of marine phytoplankton that are common inhabitants of the present coastal oceans: the diatom *Thalassiosira weissflogii* CCMP strain 105, a phycocyanin-rich cyanobacterium, *Synechococcus sp.* strain CCMP 835 and a phycoerythrin-rich cyanobacterium, *Synechococcus sp.* strain CCMP 835.

3.2 Introduction

Fundamental to the understanding of phytoplankton ecophysiology is defining the impacts of biotic and abiotic stresses. The future ocean will have elevated nutrient flux or concentrations, particularly the macro-nutrient, nitrogen that is a key factor in establishing a balance between light absorption and carbon assimilation. These factors are increasingly important because of the frequent reports correlating HAB events to ocean acidification and eutrophication (Hallegraeff 1993, 2010; Burkholder 1998; Anderson *et al.* 2002; Riebesell 2004; Moore *et al.* 2009).

Photoautotrophs have developed a number of mechanisms to acclimate to imbalances between pH, light absorption and carbon assimilation (Sabina and Latala

2012). Such mechanisms involve the elevation or depression of individual pigments in the light harvesting complexes. Under stress, phytoplankton can either decrease their light harvesting pigments concentration, increase their photoprotective pigments such as xanthophylls and carotenoids, or increase their shading photosynthetic components by accumulating UV-absorbing pigments (Marshall and Newman 2002; Harris *et al.* 2005; Falkowski and Raven 2007). However, when exposed to longer periods of excessive pH and nutrient stressors, more sufficient physiological pathways of light energy dissipation are utilized, such as photorespiration (Portis and Parry 2007) or use of NAD(P)H produced from the photosynthetic electron transport chain (ETC) by the enzyme nitrate reductase (NR) (Lomas and Gilbert 1999). Although the use of the reductant NAD(P)H, by NR to assimilate nitrate has been proposed, it is reliant on the availability of nitrogen in the environment and an increased transcription of NR genes under conditions of lower pH has currently only been observed in diatoms (Parker and Armbrust 2005).

Diatoms are responsible for roughly 40% of the total primary production in the oceans (Badger *et al.* 1998). It is understood that growth and photosynthesis of diatoms can be limited by CO₂ availability (Riebesell *et al.* 1993), and primary production may be enhanced with the increased concentration of atmospheric CO₂ (Hein and Sand-Jensen, 1997; Riebesell and Tortell 2011). However, it has been suggested that the growth rates of diatoms will not change but rather the carbon balance within the cell will alter intracellular biochemistry, leading to the accumulation of carbon-rich lipids and fats (Tortell *et al.* 2000). Most diatoms operate carbon concentrating mechanisms (CCM) that actively transport CO₂ or HCO₃⁻ across the cell membrane, to supply ribulose-1,5-bisphosphate carboxylase oxygenase (RuBisCo) with carbon. The CCMs of different phytoplankton species and their corresponding growth conditions have demonstrated

different preferences for CO₂ or HCO₃⁻ (Nimer *et al.* 1997; Burkhardt *et al.* 2001). For example, three different species of *Thalassiosira* all have different CCM: *T. punctigera* concentrates free CO₂ (Elzenga *et al.* 2000), *T. pseudonana* concentrates both CO₂ and HCO₃⁻ (Trimborn *et al.* 2009), while *T. weissflogii* operates a C₄-like pathway to concentrate intracellular carbon, whereby carbon is stored as an organic C₄ compound (malic or aspartic acid) coupled by the catalysis of phosphoenolpyruvate carboxylase before RuBisCo fixation (Reinfelder *et al.* 2000). In general, operating a CCM is energetically costly and the energy saved from down-regulating a CCM under high levels of CO₂ might stimulate growth when photosynthesis is light limited (Wu *et al.* 2010). One factor to consider is that down-regulating CCMs might result in light stress because the energy that was previously used to fuel active transport of CO₂ or HCO₃⁻ no longer serves a purpose and may lead to photoinhibition (Wu *et al.* 2010). However, it is possible that this extra light energy and the down-regulation of CCMs could result in the up-regulation of an alternate physiological process such as the accumulation of lipids.

Cyanobacteria, particularly *Synechococcus* sp., are dominant contributors to global carbon and nitrogen cycling, especially in oligotrophic gyres (Capone *et al.* 2005). It has been reported that doubling *p*CO₂ and increasing growth temperatures of *Synechococcus* sp. will significantly increase growth rates, photosynthetic capacity and cellular pigment levels (Fu *et al.* 2007). This can be attributed to the cyanobacterium down-regulating the function of their CCM under elevated CO₂ (Badger and Andrews 1982). However, there is a gap in our current knowledge of cyanobacterial responses to high *p*CO₂ in nutrient-poor waters, given the potential increase in oligotrophic gyres from future ocean warming and resulting water mass stability stratification (Rost *et al.* 2008, Hutchins *et al.* 2009). Lomas *et al.* (2012) concluded that changes in pH/*p*CO₂ within

Synechococcus are indirect and primarily controlled by the responses to other variables such as nutrient availability. Although *Synechococcus* tends to be a poorer quality food source in the diets of eukaryotic phytoplankton, their overall abundance and likelihood to grow in the future ocean warrants further investigation (Apple *et al.* 2011).

With $p\text{CO}_2$ likely to affect phytoplankton community composition, problems could arise in HAB outbreaks of *H. akashiwo*. Unlike *Thalassiosira weissflogii* and *Synechococcus* sp., *H. akashiwo* has not been found to have an active CCM. Yet, laboratory experiments have demonstrated that increasing $p\text{CO}_2$ coincided with increases in the cellular growth rates, carbon quotas and nitrogen quotas of this toxic raphidophyte (Fu *et al.* 2008). These changes were particularly accelerated under warmer temperatures predicted in our future ocean. Should growth rates as well as carbon and nitrogen quotas increase in *H. akashiwo*, this could lead to problems associated with phytoplankton community assemblages dominated by this HAB, with consequent repercussions in the marine food-web dynamic. Speciation shifts are likely to be highly dependent on nutrient availability.

This chapter will establish the relative changes in the growth and photosynthetic efficiencies in the three common phytoplankton species; *T. weissflogii*, *Synechococcus* sp. and *H. akashiwo*, which result from the compounded stressors of ocean acidification and nutrient variability in the marine environment. Furthermore, the end of the chapter will describe some physiological differences in nutrient utilization that result from ocean acidification and nutrient variability, from the assessment of phytoplankton neutral lipid accumulation. Results provide insight on the competitive advantage that *H. akashiwo* could have in the future ocean, along with the total lipid value that this HAB might have within the oceanic food web.

3.3 Materials and methods

3.3.1 Experimental design and rationale

Experiments were designed to cover three variables associated with the future ocean: 1) changes in pH; 2) changes in the level of available nitrate for growth, and 3) changes in the level of bioavailable iron for cell growth. Culture medium was adjusted to maintain a pH of 8.1, 7.8 and 7.4, which is representative of the current average ocean pH, the pH of the Eastern Boundary Upwelling System (EBUS), and the predicted future ocean pH of the year 2100, respectively (Feely *et al.* 2008). Variable nutrient conditions under each of the three-pH regimes consisted of experimental cultures at four different iron (Fe) concentrations, along with experimental cultures at two different nitrate (NO₃⁻) concentrations to mimic conditions expected in the natural EBUS of the California Current System (CCS).

3.3.2 Phytoplankton species selection

Four phytoplankton isolates were chosen among species that would be commonly found in upwelled water from the EBUS. *Thalassiosira weissflogii* a diatom strain from Culture Collection for Maine Phytoplankton (CCMP strain 1051) which was originally isolated from the North Pacific ocean on May 13, 1985. Also from the CCMP are two ecotypes of the cyanobacterium *Synechococcus* *sp.* Strain CCMP 833 is a phycoerythrin - rich cyanobacterium. Whereas the primary accessory pigment in strain CCMP 835 is phycocyanin. These were isolated from the North Atlantic Ocean in 1982 and 1985, respectively. The marine raphidophyte, *Heterosigma akashiwo* NWFSC 503, isolated from the Salish Sea in 1990, was obtained from the Northwest Fisheries Science Center (NWFSC). All isolates were maintained as unialgal, non-axenic strains.

3.3.3 Culturing conditions

Experimental culture libraries were maintained in 250 mL Erlenmeyer flasks containing 50 mL of autoclaved sterilized (heated to 121°C and 16 psi for 20 min) modified enriched seawater artificial water (ESAW) medium, modified with f/2 nutrient enrichments (ESAW + f/2) (Harrison *et al.* 1980; Berges *et al.* 2001). Cells were transferred using a 10% inoculum and maintained at a constant temperature (18°C) and continuous light irradiance of 100 $\mu\text{mol photons m}^{-2} \text{s}^{-1}$ for *T. weissflogii* and *H. akashiwo*, and 60 $\mu\text{mol photons m}^{-2} \text{s}^{-1}$ for *Synechococcus* sp. Irradiance was supplied by cool white fluorescent light and measured using a Quantum Scalar Laboratory 2100 irradiance sensor (Biospherical Instruments, San Diego, CA). To examine the dynamic variables of pH and nutrient uptake mechanisms controlling the chemistry of an acidic ocean, all laboratory experimentation (growth, photosynthetic performance and neutral lipid production) and analyses were carried out with isolates grown in batch cultures.

3.3.4 Seawater acidification and maintenance of culture pH

3.3.4a Adjustment and maintenance of culture pH

To adjust the pH of each batch culture for experimentation, 10 mM of HEPES (4-(2-hydroxyethyl)-1-piperazineethanesulfonic acid) buffer was added to autoclaved ESAW + f/2 medium in each flask to maintain culture pH during experimentation. The pH of the medium in each experimental flask was then individually titrated with 5 μL additions of either a 15% (v/v) HCl and Milli-Q® water, or a 5 M solution of NaOH until the desired pH of 7.4, 7.8 or 8.1 was reached. The solution pH was monitored using a Thermo Scientific pH meter supplied with a glass pH electrode and Stainless Steel ATC probe (VWR Catalogue Number 14004-340). After, the medium was allowed to acclimate for 1

hour (up to a maximum of 24 hours) at the desired experimental temperature, prior to cells being added.

To reduce the level of limiting nutrient transfer with inoculation, all experiments were started with cells in their stationary phase of growth. The following inoculation levels were used: *T. weissflogii* CCMP1051 was inoculated with a 20% (v/v) starting inoculum; *H. akashiwo* NWFSC 503 was inoculated with a 10% (v/v) starting inoculum; and *Synechococcus* sp. were inoculated with a 2% (v/v) starting inoculum.

3.3.4b pH measurements

For initial experiments, pH readings were taken daily to ensure experimental pH levels in the culture medium were not drifting greater than ± 0.05 pH units. Once stable pH readings were established (Appendix I), culture pH readings were taken at three time points during experimentation: 24 hours after inoculation, the exponential growth phase and the stationary growth phase. For sampling, pH was measured by removing 20 mL of the culture and pipetting it into a 20 mL glass scintillation vial. The medium was then immediately measured with the above-mentioned Thermo Scientific pH meter.

3.3.5 Iron replete and deplete experiments

To evaluate the effect of nutrient variation on the growth and neutral lipid composition of the cultures in this study, iron and nitrate additions were manipulated. All other nutrient additions to ESAW medium followed the f/2 recipe outlined in Algal Culturing Techniques (Guillard and Ryther 1962; Guillard 1975, summarized in Anderson 2005). Nutrient stock solutions were prepared with Milli-Q[®] water and filter sterilized (0.2 μ m Millipore filters). All lab-ware used for culturing and experimentation was autoclaved (heated to 121°C and 16 psi for 20 min) prior to use.

3.3.5a Iron enrichment

To explore the influence of iron on the growth and neutral lipid production in phytoplankton under the three established levels of pH, cultures were initially adjusted to the following final iron concentrations: 0.01, 0.1, 1.0 and 11.0 μM using $\text{FeCl}_3 \cdot 6\text{H}_2\text{O}$. Once a divergent iron trend was established (Appendix II), experimental iron concentrations were conducted at a 0.01 and 11.0 μM final medium concentration of $\text{FeCl}_3 \cdot 6\text{H}_2\text{O}$.

3.3.5b Nitrate enrichments

To explore the influence of nitrate on the dynamics of growth and neutral lipid production at the desired pH variations, experiments were initially conducted at the standard f/2 level of 882 μM of NaNO_3 . Then employing a NO_3^- concentration more representative of EBUS, a final NaNO_3 concentration of 80 μM was chosen to assess whether a more limited NO_3^- concentration would change the physiological principles that were analyzed in the study.

3.3.6 Methods of analyses: growth measurements

Cell counts were conducted throughout all experimentation to quantify the effects of growth by the combinational pressures of either high or low nutrients (Fe and NO_3^-) and high or low pH. *H. akashiwo* NWFSC 503 samples were counted using the PhytoCyt™ Flow Cytometer (Turner Designs, Inc.), while *T. weissflogii* samples were counted either under the microscope using a haemocytometer or optical density using spectrophotometry, and *Synechococcus* sp. samples were counted using optical density through spectrophotometry.

For all count metrics, maximal yields ($\text{yield}_{\text{max}}$ in units cells mL^{-1}) were averaged from three consecutive days, on four separate cultures. Maximal growth rates (μ_{max} in

units day⁻¹) were determined from the slope of a linear regression (the coefficient of correlation [R^2] ≥ 0.95) of the natural logarithm of cell density versus time during exponential growth (Guillard, 1973). For all species, the length of the lag phase was calculated based on the number of days preceding exponential growth.

3.3.6a Flow Cytometry counts

Daily samples of *H. akashiwo* NWFSC 503 (0.5 mL in 1.5mL Eppendorf® Safe-Lock microcentrifuge tubes) were removed from culture under a Laminar flow hood and counted using the PhytoCyt™ Flow Cytometer (Turner Designs, Inc.). The flow cytometer was setup to measure endogenous fluorophores common to *H. akashiwo* NWFSC 503 (primarily chlorophyll-*a*; cytometer detector FL-3) against the forward scatter (FSC) of particles. Cells from a 50-μL subsample were counted and converted to cells mL⁻¹. Multiple sub-sampling counteracted instrument variation.

3.3.6b Haemocytometer

Direct cell counts were performed using a haemocytometer to calculate cell density (in units cells mL⁻¹). For each treatment, a culture sample was enumerated on a haemocytometer such that a minimum of six fields were counted until the percentage standardized variation (% SV) for the number of cells per field was less than 10%, according to the following equation:

$$\%SV = \frac{\left(\frac{s}{\sqrt{n}}\right)}{X} \times 100$$

where *s* is the standard deviation, *x* is the mean of the number of cells per field, and *n* is the number of fields counted.

3.3.6c Spectrophotometer

Optical density, calculated by measuring absorbance at 720 nm with a DU 640 spectrophotometer (Beckman Coulter), calibrated to flow cytometry or haemocytometer measurements, was used to measure phytoplankton density (Held, 2011). To avoid performing cell counts on cylindrical isolates, such as *T. weissflogii* CCMP 1051 and small isolates, such as *Synechococcus* sp., optical density was used as a proxy for cell densities.

3.3.7 Photosynthetic performance

The photosynthetic performance of cultures grown under the combinational pressures of pH and nutrient regimes was evaluated using light specific oxygen evolution (P vs. E) and Pulse Amplitude Modulatory (PAM) fluorometry methodology. Photosynthetic performance was measured for each sample on selected days: time zero (the day of inoculation), the exponential growth phase and the stationary growth phase. Over this timeframe, cells were kept at their optimal growth conditions and reassessed for any variance in their efficiency of capturing light for metabolism. On the selected days of analyses, the samples of each treatment were concentrated to achieve stronger instrument readings.

3.3.7a Sample concentration

Prior to assessing photosynthetic performance, cultures from a 15% (v/v) stationary inoculum of *T. weissflogii* CMPP 1051 were concentrated 20 fold. The 20 fold concentration was performed by pipetting 32 mL of each treatment in Oak Ridge Nalgene polysulfone centrifuge tubes and concentrating the sample by centrifuging the volumes at a relative centrifugal force (RCF) of 3,000 g for 5 minutes using the Avanti J-25I and J-E Beckman Coulter centrifuge. Cultures from a 4% (v/v) starting inoculum of *Synechococcus* sp. and a 20% (v/v) starting inoculum of *H. akashiwo* NWFSC 503 were

pipetted in Oak Ridge Nalgene polysulfone centrifuge tubes. Samples were spun for 15 minutes at a RCF of 1500g in the Avanti J-25I and J-E Beckman Coulter centrifuge to achieve a 50-fold concentration. The resulting supernatants were decanted to obtain a pellet of cells. Each pellet was resuspended in 1.6 mL of the supernatant and pipetted into a 2 mL Eppendorf® Safe-Lock microcentrifuge tubes. Samples were dark incubated for 30 minutes prior to testing.

3.3.7b Pulse Amplitude Modulatory Fluorometry (PAM)

After cell concentration, a PAM-2500 High-performance chlorophyll fluorometer with PamWin-3 software (Heinz Walz GmbH, 2008, Germany) was used to evaluate *in vivo* cellular fluorescence capacity through variable fluorescence (F_v/F_m), effectively measuring the quantum efficiency of photosystem II, an indicator of stress. Exposure times of 30-second pulses of actinic light (ranging from 0 to 825 $\mu\text{mol}/\text{m}^2/\text{sec}$) were evaluated. After PAM fluorometry was employed, the samples were placed back into their respective microcentrifuge tubes and dark incubated for another 30 minutes prior to oxygen-evolution analyses.

3.3.7c Oxygen evolution

With the same samples used for PAM fluorometry, photosynthetic performance was examined by measuring oxygen production rates ($\mu\text{mol O}_2 \text{ m}^{-1}$) under increasing light exposure (P vs. E). Cells were evaluated for their ability to harvest light energy and effectively process the energy needed for carbon acquisition, by determining oxygen evolution rates using a Clark-type O_2 electrode (Oxy-lab 2.0, 2004, Hansatech Instrument Ltd., England with Oxylab32 software) (Appendix III).

The oxygen electrode was calibrated using ambient air to set the maximum oxygen evolution capacity and nitrogen dioxide gas for the minimum oxygen evolution capacity. Calibration and measurement guidelines were closely followed in the LD 2/3 Hansatech Instruments Oxygen Electrode Chamber operating manual to measure oxygen evolution rates. A template was created to assess the amount of oxygen released from the cells at increasing light irradiances over a period of 26 minutes at a specific light flux ranging from 0 - 800 $\mu\text{mol quanta m}^{-2} \text{s}^{-1}$. Additionally, a 1 M solution of sodium bicarbonate was prepared by dissolving 0.084 grams of sodium bicarbonate in 1 mL of distilled water.

After calibration, 1.5 mL of the concentrated sample was added to the sample chamber along with 7.5 μL of the 1 M sodium bicarbonate solution to ensure photosynthesis was not limited by the lack of carbon dioxide in the closed chamber. At 13 intervals of 2 minutes over a 26 minute time period, the following light irradiances were applied to each sample: 0, 20, 40, 60, 80, 100, 150, 200, 250, 300, 400, 500 and 800 ($\mu\text{mol quanta m}^{-2} \text{s}^{-1}$). Oxygen evolution rates were recorded for each 2-minute time interval.

3.3.7d Chlorophyll-a isolation

After all photosynthetic analyses were performed, chlorophyll-*a* was extracted to normalize photosynthetic rates to chlorophyll-*a* cell^{-1} . Chlorophyll was extracted according to the method described in Morgan-Kiss *et al.* (2002). Cells were pelleted by centrifugation (Eppendorf minifuge) at 12,000 rotations per minute (RPM) for 5 min. After centrifugation, the supernatant was removed and samples were placed on ice. The pellet was re-suspended in 1.5 mL of 90% acetone and fractioned with 0.1mm silica beads for 30 seconds using a bead beater. Samples were placed on ice between

fractionation. After the beads and debris settled, the supernatant was transferred to a microcentrifuge tube and centrifuged for 5 minutes at 12,000 RPM. The absorption of 1 mL of the supernatant was measured in a 1 mL (1 cm length) quartz cuvette in the DU 640 spectrophotometer (Beckman Coulter) at 664 nm (A_{664}) and 647 nm (A_{647}) and total chlorophyll content was calculated according to the formula outlined in Jeffrey and Humphrey (1975):

$$\text{Total Chlorophyll } (\mu\text{g mL}^{-1}) = [\text{Chlorophyll-}a: 11.93 A_{664} - 1.93 A_{647}] + [\text{Chlorophyll-}b: 20.36 A_{647} - 5.50 A_{664}]$$

3.3.8 Nile red lipid analyses

Total intracellular neutral lipid content was estimated using a Nile Red fluorescence assay (Bjornsson 2009) and a fluorescence spectrophotometer (Cary Eclipse, Varian) fixed with a multi-well plate attachment set to read chemi/bio-luminescence from 540 nm to 700 nm.

The fluorescent probe Nile red (9-(diethylamino)-5H benzo phenoxa-zin-5-one), stains intracellular lipid droplets and allows for a semi-quantitative estimate of total neutral lipid content to be made based on its fluorescence emission intensity in the spectrophotometer (Bjornsson 2009; Held *et al.* 2011). The degree to which the sample fluoresced served as a proxy for intracellular lipid content. Samples were prepared in a 2 mL deep 96-multiwell plate (MWP) (BD, Bioscience) and evaluated on the plate reader in 300 μL analytical triplicates using a 300 μL deep 96-MWP. The MWPs were arranged according to Appendix IV.

3.4 Results

Ocean acidification leads to a decrease in the pH of seawater, which in some cases affected the chemistry of nutrients, in particular, iron (Fe) and nitrogen (N), thereby

altering phytoplankton homeostasis. My experimental focus was to observe the combined effects of pH change and the bioavailability of iron. Prior to working with different iron concentrations and pH values as variables, preliminary work was essential to establish a method of acidification that would not change the growth rate of the phytoplankton species examined. Two methods were used to acidify laboratory cultures: acid/base titration and CO₂-bubbling, the former was examined first.

3.4.1. Acidification

3.4.1a Examining acid/base titration pH changes in media without cell culture

HCl was used to adjust the pH of ESAW medium to 7.4, 7.8 or 8.1. As shown in Figure 3.1, in the absence of cells, the pH remained stable over time. This was a key starting point to confirm that any pH fluctuation to occur after cultures were inoculated for experimentation was solely the result of algal activity, and not ambient air diffusion into the medium. The average pH and deviation of pH changes in treatments titrated to pH 7.4, 7.8 and 8.1 over the 5 day time frame was: 7.46 ± 0.08 , 7.81 ± 0.02 and 8.08 ± 0.03 , respectively. The standard deviation values represent the average change in pH that can be expected through future experimentation.

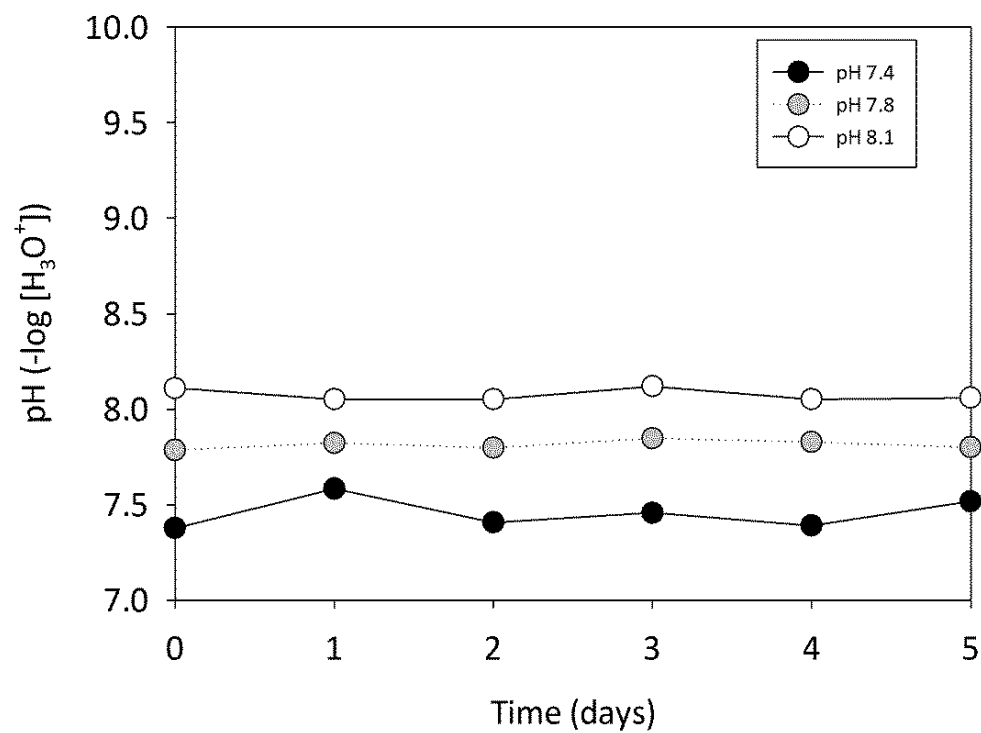


Figure 3.1 pH readings over 5 days of ESW medium adjusted to pH 7.4, 7.8 and 8.1 with HCl, in the absence of cells. The average pH and deviation of pH changes over the 5 day time frame was: 7.46 ± 0.080 , 7.81 ± 0.023 and 8.08 ± 0.033 , respectively (n=1).

3.4.1b Examining pH changes in media with phytoplankton

When phytoplankton are grown in artificial seawater medium (ESAW), one of their primary sources of carbon comes from the addition of bicarbonate (HCO_3^-). HCO_3^- has an intrinsic buffering capability to maintain the pH of the medium that phytoplankton are grown in, because cells utilize HCO_3^- for carbon acquisition for photosynthesis. The intrinsic buffering capability of HCO_3^- in ESAW medium adjusted with HCl was examined with the addition of *Synechococcus* sp. cells. As shown in Fig. 3.2, when ESAW medium was adjusted to the desired pH using HCl and phytoplankton cells were then added, the pH of the culture rose to an average of 9.4, irrespective of the starting pH adjustment. These results demonstrated the necessity of adding an additional buffering agent to maintain the pH for ocean acidification experiments involving the acid/base titration method. A pH of 7.4 represents 40 nM L^{-1} ($4 \times 10^{-8} \text{ M}$) of H^+ ions, pH 7.8 represents 1.5 nM L^{-1} ($1.5 \times 10^{-8} \text{ M}$) of H^+ ions, 8.1 represents 7.9 nM L^{-1} ($7.9 \times 10^{-9} \text{ M}$) of H^+ ions, and these values all rose to an average of pH 9.4, which represents 0.4 nM L^{-1} ($4.0 \times 10^{-10} \text{ M}$) of H^+ ions in solution. To illustrate, a pH change from 7.4 to 9.4 represents $100\times$ more H^+ ions, 7.8 to 9.4 represents $37.5 \times$ more H^+ ions and pH 8.1 to 9.4 represents $19.75 \times$ more H^+ ions in solution.

3.4.1c Buffer selection

ESAW medium has a weak intrinsic buffering ability to resist changes in pH that occur as phytoplankton grow and utilize carbon, through the addition of HCO_3^{2-} . To determine the effects of adding an additional chemical buffering agent to the pH of the ESAW medium, three commercial buffers (Good's buffers) were examined: HEPES, TES and Tricine (Appendix I). Three levels of buffers were investigated for their ability to resist pH change over time (0.56 mM, 2.7 mM and 10 mM). The addition of HEPES

buffer was found to be the most effective at resisting pH change (Fig. 3.3), while not affecting cell growth rates (Table 3.1) and cell yields (Table 3.2). The results confirmed the necessity of adding a buffering agent to resist pH changes that resulted from biological activity to all experimental cultures for acid/base pH manipulation.

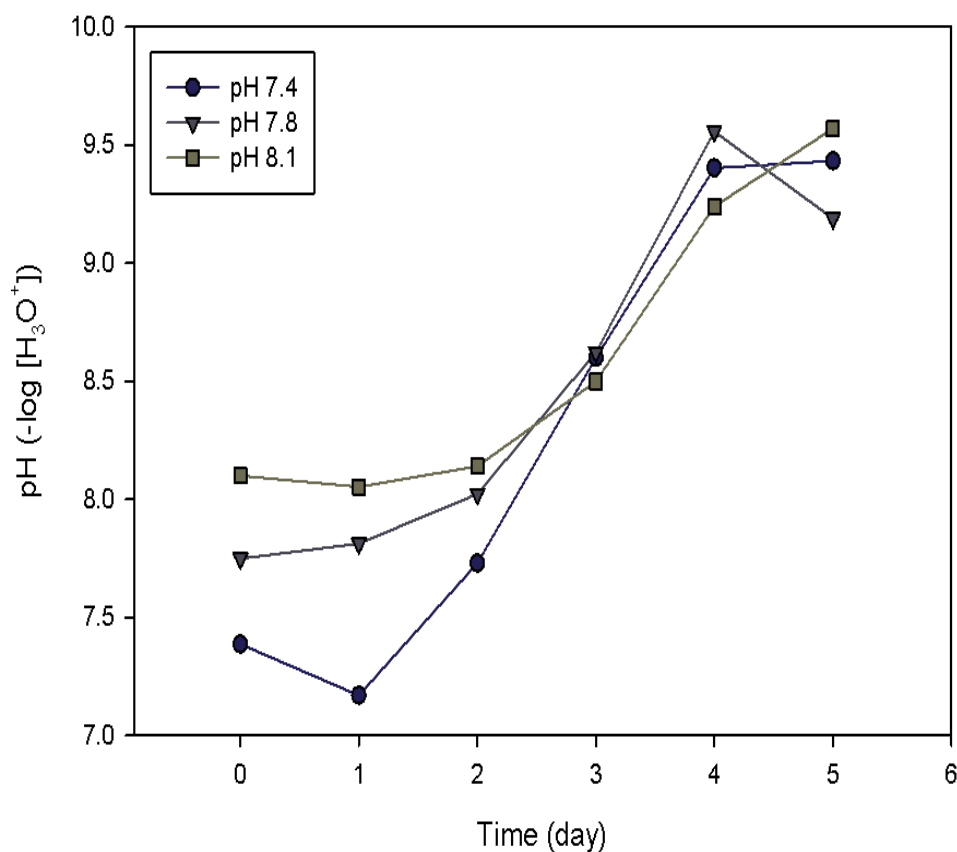


Figure 3.2 Non-buffered *Synechococcus* sp. CCMP 833 in ESAW medium adjusted to a pH of 7.4, 7.8, and 8.1 with 10% HCl.

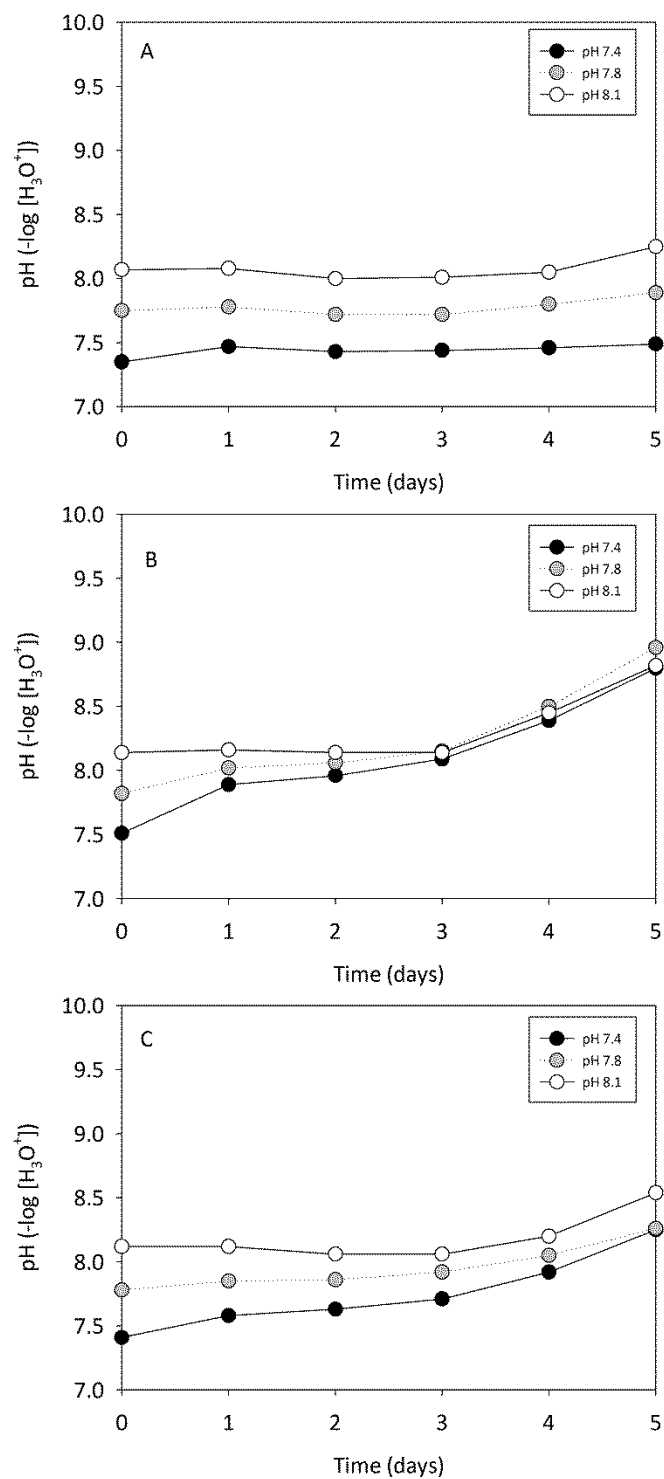


Figure 3.3. pH changes in acid/base titrated cultures over a 5-day growth period for *Synechococcus* sp. CCMP 833 grown in ESAW medium (880 μ M N) with the addition of HEPES buffer at a concentration of A) 0.56 mM B) 2.7 mM and C) 10 mM (n=1).

	0.56 mM	2.7 mM	10mM	No buffer
pH 7.4	0.823	0.815	0.801	
pH 7.8	0.803	0.767	0.724	
pH 8.1	0.863	0.793	0.863	
Control				0.84

Table 3.1 Growth rates (divisions day⁻¹) of *Synechococcus* sp. CCMP 833 grown in ESAW (+ f/2 nutrients), supplemented with three different concentrations of HEPES buffer.

	0.56 mM	2.7 mM	10mM	No buffer
pH 7.4	0.048	0.051	0.054	
pH 7.8	0.057	0.036	0.062	
pH 8.1	0.052	0.041	0.054	
Control				0.051

Table 3.2 Optical density (720 nm) as a proxy for cell yield of *Synechococcus* sp. CCVMP 833 grown in ESAW (+f/2 nutrients), supplemented with three different concentrations of HEPES buffer.

3.4.1d Fe selection

Growth for *Synechococcus* sp. CCMP 833 under the combined stresses of pH and iron was examined (with the addition of HEPES buffer) to confirm any growth changes that the buffer might impose on the algae (Fig. 3.4). It was critical to assess this parameter to verify that any changes in growth were due to the pressures of pH or iron concentrations, and not the result of adding a buffering agent. HEPES buffer did not affect the algal growth rate or growth yield, however, acid/base titration limited biomass, as will be noted in section 3.4.8.

In order to select two iron enrichments to add to ESAW medium (one to maximize algal growth and one to restrict algal growth), four iron concentrations were examined. Cell density for each pH (7.4, 7.8 and 8.1) treatment in Fe-rich conditions (1.0 μM FeCl_3 and 11.0 μM FeCl_3) and low iron growth conditions (0.01 μM FeCl_3 and 0.1 μM FeCl_3) were examined to assess combined effects of pH and Fe. It was noted that growth rates (day^{-1}) in the Fe-poor conditions (0.01 μM FeCl_3 and 0.1 μM FeCl_3) were not different from one another, and growth rates within the Fe-rich conditions (1.0 μM FeCl_3 and 11.0 μM FeCl_3) were not different from one another. Additionally, the growth rates among pH treatments were not different within the Fe-poor conditions (0.01 μM FeCl_3 and 0.1 μM FeCl_3) and within the Fe-rich conditions (1.0 μM FeCl_3 and 11.0 μM FeCl_3) meaning that pH stress is what restricted growth rates of the system, since growth rates decrease with decreasing pH (Fig. 3.4).

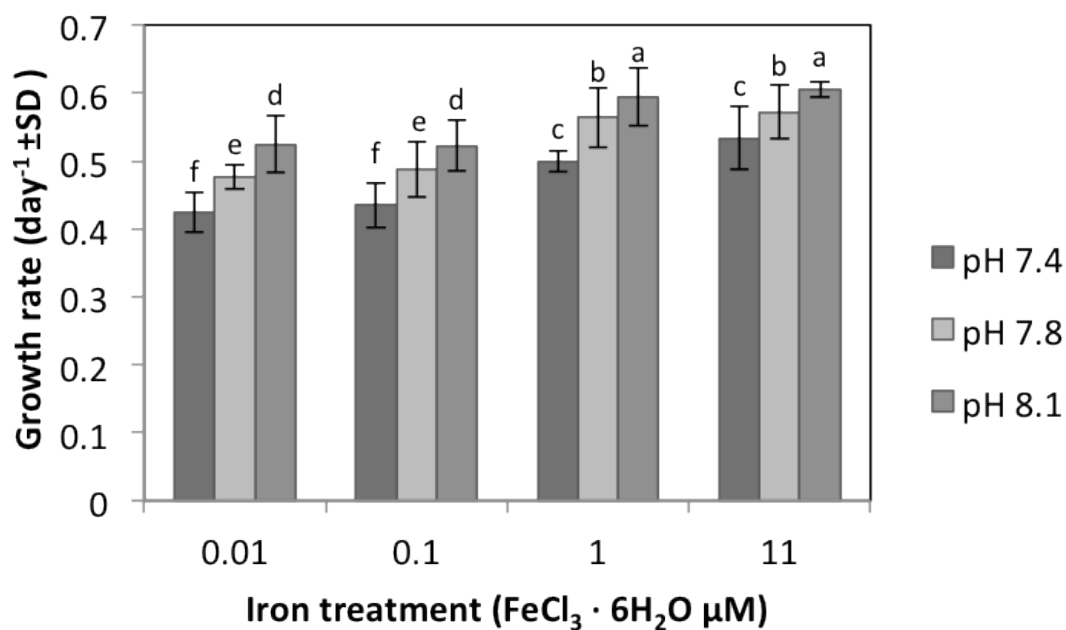


Figure 3.4 Average growth rate ($\text{day}^{-1} \pm \text{SD}$) of *Synechococcus* sp. CCMP 833 grown in ESAW medium ($880 \mu\text{M N}$) at varying iron concentrations ($0.01 \mu\text{M}$, $0.1 \mu\text{M}$, $1.0 \mu\text{M}$ and $11.0 \mu\text{M FeCl}_3$) and pH levels (7.4, 7.8 and 8.1). Bars with different letters represent statistically different treatment effects based on Tukey's b post hoc test ($n = 3$), ($F=36.331$, $df=2$, $p<0.001$).

Since there was no difference in growth rates of *Synechococcus* sp. CCMP 833 cultures among the Fe-poor conditions (0.01 μM FeCl_3 and 0.1 μM FeCl_3) and among the Fe-rich conditions (1.0 μM FeCl_3 and 11.0 μM FeCl_3), all future experiments were conducted at only two of these chosen iron concentrations: low iron (0.01 μM FeCl_3) and high iron (11.0 μM FeCl_3). Growth curves for *Synechococcus* sp. CCMP 833 (Figure 3.5) and *Synechococcus* sp. CCMP 835 (Fig. 3.6) were similar, however, in the diatom species *T. weissflogii* CCMP 1051, pH and iron had no effect on growth rate (Fig. 3.7).

For the flagellate *H. akashiwo* NWFSC 503 examined in this study, there was once again no difference in growth rates or cell density between the two Fe-poor enrichments (0.01 μM FeCl_3 and 0.1 μM FeCl_3) or between the two Fe-rich enrichments (1.0 μM FeCl_3 and 11.0 μM FeCl_3). Iron was growth limiting at the two lowest levels of iron (based on the reduced cell yield). Yet the growth rates of *H. akashiwo* NWFSC 503 was not impacted under any of the pH conditions (Figs. 3.8 and 3.9).

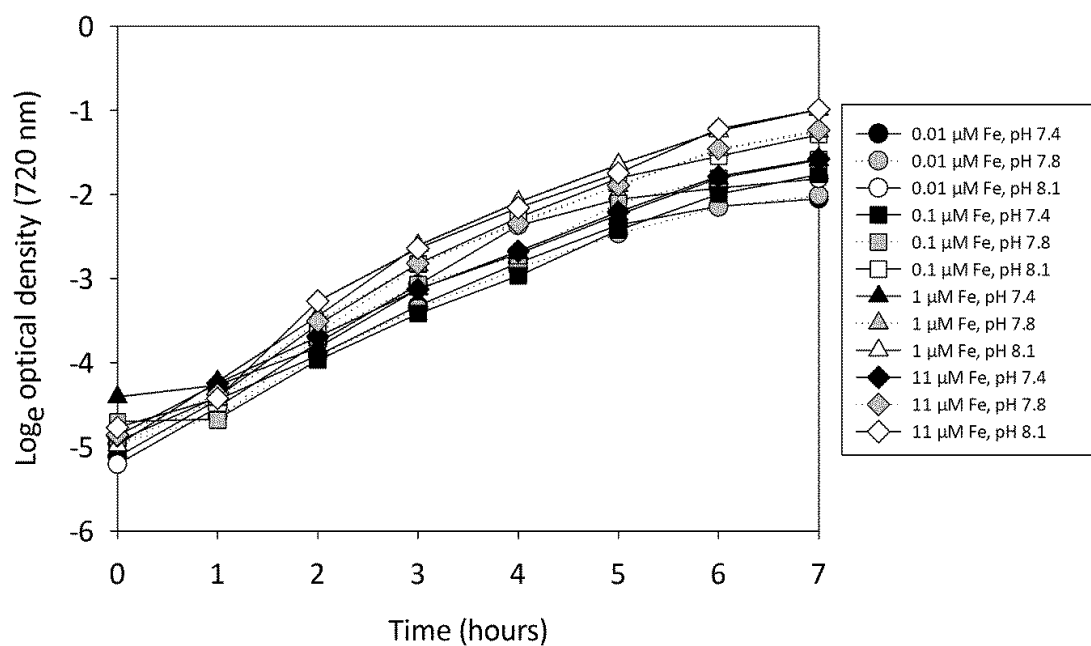


Figure 3.5 Growth curve of *Synechococcus* sp. CCMP 833 grown in ESAW medium (880 μM N) with altered iron concentrations and pH levels. Growth is expressed as the natural logarithm of cell density (n=3).

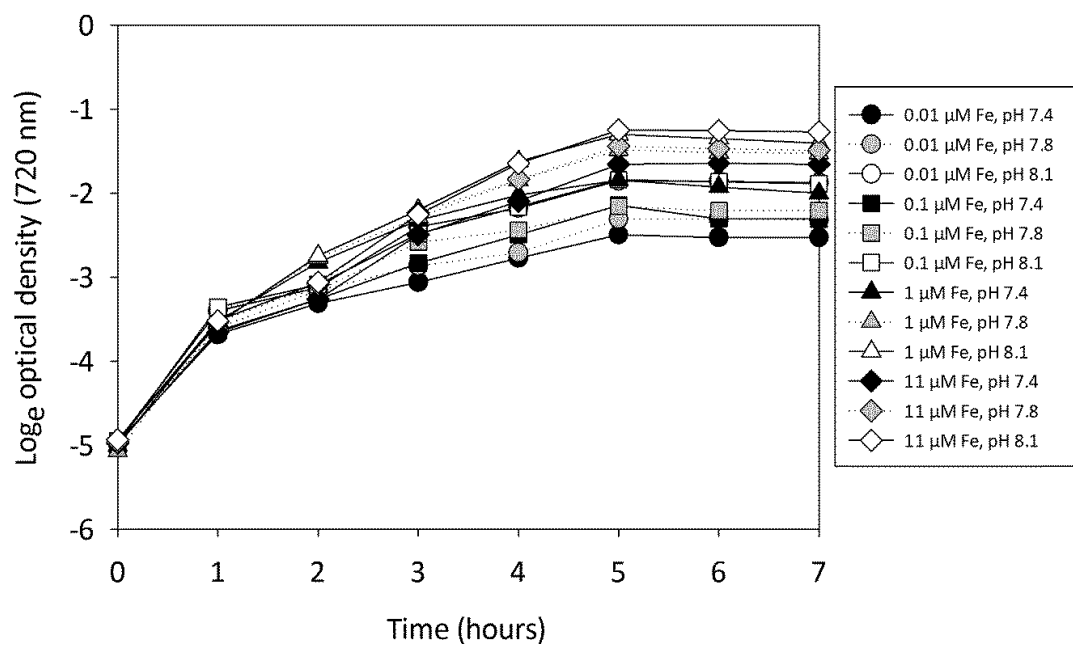


Figure 3.6 Growth curve of *Synechococcus* sp. CCMP 835 grown in ESAW medium (880 μ M N) with altered iron concentrations and pH levels. Growth is expressed as the natural logarithm of cell density (n=3).

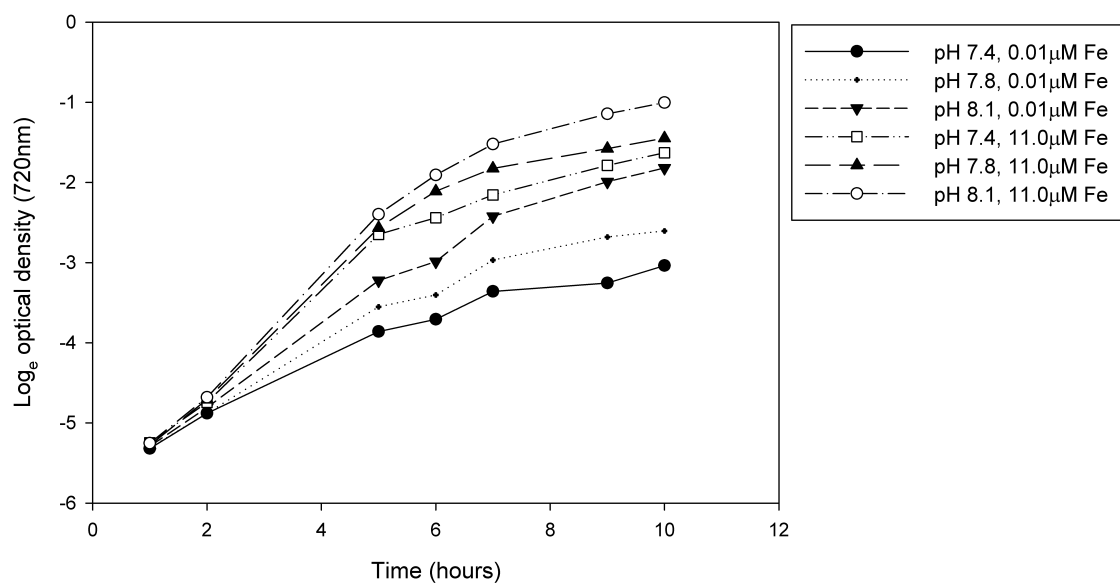


Figure 3.7 Growth curve of *Thalassiosira weissflogii* CCMP 1051 grown in ESAW medium (880 μM N) with altered iron concentrations and pH levels. Growth is expressed as the natural logarithm of cell density (n=3).

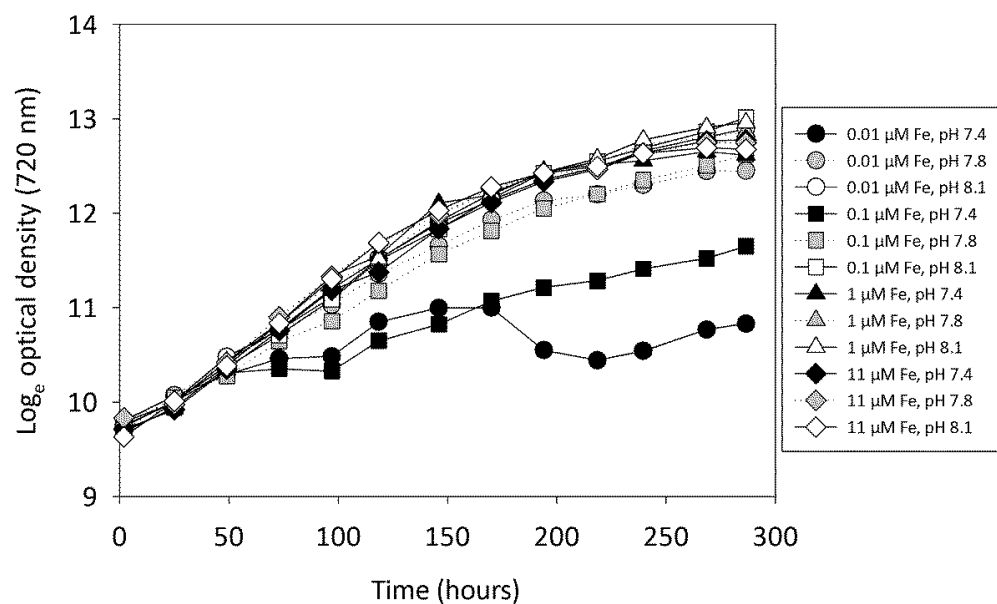


Figure 3.8 Growth curve of *H. akashiwo* NWFSC 503 grown in ESAW medium (880 μM N) with altered iron concentrations and pH levels. Growth is expressed as the natural logarithm of cell density (n=3).

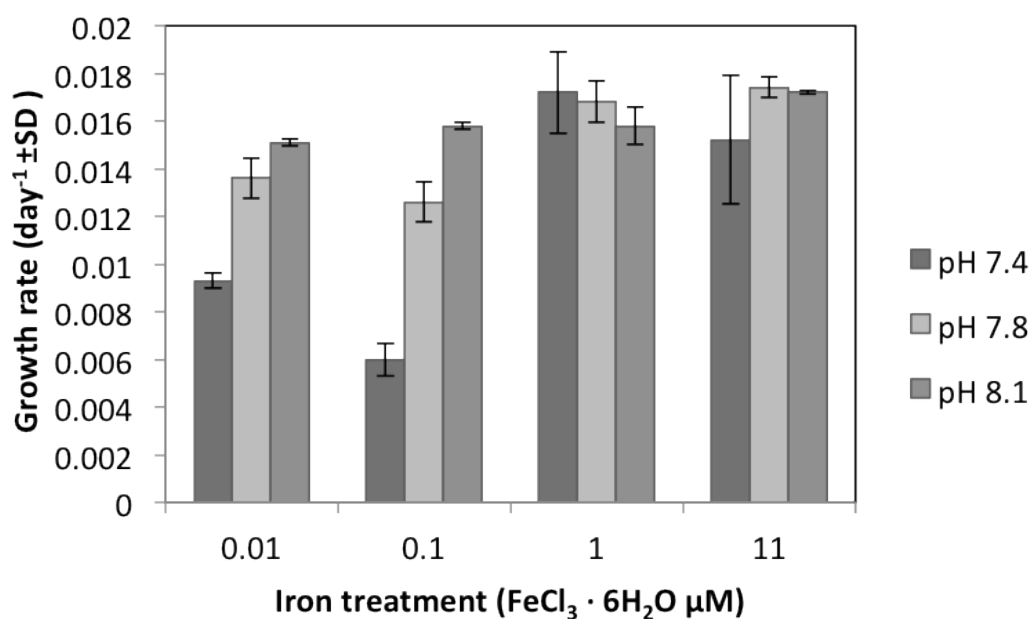


Figure 3.9 Mean growth rate (day⁻¹ ± SD) of *H. akashiwo* NWFSC 503 grown in ESAW medium (880 μM N) at varying iron concentrations and pH levels (n = 3). Significant differences were observed across iron limited levels (0.01 and 0.1 μM Fe) and pH levels, but there was no observed significant interaction effect between pH or high iron levels (0.01 and 0.1 μM Fe), (iron: F=4.328, Df= 3, 22, P= 0.0166; pH: F=3.565, Df= 2, 22, P= 0.04561).

3.4.2 Algal growth

To assess whether ocean acidification in Fe-rich and Fe-poor medium would alter growth characteristics of phytoplankton, growth rates were assessed. In both *Synechococcus* sp. CCMP 835 (Fig. 3.10) and *Synechococcus* sp. CCMP 833 (Fig. 3.11), there was not a significant difference in the mean growth rates among different levels of pH, but there was a significant difference in the mean growth rates among the different levels of iron (within any given pH treatment). Therefore, acidification using an acid/base buffering method to change pH did not drive growth rate differences. Except in the case of *Synechococcus* sp. In comparison, growth rates in the diatom, *T. weissflogii* CCMP 1051, were not different among any pH or iron treatments (Fig. 3.12).

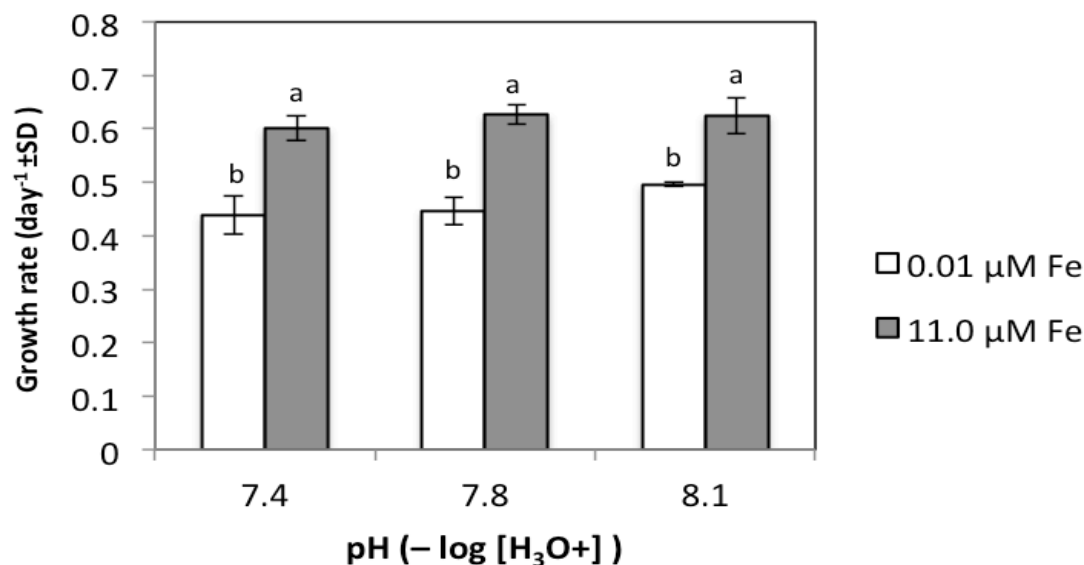


Figure 3.10 Mean growth rate (day⁻¹ ± SD) of *Synechococcus* sp. 835 at grown in ESAW medium (880 μM N) at varying iron concentrations and pH levels. Bars with different letters represent statistically different treatment effects based on Tukey's b post hoc test (n = 3), (F=1.257, df=2, p<0.001).

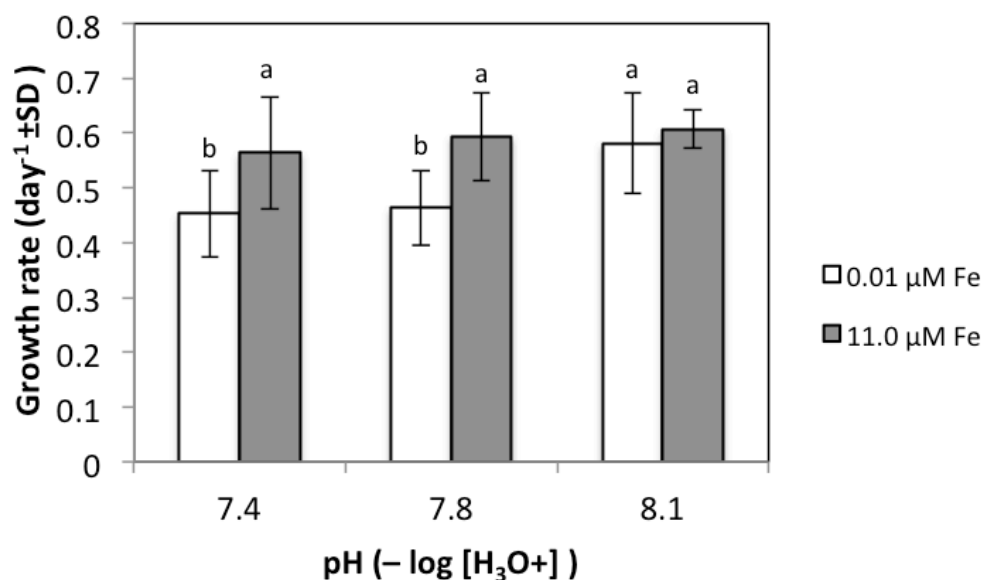


Figure 3.11 Mean growth rate (day⁻¹ ± SD) of *Synechococcus* sp. CCMP 833 grown in ESAW medium (880 μM N) at varying iron concentrations and pH levels. Bars with different letters represent statistically different treatment effects based on Tukey's b post hoc test (n = 3), (F=2.405, df=2, p<0.001).

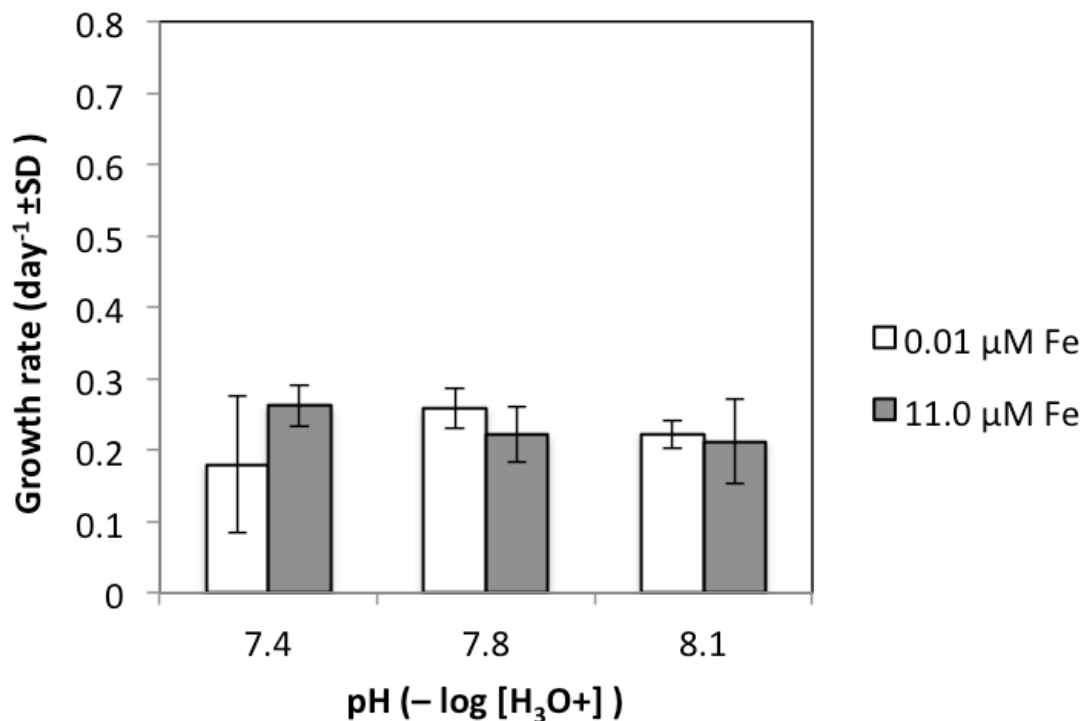


Figure 3.12 Mean growth rate (day⁻¹ ± SD) of *T. weissflogii* CCMP 1051 grown in ESAW medium (880 μM N) at varying iron concentrations and pH levels (n =3) representing no significant difference between iron and pH level (F=2.485, df=2, p=0.138).

3.4.3 Cell density variation among iron and pH treatments

Photoautotrophs have developed a number of mechanisms to acclimate to imbalances between pH, light absorption and carbon assimilation. Such mechanisms involve light harvesting complexes, where cells can either decrease the concentrations of their light harvesting pigments, increase their photoprotective pigments such as xanthophylls and carotenoids, or increase their shading photosynthetic components. To assess these plausible changes, cell density was observed. In *Synechococcus* sp., there was an observable density variation between the iron-limited enrichments (0.01 μM FeCl₃

and 0.1 μM FeCl_3) and the iron-rich enrichments (1.0 μM FeCl_3 and 11.0 μM FeCl_3). Less pigment (meaning either low cell density and/or less chlorophyll per cell) was displayed in Fe-poor enrichments, as predicted due to lower nutrient concentrations- a driver of cell density changes. Not only was there cell pigment density variation among iron enrichments (as shown across the rows in Fig. 3.13), but also density/pigment variation was visible between pH levels. With decreasing pH, there was less density/pigments in all phytoplankton isolates, with the exception of the diatom, *T. weissflogii* CCMP 1051, which only exhibited less density/pigments in the iron-poor treatment at pH 7.4.

3.4.4 Chlorophyll

Chlorophyll production was used as an indicator of algal light harvesting potential under the combined stresses of pH and iron availability. Before examining chlorophyll production, assessing whether the use of HEPES buffer would alter the raw chlorophyll fluorescence (RFU) produced by phytoplankton (thereby changing the amount of chlorophyll), was tested. HEPES buffer did not have an impact on chlorophyll fluorescence when a control culture grown without the addition of HEPES and an experimental culture grown with the addition HEPES was compared (results not shown).

Results of total chlorophyll-*a* production from cultures grown in ESAW (880 μM N) were used as a proxy for growth, and showed a similar pattern to growth rate measurements. In the iron-poor enrichments (0.01 μM FeCl_3), the low iron concentrations are what limited the total isolated chlorophyll-*a* (mg). Therefore, when iron was limited, there was no significant difference in the amount of chlorophyll-*a* produced between different pH levels in both cyanobacterium isolates examined, *Synechococcus* sp. CCMP

835 (Fig. 3.14) and *Synechococcus* sp. CCMP 833 (Fig. 3.15). When the iron enrichment was high (11.0 μM FeCl_3), however, there was a significant difference in the amount of chlorophyll-*a* produced in both cyanobacterium isolates, but there was not a significant interaction between pH and iron for *Synechococcus* sp. CCMP 835 (Fig. 3.14) and *Synechococcus* sp. CCMP 833 (Fig. 3.15). Two reasons could explain this result: this could be the result of either less cells or less chlorophyll within each cell.

A different trend was noted in the phytoplankton isolates: *T. weissflogii* CCMP 1051 and *H. akashiwo* NWFSC 503 grown in ESAW medium (880 μM N). In the iron-poor and iron-rich enrichments (0.01 μM FeCl_3 and 11.0 μM FeCl_3) for *T. weissflogii* CCMP 1051, the total isolated chlorophyll-*a* levels were lowest in only the treatment that had a combined stress of acidification at pH 7.4 and iron limitation at 0.01 μM FeCl_3 , which explains why this was the only treatment with the lowest visible pigment (or cell density as noted in the previous section). All other treatments demonstrated no difference in the amount of chlorophyll-*a* (mg) present between pH levels and iron concentrations (Fig. 3.16).

In *H. akashiwo* NWFSC 503, when iron enrichment was low, chlorophyll-*a* production was highest at a moderate pH level of 7.8, compared to the acidic (7.4) and ambient (8.1) pH treatments. Within the high iron enrichments, there was no difference in chlorophyll-*a* production at any of the pH levels examined. Similarly to the cyanobacteria examined in this study, it was the limitation of iron and not pH that drove differences in chlorophyll-*a* production for *H. akashiwo* NWFSC 503 (Fig. 3.17).

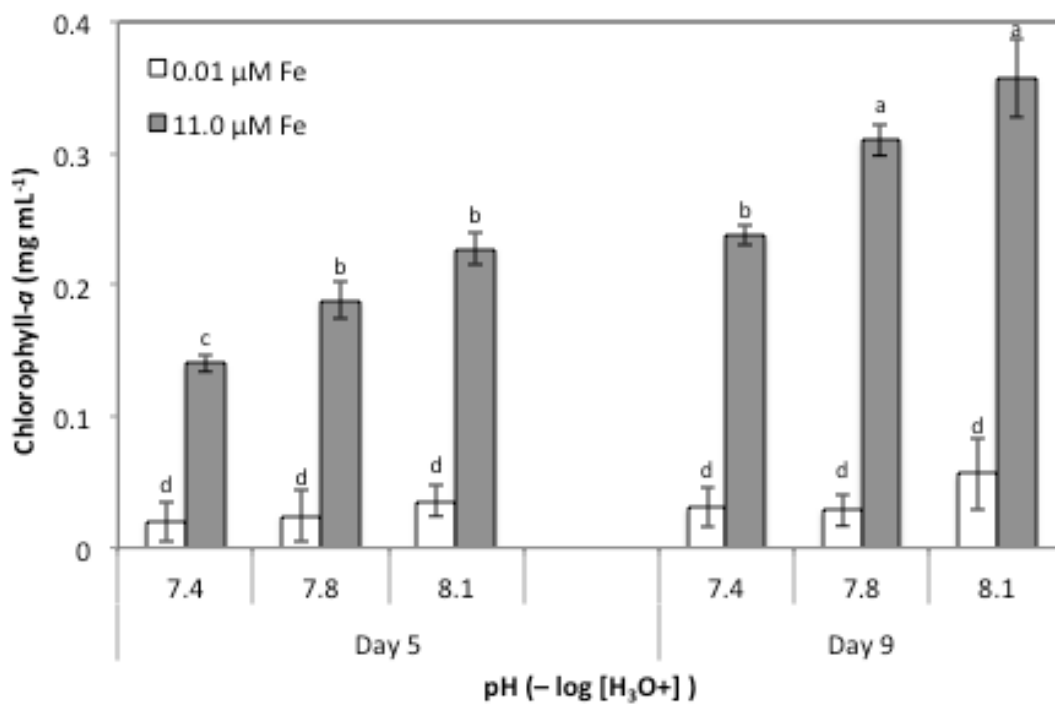


Figure 3.14 Mean chlorophyll-*a* values (mg/mL) on day 5 and day 9 of growth for *Synechococcus* sp. CCMP 835 grown in ESAW medium with 880 μM N. Within day 5 and day 9, bars with different letters indicate statistically significant chlorophyll differences among treatments, based on Tukey's b post hoc test (n = 3).

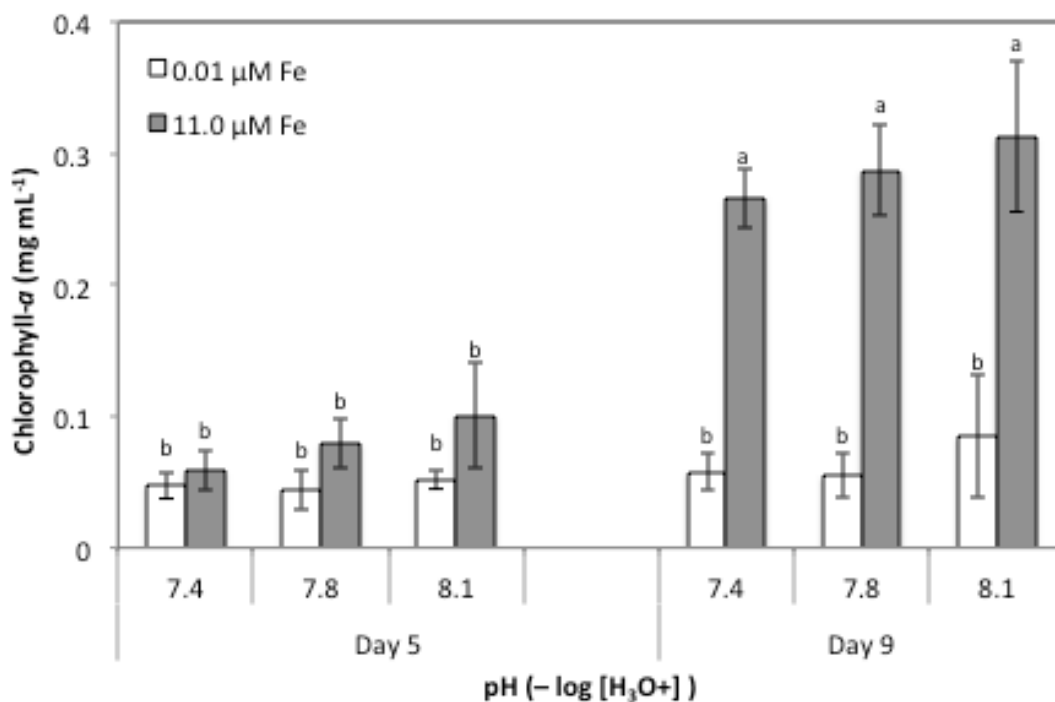


Figure 3.15 Mean chlorophyll-*a* values (mg/mL) on day 5 and day 9 of growth for *Synechococcus* sp. CCMP 833 grown in ESAW medium with 880 μM N. Within day 5 and day 9, bars with different letters indicate statistically significant chlorophyll differences among treatments, based on Tukey's b post hoc test ($n = 3$).

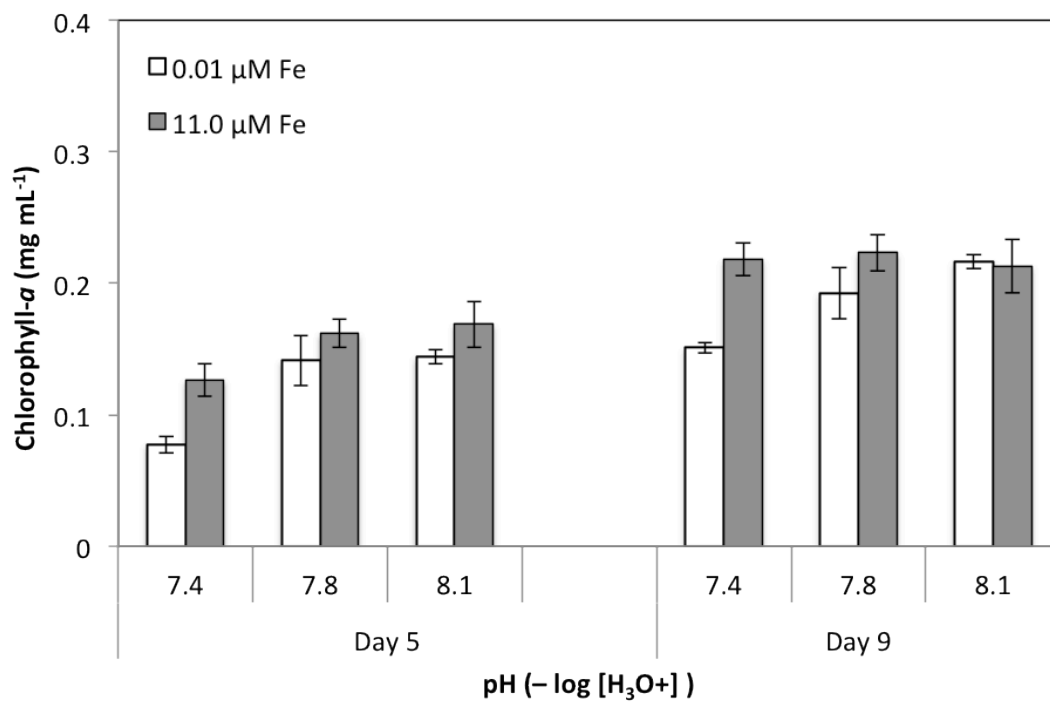


Figure 3.16 Mean chlorophyll-*a* values (mg/mL) on day 5 and day 9 of growth for *T. weissflogii* CCMP1051 grown in ESAW medium with 880 $\mu\text{M N}$ ($n = 3$).

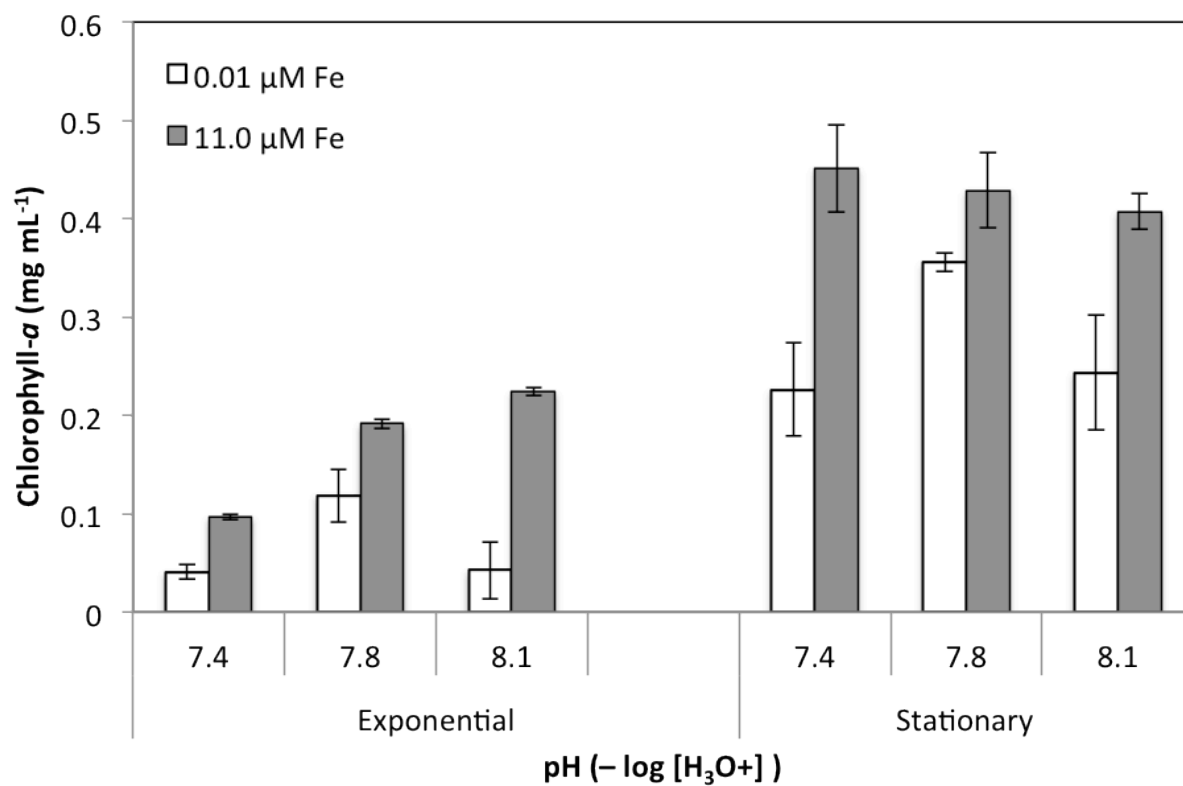


Figure 3.17 Mean chlorophyll-*a* values (mg/mL) on day 5 and day 9 of growth for *H. akashiwo* NWFSC 503 grown in ESAW medium with 880 $\mu\text{M N}$ (n=3).

3.4.5 Oxygen evolution

It has been suggested that it is unlikely that an increase in CO₂ expected by the year 2100 (pH 7.4) will have a significant direct effect on photosynthesis in phytoplankton because of their ability to concentrate carbon using a CCM (ref). However, pH affects the availability of nutrients, and this has been proposed to alter their rate of growth and photosynthesis (The Royal Society, 2005). To assess if photosynthetic ability in planktonic algae is impaired resulting from ocean acidification, photosynthesis (that is, oxygen evolution) was examined at each pH level (7.4, 7.8 and 8.1) in iron-poor (0.01 µM FeCl₃) and iron-rich (11.0 µM FeCl₃) enrichments with cells grown in ESAW medium (880 µM N enrichment). Photosynthetic efficiency, apparent and true photosynthetic capacity, and photorespiration were examined and results are outlined at low iron (0.01µM) in Table 3.3 (A), and high iron (11.0 µM) in Table 3.3 (B).

A)	Photosynthetic efficiency			True photosynthetic capacity			Apparent photosynthetic capacity			% True photosynthesis			Photorespiration		
	pH 7.4	pH 7.8	pH 8.1	pH 7.4	pH 7.8	pH 8.1	pH 7.4	pH 7.8	pH 8.1	pH 7.4	pH 7.8	pH 8.1	pH 7.4	pH 7.8	pH 8.1
<i>Synechococcus</i> spp. 833	8X10 ⁻⁵	1X10 ⁻⁴	1X10 ⁻⁴	0.028	0.023	0.023	0.016	0.019	0.014	43	17	39	0.012	0.004	0.009
<i>Synechococcus</i> spp. 835	8X10 ⁻⁵	8X10 ⁻⁵	9X10 ⁻⁷	0.024	0.01	0.013	0.007	0.006	0.008	71	40	38	0.017	0.004	0.005
<i>T. weissflogii</i> 1051	3X10 ⁻⁵	5X10 ⁻⁵	7X10 ⁻⁵	0.006	0.008	0.008	0.004	0.004	0.003	33	50	63	0.002	0.004	0.005
<i>H. akashiwo</i> 503	3X10 ⁻⁵	1X10 ⁻⁵	1X10 ⁻⁵	0.005	0.003	0.002	0.002	0.002	0.001	60	33	50	0.003	0.001	0.001
B)	Photosynthetic efficiency			True photosynthetic capacity			Apparent photosynthetic capacity			% True photosynthesis			Photorespiration		
	pH 7.4	pH 7.8	pH 8.1	pH 7.4	pH 7.8	pH 8.1	pH 7.4	pH 7.8	pH 8.1	pH 7.4	pH 7.8	pH 8.1	pH 7.4	pH 7.8	pH 8.1
<i>Synechococcus</i> spp. 833	7X10 ⁻⁵	6X10 ⁻⁵	6X10 ⁻⁵	0.016	0.012	0.015	0.009	0.005	0.009	44	58	40	0.007	0.007	0.006
<i>Synechococcus</i> spp. 835	2X10 ⁻⁵	3X10 ⁻⁵	4X10 ⁻⁵	0.014	0.007	0.005	0.001	0.001	0.001	93	86	80	0.013	0.006	0.004
<i>T. weissflogii</i> 1051	6X10 ⁻⁵	5X10 ⁻⁵	7X10 ⁻⁵	0.008	0.008	0.011	0.005	0.004	0.004	38	50	64	0.003	0.004	0.007
<i>H. akashiwo</i> 503	1X10 ⁻⁵	1X10 ⁻⁵	1X10 ⁻⁵	0.003	0.003	0.003	0.002	0.002	0.001	33	33	67	0.001	0.001	0.002

Table 3.3 Photosynthetic efficiency, apparent and true photosynthetic capacity, and photorespiration of *Synechococcus* sp. CCMP 833, *Synechococcus* sp. CCMP 835, *T. weissflogii* CCMP 1051, and *H. akashiwo* NWFSC 503 at: a) low Fe (0.01 μ M). and b) high Fe (11.0 μ M).

A difference in the response of growth rates to CO₂ does not necessarily translate to similar differences in photosynthetic affinity for CO₂ (Raven *et al.* 1993; Beardall *et al.* 1998). For this reason, oxygen evolution rates were used as a proxy to examine carbon acquisition rates in phytoplankton, as O₂-evolution occurs in a 1:1 ratio with CO₂-uptake. Since photoautotrophic algae have different photosynthetic responses to inorganic carbon concentration, algae are likely to respond differently to current and future changes in ocean pH (or atmospheric CO₂). When examining oxygen evolution rates, a similar pattern was observed in the cyanobacteria *Synechococcus* sp. CCMP 835 (Fig. 3.18), *Synechococcus* sp. CCMP 833 (Fig. 3.19) and in the flagellate *H. akashiwo* NWFSC 503 (Fig. 3.20), but a different trend was noticed in the oxygen evolution curves of the diatom *T. weissflogii* CCMP 1051 (Fig. 3.21).

For the cyanobacteria and *H. akashiwo*, low iron enrichment and acidic (pH 7.4) conditions resulted in cells having the highest rates of oxygen evolution. By stationary growth, the cells with low iron enrichment exhibited no change in photosynthesis whereas the cells with high iron enrichment showed a significantly lower maximum photosynthetic capacity.

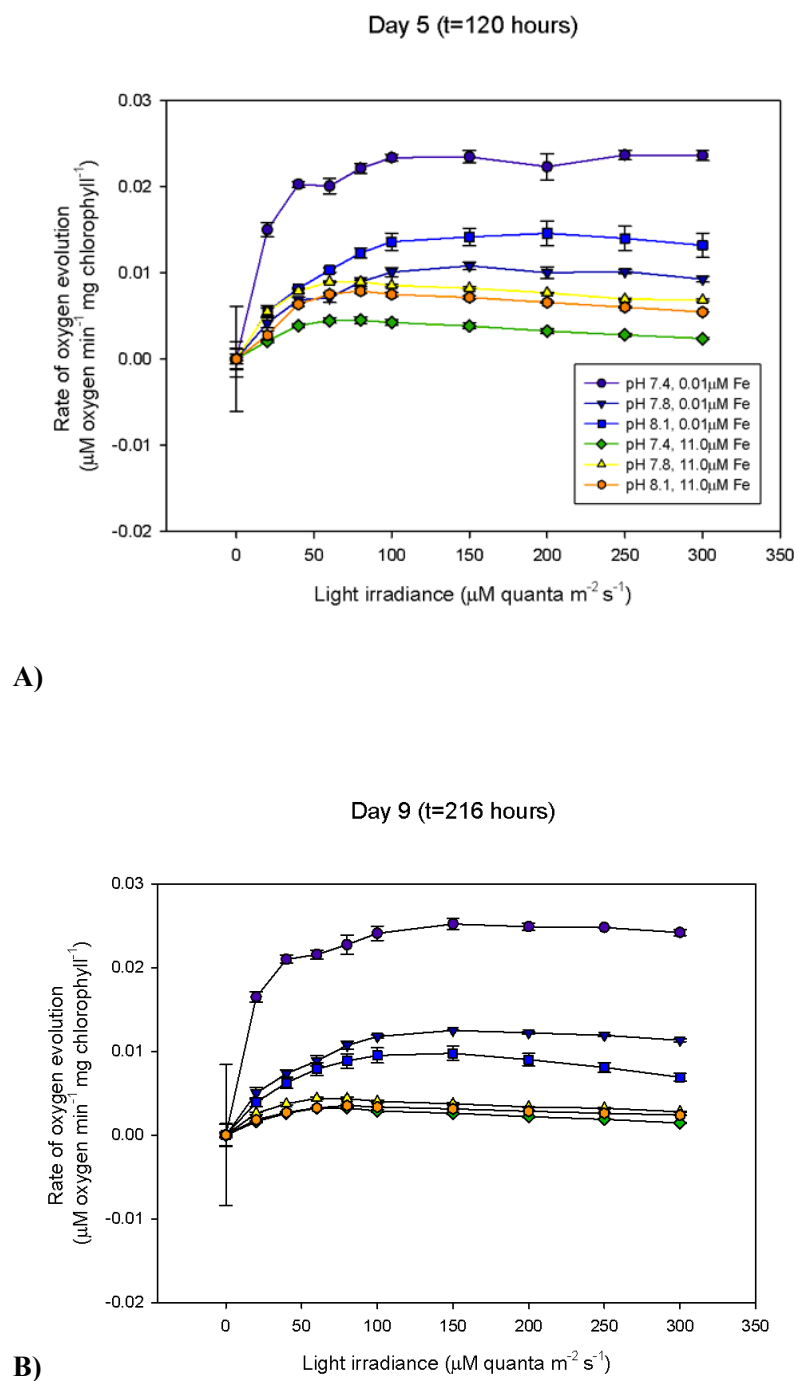


Figure 3.18 Oxygen evolution of *Synechococcus* sp. CCMP 835 grown in ESAW medium (880 μM) at varying iron enrichments (0.01 and 11.0 μM) and pH levels (7.4, 7.8 and 8.1) during: A) exponential growth phase and B) stationary growth phase (n=3).

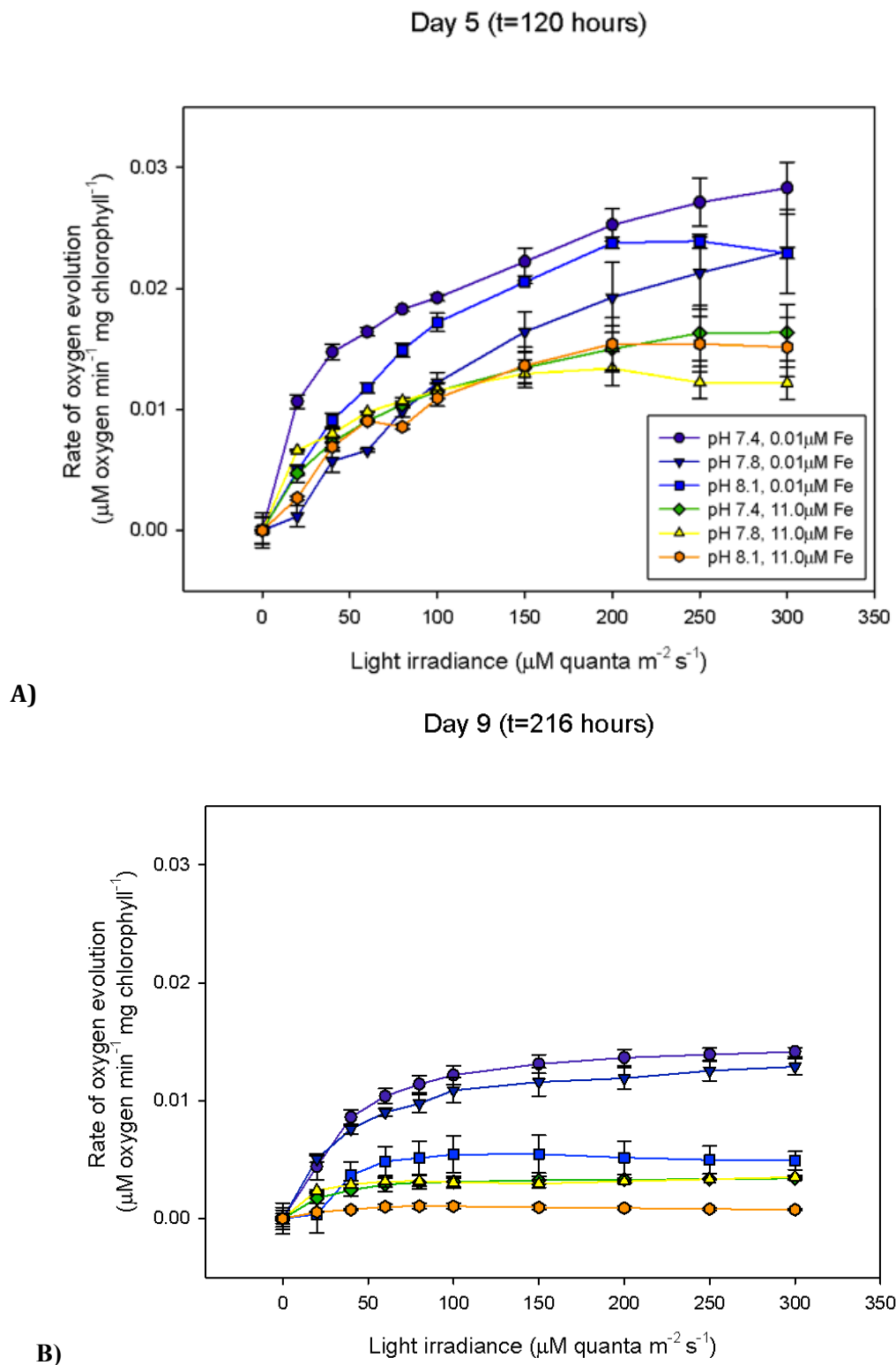


Figure 3.19 Oxygen evolution of *Synechococcus* sp. CCMP 833 grown in ESAW medium (880 μM) at varying iron enrichments (0.01 and 11.0 μM) and pH levels (7.4, 7.8 and 8.1) during: A) exponential growth phase and B) stationary growth phase ($n = 3$).

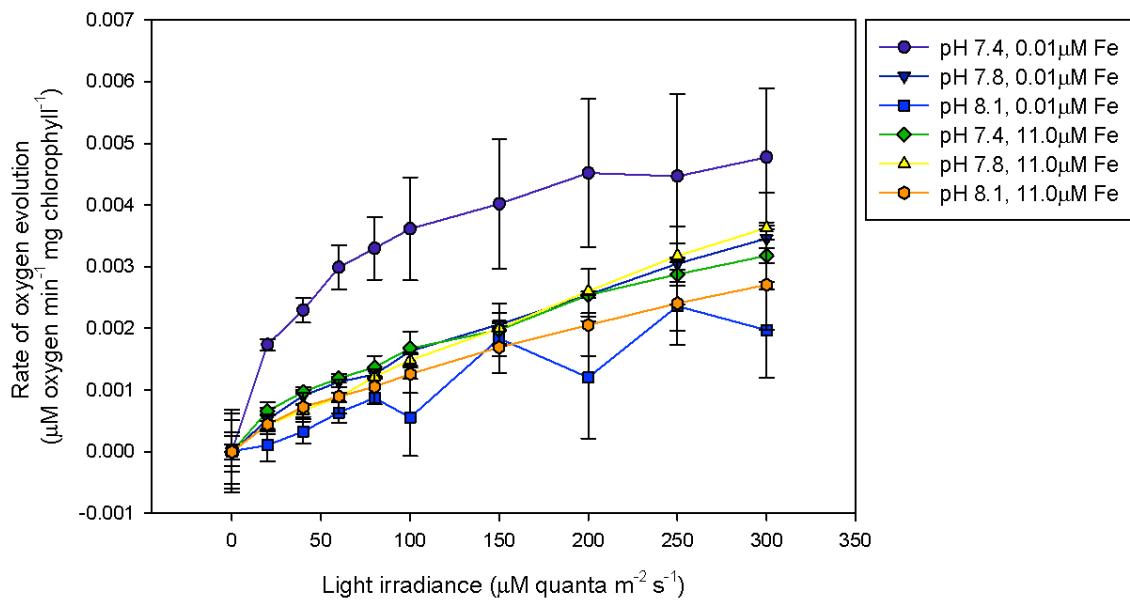


Figure 3.20 Oxygen evolution of *Heterosigma akashiwo* NWFSC 503 grown in ESAW medium (880 μM) at varying iron enrichments (0.01 and 11.0 μM) and levels of acidity pH (7.4, 7.8 and 8.1) during exponential growth ($n = 2$). There was a significant interaction between low pH and oxygen evolution in the low iron treatment compared ($F=7.288$, $df=1.8$, 29 , $p=0.0115$), but no interaction with irradiance and high pH with high iron ($F=60.688$, $df= 1$, 29 , $p=0.0283$).

Unlike the phytoplankton isolates described above, the diatom *T. weissflogii* CCMP 1051 demonstrated a different photosynthetic efficiency and photosynthetic capacity trend in the oxygen evolution rates (Fig. 3.21). During, the cells grown at ambient pH (8.1) with a high iron enrichment (11 μM) had the highest rate of oxygen evolution compared to the acidified cells at pH (7.4) with a low iron enrichment (0.01 μM). All other iron enrichments and pH conditions residing between the two treatment extremes were not different from one another. By stationary growth, there was no significant difference in the rates of oxygen evolution among any treatment, as the overall rates decreased with the aging algal population.

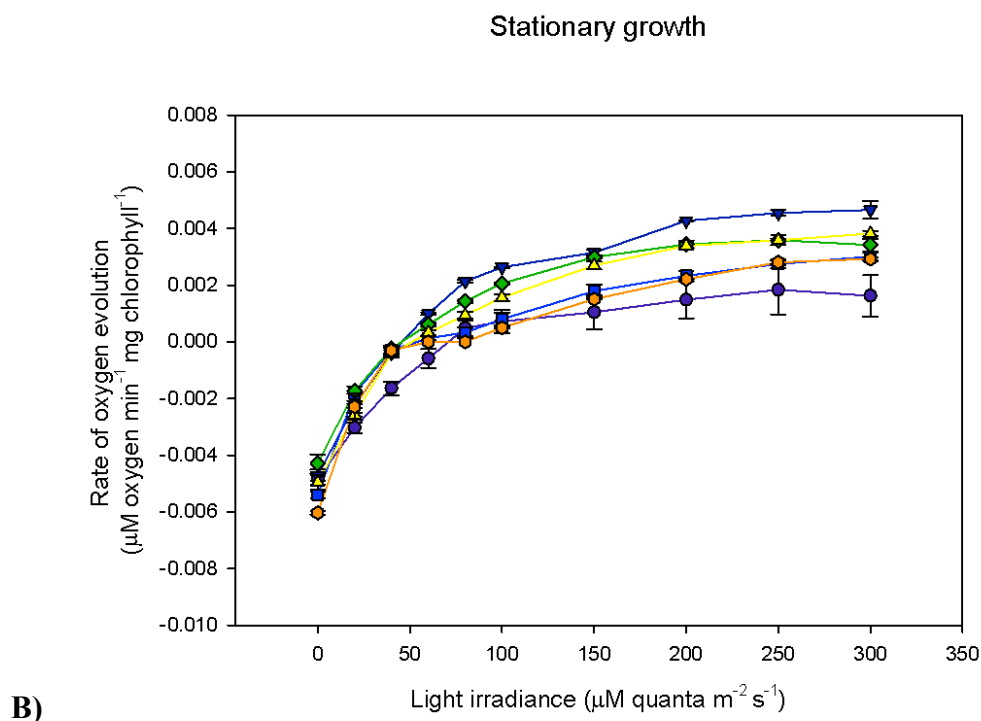
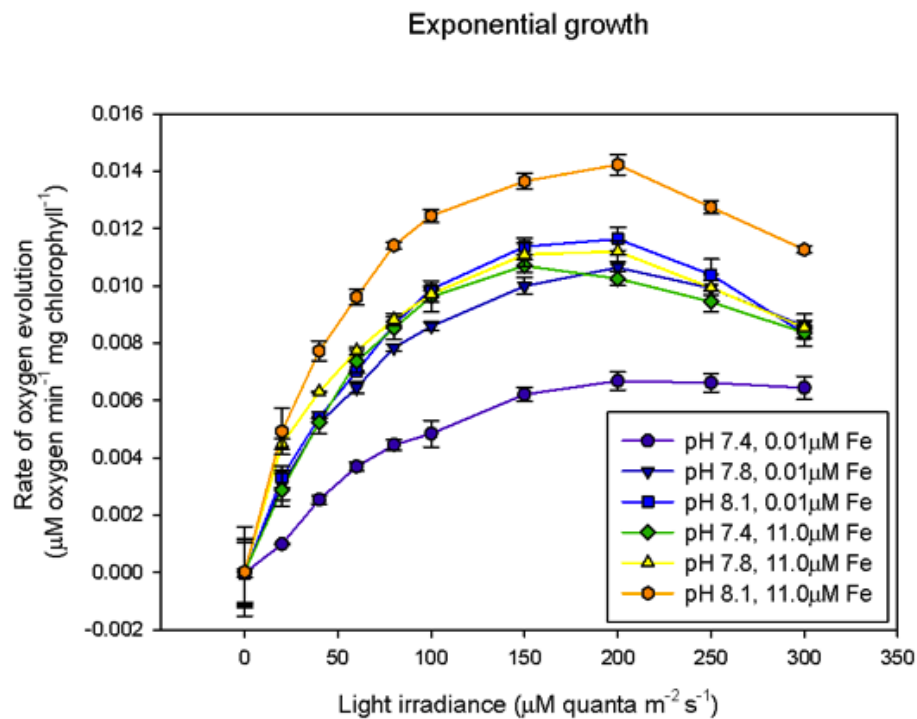


Figure 3.21 Oxygen evolution curve of *T. weissgloffi* CCMP 1051 grown in ESAW medium (880 μM) at varying iron concentrations (0.01 and 11.0 μM) and levels of acidity pH (7.4, 7.8 and 8.1) during: A) exponential growth phase and B) stationary growth phase (n=3).

3.4.6 Nitrogen enrichments on lipid production

Several studies have pointed out the link between overabundant nitrogen enrichment inducing greater cell yield and their interaction with fatty acid biosynthesis (refs). With ESAW + f/2 nutrients containing 880 μM N, it was thought that this N concentration might be too high for the accurate conclusion that potential fatty acid changes to be seen are the result of acidification, and not the lack of carbon available *in vitro* from the N concentration being in abundance. The decision to re-examine phytoplankton physiological effects by moving to a lowered N concentration (in balance with C-enrichment via bicarbonate) were evident. Upon examining the growth curves of *H. akashiwo* NWFSC 503 at various N-concentrations (Fig. 3.22) and observing the differences in cell yield of *H. akashiwo* NWFSC 503 (Table 3.4), an N-concentration of 80 μM was chosen to proceed with fatty acid experimentation. At this concentration, nutrients were limited in a carbon, nitrogen and phosphate ratio of 258:10:1- three nutrients known to induce cell density changes, thereby affecting growth and fatty acid biosynthesis. By limiting N in balance with C and P, one may conclude that any fatty acid changes are the result of ocean acidification pH effects, and not the lack of available carbon due to the overabundance of N.

Nitrogen concentration (μM)	Growth rate (divisions day^{-1})	Yield (cells mL^{-1})
88	0.5695	42940
176	0.5314	117146
441	0.6111	202006
882	0.6206	295080
1764	0.5946	310986

Table 3.4 Growth rate (divisions day^{-1}) and cell yield (cells mL^{-1}) of *H. akashiwo* NWFSC 503 grown in ESAW medium at various initial N concentrations. More details required. At what days were these measurements made? How can the number of divisions/day be essentially the same, but the cell yield be so different?

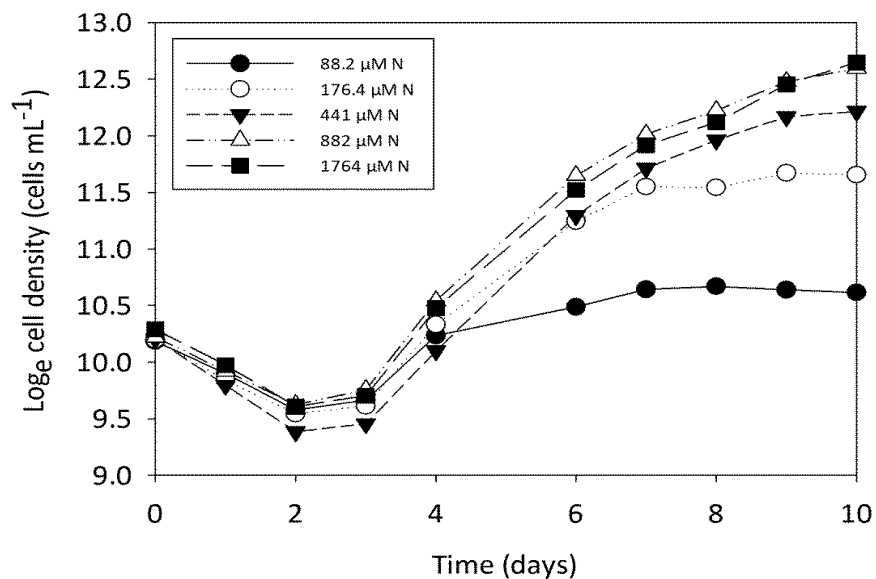


Figure 3.22 Log normalized growth curve of *H. akashiwo* NWFSC 503 grown in ESAW medium +f/2 nutrients at varying N-concentrations (n=1).

As shown in Fig. 3.23, neutral lipid production in *H. akashiwo* NWFSC 503, as measured by the Nile red assay was highest in the low N treatment when the culture was 3 days into its stationary growth phase. As the culture began to senesce, total neutral lipid production decreased. These results reinforced the selection of choosing a low N concentration for future experimentations.

H. akashiwo 503

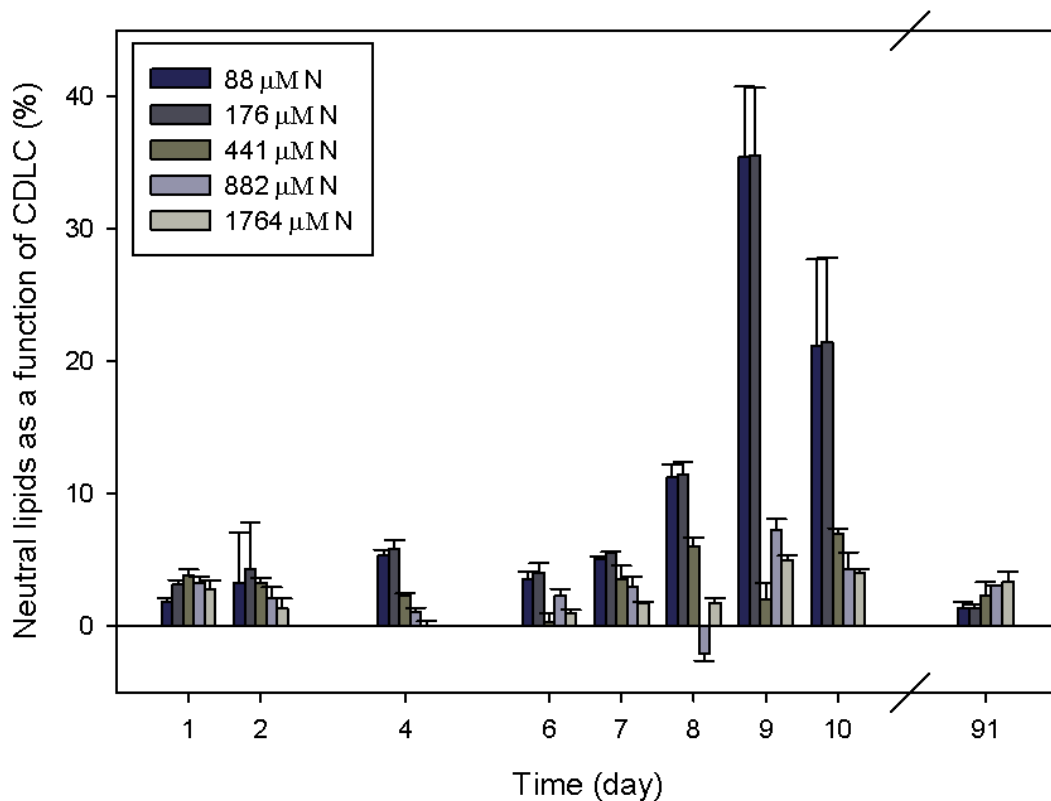


Figure 3.23 Neutral lipid content (% of the Chemically Defined Lipid Concentrate, CDLC) over time in *H. akashiwo* 503 at varying N concentrations. Nitrogen limitation showed a significant effect in enhancing lipid content ($F=14.46$, $Df= 4, 134$, $P= 7.68 \times 10^{-10}$) which also was significant based on day of growth ($F=13.757$, $Df= 9, 134$, $P= 7.68 \times 10^{-15}$).

3.4.7 Low N enrichment on growth and lipid production

The following experiments were conducted with cultures grown in ESAW medium +f/2 nutrients with 80 μM N at a nutrient ratio concentration of C:N:P (258:10:1) based on the nitrogen selection results from section 3.3.6. It is interesting to note the differences in the results with cultures grown at 80 μM N compared to the results from sections 3.3.2-3.3.5, using 880 μM N. With the aforementioned nutrient enrichments, each culture consisted of a treatment of low and high iron (0.01 μM and 11.0 μM , respectively) at a low and high pH (7.4 and 8.1, respectively) that was acidified using the acid/base titration methodology.

3.4.7a Algal growth

There were no growth rate or growth yield differences between any algal isolates examined at any of the iron or pH treatments with the exception of both cyanobacterium isolates examined: *Synechococcus* sp. CCMP 833 and *Synechococcus* sp. CCMP 835 (Fig. 3.24). The cyanobacteria experienced a slower growth rate under the combinational pressures of a pH of 7.4 and an iron enrichment of 0.01 μM compared to all other treatments. Therefore, when N concentrations are low, growth rate and growth yield generally remain unaffected by ocean acidification at varying iron concentrations.

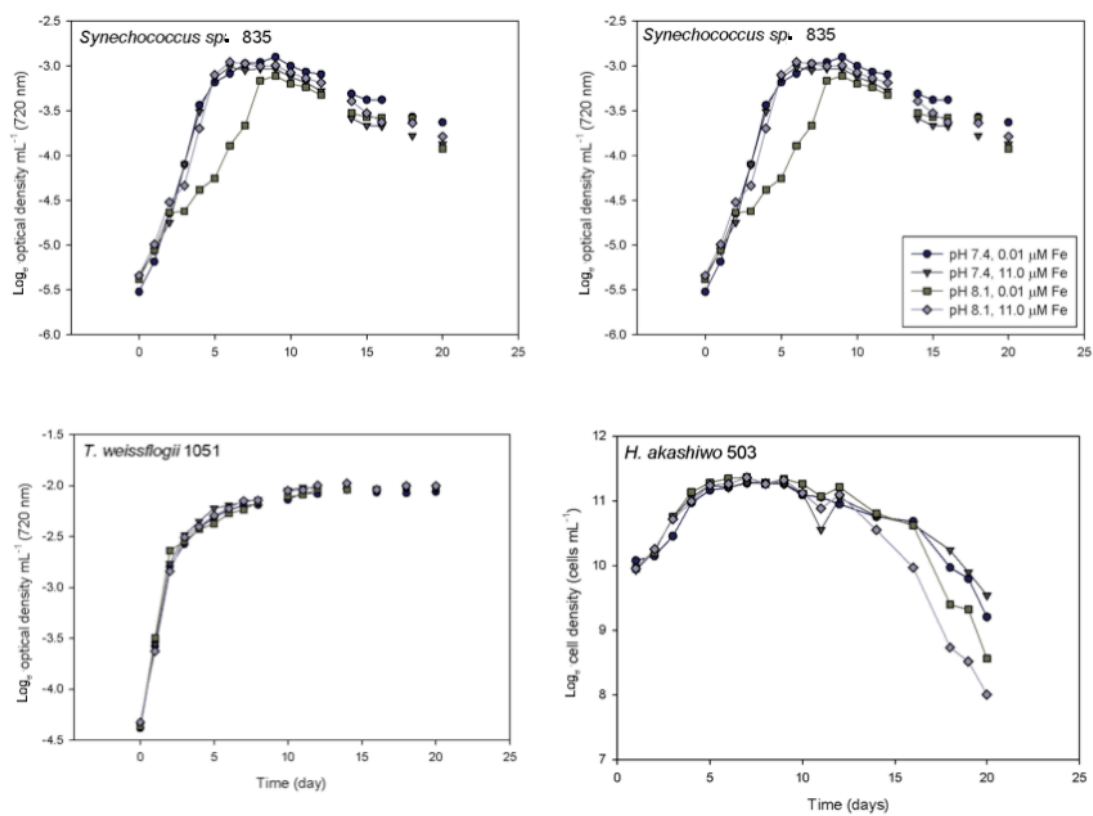


Figure 3.24 Growth curve of *Synechococcus* sp. CCMP 833, *Synechococcus* sp. CCMP 835, *T. weissflogii* CCMP 1051, and *H. akashiwo* NWFSC 503 over a 20-day time period at a low iron concentration of 0.01 μ M, a high iron concentration of 11.0 μ M and a pH of 7.4 and 8.1. Growth rate (α) and yield (β) were not different among treatments, with the exception of a lowered growth rate in *Synechococcus* sp. CCMP 833 and *Synechococcus* sp. CCMP 835 at a pH of 7.4 and 0.01 μ M Fe (n=1 for each treatment).

3.4.7b Chlorophyll production

For all phytoplankton isolates examined, total chlorophyll-*a* production was not different between iron concentrations (0.01 μM and 11.0 μM) at the high or low pH level examined (8.1 and 7.4) (Fig. 3.25). Therefore, when N concentrations are low, acidification does not limit chlorophyll-*a* production, regardless of whether iron is limiting or in excess.

3.4.7c PAM

For all phytoplankton isolates examined, total photochemical (PSII) efficiency was examined using variable over maximal fluorescence (F_v/F_m) and was not drastically different between iron concentrations (0.01 μM and 11.0 μM) at the high or low pH level examined (8.1 and 7.4) (Fig. 3.26). F_v/F_m values were only slightly higher at an iron concentration of 11.0 μM , but this increase is not statistically significant. Therefore, when N concentrations are low, there are no changes in F_v/F_m of phytoplankton during either exponential or stationary growth phases.

3.4.7d Oxygen evolution

Results from the oxygen evolution curves at a lowered N concentration (80 μM N) were similar to the results observed at the higher N concentration (880 μM N) in *T. weissflogii* CCMP 1051 (Fig. 3.27). During exponential growth, treatment with 11 μM iron at a pH of 8.1 resulted in the highest photosynthetic capacity, but during stationary growth, the treatment of 0.01 μM iron at a pH of 7.4 resulted in the highest photosynthetic capacity. Results were similar in both cyanobacterium isolates examined: *Synechococcus* sp. CCMP 833 and *Synechococcus* sp. CCMP 835. (*H. akashiwo* data unavailable.)

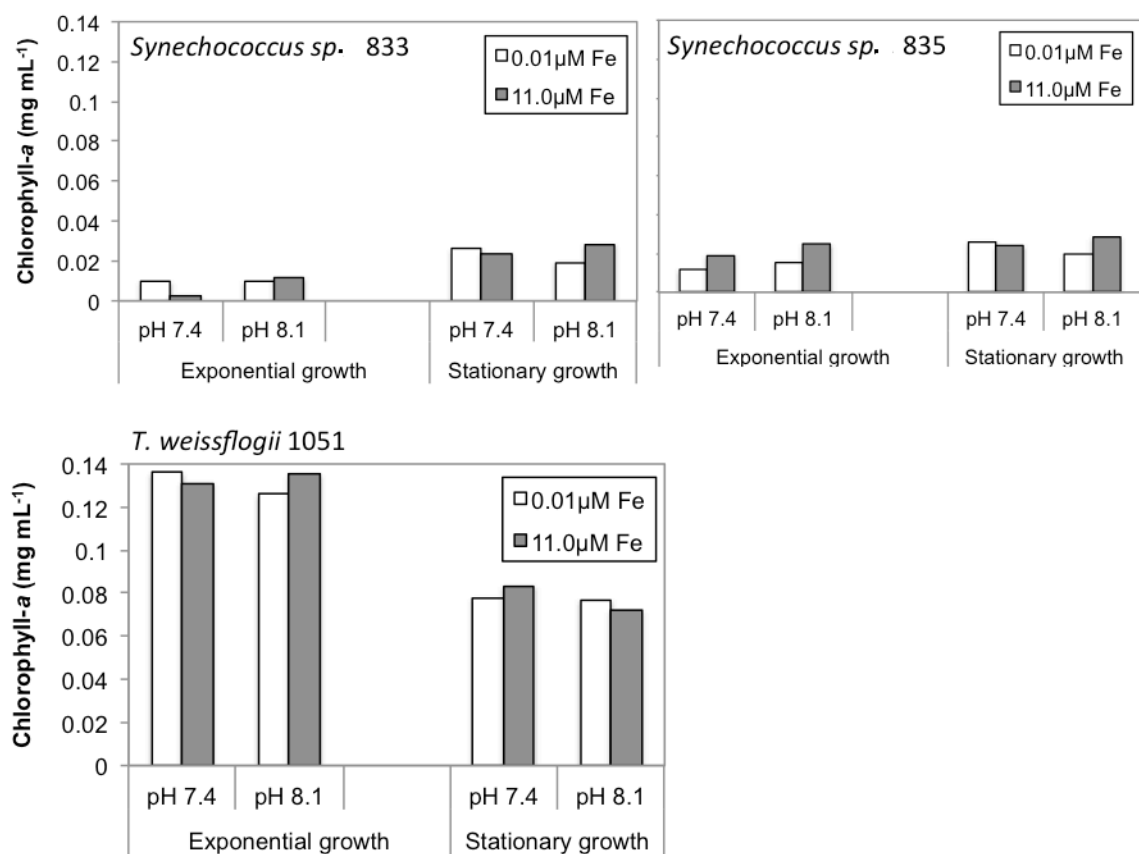


Figure 3.25 Total chlorophyll-a of *Synechococcus* sp. CCMP 833, *Synechococcus* sp. CCMP 835 and *T. weissflogii* CCMP 1051 was not different between the two iron concentrations examined (0.01 μM or 11.0 μM) and between the two pH treatments (7.4 or 8.1) during either the exponential growth period, or the stationary growth period (n=1 for each treatment).

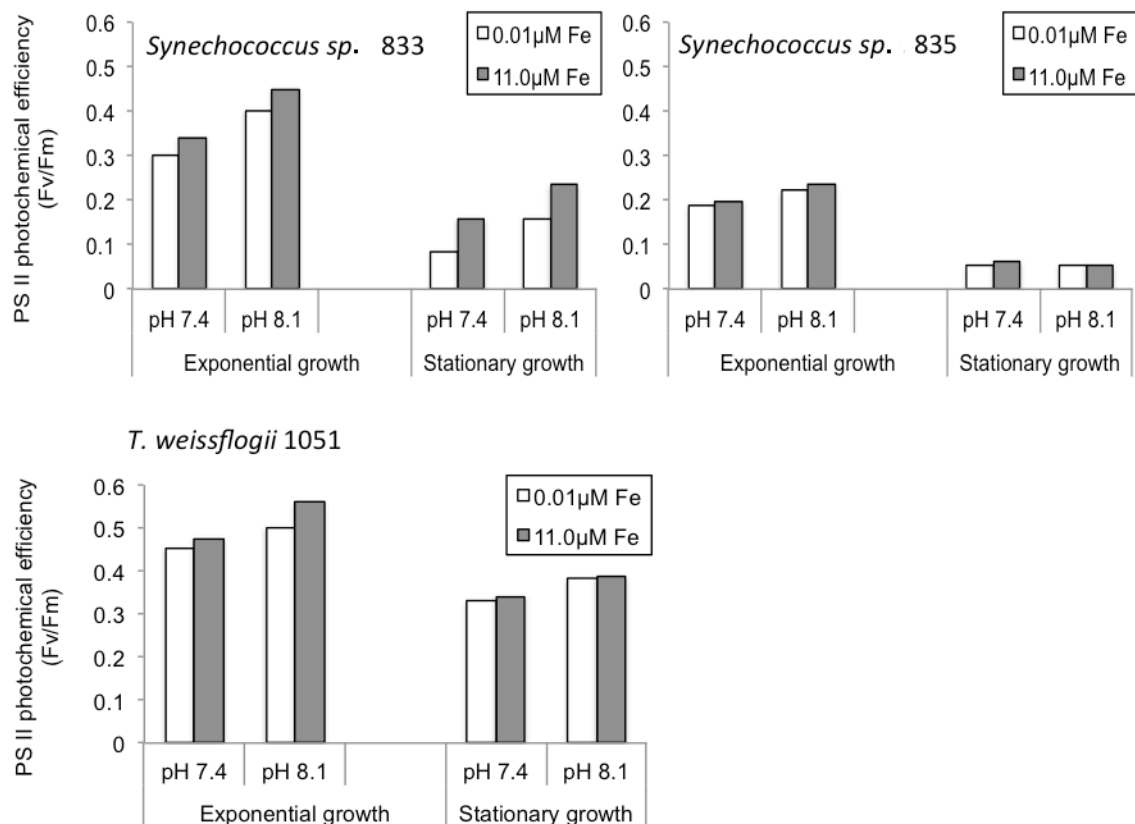


Figure 3.26 PSII efficiency of *Synechococcus* sp. CCMP 833, *Synechococcus* sp. CCMP 835 and *T. weissflogii* CCMP 1051 was not different between the two iron concentrations examined (0.01 μM or 11.0 μM) and between the two pH treatments (7.4 or 8.1) during either the exponential growth period, or the stationary growth period (n=1 for each treatment).

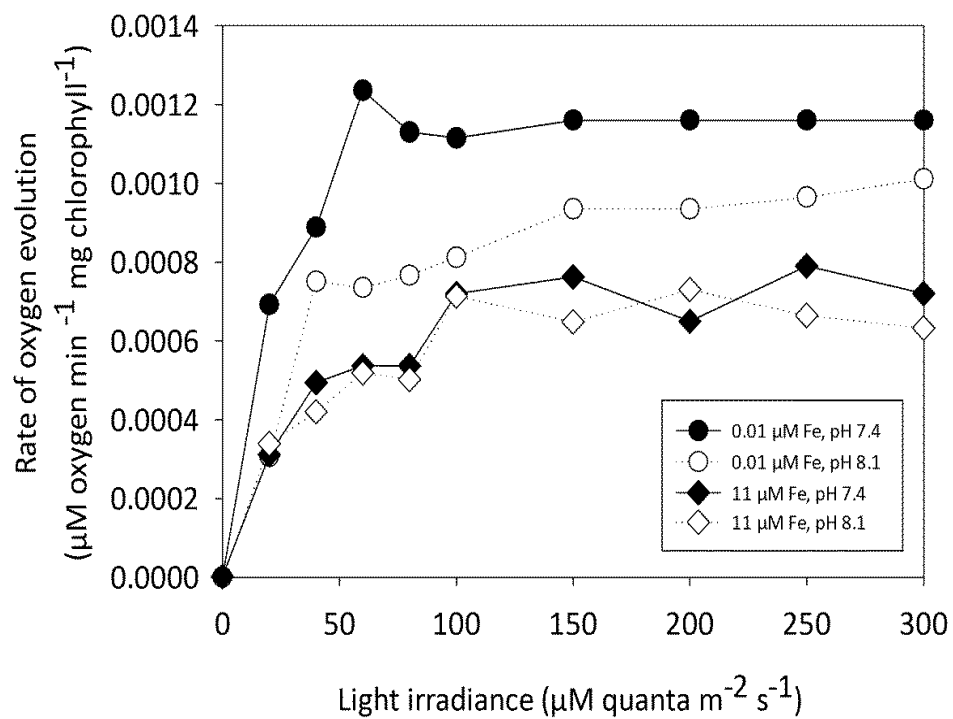


Figure 3.27 Oxygen evolution curve of *T. weissgloffi* CCMP 1051 grown in ESAW medium (80 $\mu\text{M N}$) at varying iron concentrations (0.01 and 11.0 μM) and levels of acidity pH (7.4, 7.8 and 8.1) during: A) exponential growth phase and B) stationary growth phase ($n=1$ for each treatment).

3.4.7e Lipid production

For all phytoplankton isolates examined, neutral lipid production was highest during exponential growth phases at a low iron concentration of 0.01 μM Fe, irrespective of the culture pH, but as the cultures began to shift into their stationary growth, neutral lipid production began to accumulate in cultures that were grown at a high iron concentration of 11.0 μM Fe, irrespective of the culture pH (Fig. 3.28). Therefore, ocean acidification does not appear to change or limit neutral lipid production in phytoplankton, rather, it is the abundance or limitation of iron within the water column that induces these changes in laboratory experiments that use the acid/base acidification methodology.

3.4.8 Examining density changes in acid/base buffered cell cultures

Synechococcus sp. CCMP 833 culture was adjusted to a pH of 7.4, 7.8 and 8.1 with 10% HCl. Fig. 3.29 demonstrated an artifactual change that occurred when cultures were titrated with acid, because the culture with no titrated pH adjustment continued to grow after 6 days whereas the pH adjusted cultures senesced after 4 days of growth. The result exemplified the subliminal changes in phytoplankton ecophysiology that can lead to potential bias in some ocean acidification research conclusions. This result led to the consensus that a truer methodology to manipulate ocean acidification would be to move to a CO₂-bubbling system.

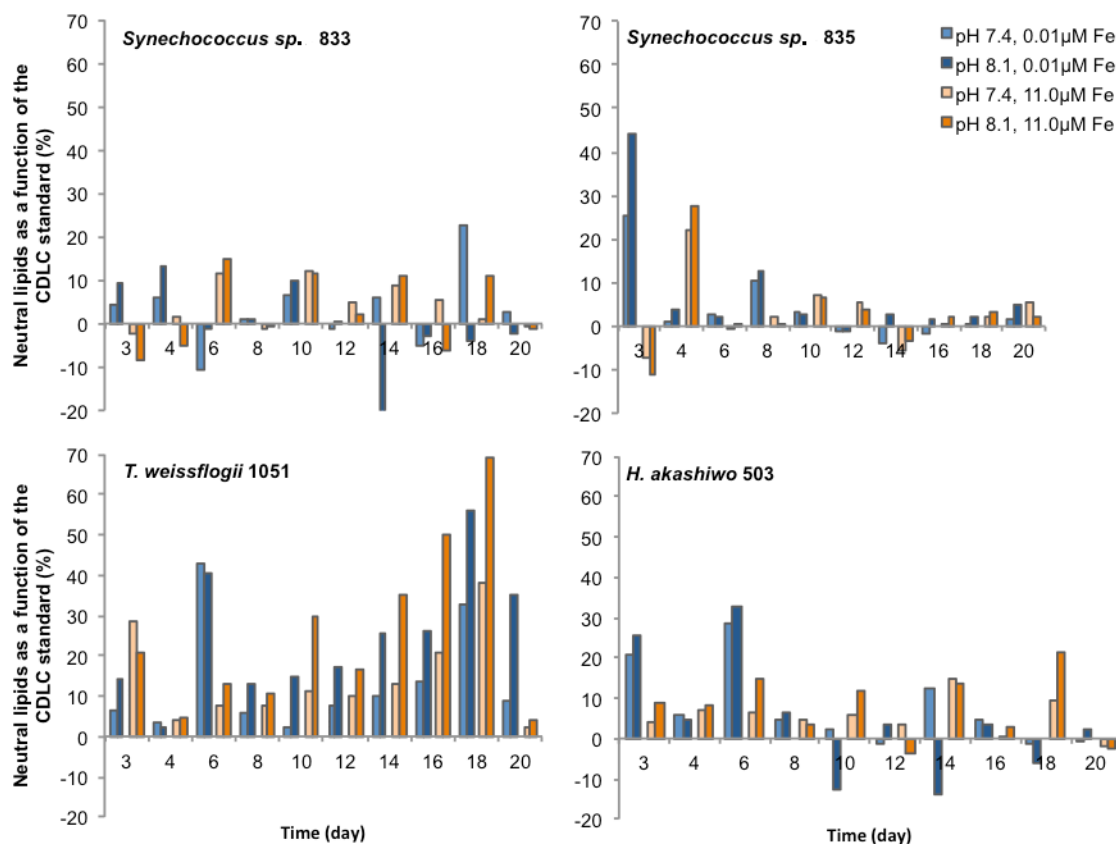


Figure 3.28 Neutral lipid production (as a % of the CDLC) over time in *Synechococcus* sp. 833, *Synechococcus* sp. 835, *T. weissflogii* 1051, and *H. akashiwo* NWFSC 503 over a 20 day time period at a low iron concentration of 0.01μM, a high iron concentration of 11.0μM and a pH of 7.4 and 8.1. Cultures were grown in ESAW medium +f/2 nutrients (80 μM N) (n=1 for each treatment).

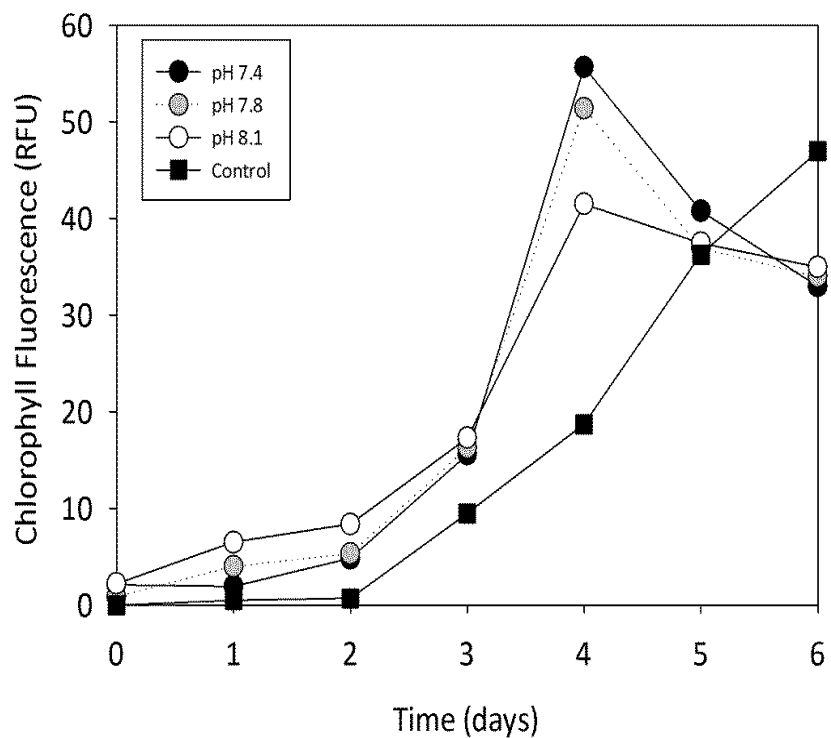


Figure 3.29 Chlorophyll fluorescence was used to quantify cell density changes in *Synechococcus* sp. CCMP 833 grown in ESAW (880 μ M N) with no buffer added, and illustrated that cell cultures with an HCl acidified pH of 7.4, 7.8 and 8.1 have a shorter growth period than cultures that have had no pH manipulation with HCl titration (n=1 for each treatment).

3.5 Discussion

3.5.1 Acid/base buffering

It is worthwhile to note that while some acidification studies that use the acid/base-addition method often do not involve supplementing cultures with a buffering agent, organic buffers are commonly used to control pH in many other phytoplankton studies, and are necessary to reduce variability in culture conditions during long-term experiments (Crawford *et al.* 2011). In this study, the addition of minimal buffer was desired to counter photosynthetic carbon uptake-derived pH changes throughout the life cycle of each species examined. Although it has been suggested that organic buffers may form complexes with metals, reducing availability to phytoplankton, the HEPES buffer used resulted in no apparent change in the growth rate or yield of any species (Shi *et al.*, 2009). HEPES was chosen because it provided no additional nutritional benefit to the culture, and is commonly used for cell cultures that live between a biological pH range of 6-8. These characteristics of HEPES explained its efficiency at maintaining a constant pH under given conditions. Other acid/base-methodology studies that do not supplement cultures with a buffering agent are limited in that they cannot sufficiently state results were due to pH differences. Using the addition of a buffer for acid/base ocean acidification experiments is recommended when employing this methodology. With these factors in mind, Crawford *et al.* (2011) found that high buffer concentrations had adverse effects on the growth rate of a diatom species, where cell densities of buffered cultures were found to be less than unbuffered controls. Therefore, buffering effects may be species specific and alternative approaches to control culture pH, namely CO₂-bubbling, are recommended whenever possible. For this reason, CO₂-bubbling was explored in Chapter 4.

3.5.2 Algal growth kinetics and photosynthetic changes to ocean acidification

Changes in pH affect the availability of nutrients, and this has been proposed to alter the rate of growth and photosynthesis in marine phytoplankton (The Royal Society, 2005). Seasonal changes such as those in temperature and biological productivity (namely, variations in photosynthesis and respiration), contribute to fluctuations in ocean pH (Gonzalez-Davila *et al.* 2003). When examining growth rates under acid/base-addition experiments, Berge *et al.* 2010 noted that a lowered pH neither increased nor decreased growth rates of the phytoplankton species examined in their study: diatoms, dinoflagellates, cryptophytes and haptophytes. These results agree with the steady growth rate results shown herein, where there was no significant difference between growth rates at each of the three pH levels used (7.4, 7.8 and 8.1) for any of the phytoplankton species examined: *Synechococcus* sp. CCMP 833, *Synechococcus* sp. CCMP 835, and *T. weissflogii* CCMP 1051, with the exception of *H. akashiwo* NWFSC 503 that only experienced a decreased growth rate under the combined stresses of low pH and low Fe.

In the photosynthetic species, *Synechococcus* sp. and *H. akashiwo*, the decrease in absolute cell density, growth rate and chlorophyll-*a* did not coincide with a decrease in pH, but rather coincided with a decrease in Fe enrichments only when there was a surplus of N (880 μ M) available to the cells. When N was more limited (80 μ M), there was no difference in the cell density, growth rates, or amount of chlorophyll-*a* produced by the cells at any of the pH or iron enrichments examined- eluding that future ocean acidification will not give *Synechococcus* sp. or *H. akashiwo* a competitive advantage in the new ocean. This result may suggest that pH levels do not change the ability these species to acquire key elements (such as carbon, iron or nitrogen) required for processes like growth and photosynthesis in an upwelling area that is routinely subjected with a

surplus of nutrients and acidified waters. The result can be explained by observations from Lomas *et al.* (2012) and Fu *et al.* (2007), who found small and non-significant effects of decreased pH (using the acid/base buffering method) on *Synechococcus* sp. growth, density and physiological parameters.

Photoautotrophs have developed a number of mechanisms to acclimate to imbalances between pH, light absorption and carbon assimilation. Such mechanisms involve changes to light harvesting complexes, where cells can either decrease the concentration of light harvesting pigments, increase the levels of photoprotective pigments such as xanthophylls and carotenoids, or increase the shading of photosynthetic components by accumulating UV-absorbing pigments (Marshall and Newman 2002; Harris *et al.* 2005; Falkowski and Raven 2007). The effects of high and low Fe enrichments on the cell density (or light harvesting pigments) of *Synechococcus* sp. and *H. akashiwo* were expected. These phytoplankton species adapted to Fe-limiting environments by undergoing physiological and chemical changes such as decreasing light harvesting pigment levels, in order to decrease Fe requirements (Boyer *et al.* 1987; Odom *et al.* 1993; Sherman and Sherman, 1983). This described why more pigment was visible at higher Fe concentrations, even though cell yield was unchanged. Pigment variation among pH levels may also be due to physiological changes to initial pH stress, since cultures were not given time to adapt to pH changes prior to experimentation. It is likely that lower pH levels could have affected the cell's ability to obtain nutrients, in particular iron, therefore more energy was being diverted from light harvesting pigments to nutrient acquisition.

Additionally, HEPES buffer added to cell cultures of *Synechococcus* sp. and *H. akashiwo* could have affected their ability to acquire Fe since it has been suggested that

organic buffers may form complexes with metals, reducing availability to phytoplankton (Shi *et al.*, 2009). This would explain why more pigment was visible when Fe was added to cultures in excess. Iron requirements are slightly higher for *Synechococcus* than pelagic marine species due to their natural coastal marine habitats- environments characterized by a surplus of nutrients (Brand 1991). The iron-poor conditions (0.01 μM FeCl_3 and 0.1 μM FeCl_3) were not as conducive for *Synechococcus* sp. or *H. akashiwo* in achieving the same pigment as the Fe-rich conditions (1.0 μM FeCl_3 and 11.0 μM FeCl_3). When comparing these results to a study on *Synechococcus* sp. using $p\text{CO}_2$ -bubbling, the result showed the opposite trend, where cellular pigment levels, growth rates and photosynthetic capacities were higher in acidified treatments (Fu *et al.* 2007). This difference demonstrates the disparity between the two methods of acidification. Still, pH measurements are known to be a substantial indicator of change in seawater $p\text{CO}_2$ concentrations resulting from CO_2 consumption or gas exchange (Gattuso *et al.* 2010).

In many laboratory studies, evidence for the lack of pH effects on photosynthesis due to changes in CO_2 concentrations has been derived. Many laboratory experiments have involved artificially altering the total inorganic carbon concentrations, the pH value, or both. As a result, the ratios of CO_2 and HCO_3^- do not mimic the change that would be found if atmospheric CO_2 increased (Giordano *et al.* 2005). These experiments, however, are generally performed on a short time frame. When exposed to longer periods of excessive pH and nutrient stressors, more sufficient physiological pathways of light energy dissipation for photosynthesis are utilized, such as: photorespiration (Portis and Parry 2007) or use of NAD(P)H produced from the photosynthetic electron transport chain (ETC) by the enzyme nitrate reductase (NR) (Lomas and Gilbert 1999). Although the use of the reductant NAD(P)H by NR to assimilate nitrate has been proposed, it is

reliant on the abundance of nitrogen in the environment and an increased transcription of NR genes has currently only been observed in diatoms (Parker and Armbrust 2005). Observations of high NR activity in the HAB species, *H. akashiwo* warrants further investigation.

To acclimate to a changed pH environment under an iron-poor scenario, light energy may be diverted away from chlorophyll fluorescence to a process that would aid in acquiring key elements. Badger and Andrews (1982) found that *Synechococcus* sp. diverted more light energy to carbon concentrating mechanisms (CCMs) to acquire inorganic carbon when CO₂ levels were low, rather than fluorescence. This result explains why there was more pigment visible in high pH and iron-rich cultures compared to treatments acidified under iron-limited conditions. The result was further explored by measuring oxygen evolution when both pH and Fe concentrations were examined in combination. While a short term pH response may be demonstrated in this cyanobacterium (that is, a depression of CO₂ fixation at high pH) it has been suggested that *Synechococcus* sp. can rapidly acclimate and up-regulate photosynthetic capacity where pH-dependent responses are no longer evident after only a few days of growth (Lomas *et al.* 2012).

Other studies have suggested that cyanobacteria are able to change their relative affinities for different forms inorganic carbon to undergo photosynthesis depending on the external environment (Badger *et. al* 1981). Therefore, when the environment was iron-limiting, one would expect cells to designate more energy toward acquiring Fe for survival and sacrifice the affinity for carbon resulting in lower photosynthesis, chlorophyll production and growth rates. However, the results presented here show the opposite trend, where photosynthetic capacity was optimal in a combined low pH and Fe

environment for both cyanobacteria examined. Cyanobacteria are known to be capable of using CCMs to store carbon intracellularly. It is possible that the inorganic carbon stored in the cell was either insufficient for optimal photosynthesizing capabilities or the CCM was less efficient for inorganic carbon storage at either an ambient pH environment or when Fe was present in excess. Unlike *Synechococcus* sp. and *H. akashiwo*, the diatom, *T. weissflogii* did not exhibit changes in pigments from pH or Fe alterations, meaning that photoprotective pigments would not likely be affected by ocean acidification under a mosaic of nutrient conditions.

A difference in the response of growth rates to CO₂ does not necessarily translate to similar differences in photosynthetic affinity for CO₂ (Raven *et al.* 1993; Beardall *et al.* 1998). When *Synechococcus* sp. and *H. akashiwo* were grown in media with high and low pH, surprisingly, an increased growth rate and chlorophyll-*a* production was only demonstrated when iron was in excess - which coincided with corresponding changes in photosynthetic activity. As growth rates and total chlorophyll-*a* production remained the same at each pH (but decreased with low iron concentrations), the true photosynthetic capacities must have increased. In other words, there was a higher photosynthetic capacity in cultures that were grown at limiting iron concentrations with a pH of 7.4, a finding that was unexpected. Badger and Andrews (1982) stated that in environments when CO₂ was low (meaning, high pH), more light energy is diverted into the transport of inorganic carbon to the cell since an accumulation of HCO₃⁻ is dependent on light. This being said, lower pH environments would have a negative impact on CCMs for *Synechococcus* sp., as well as resulting in a decrease in light use efficiency. This would result in less accumulation of inorganic carbon within the cell for photosynthesis. With a lack of a constant addition of carbon dioxide (CO₂), *Synechococcus* sp. could have been

limited in the ability to carry out photosynthesis. Since results from the photosynthesis experiments presented here were conducted with an acid/base acidification technique, this is the probable reason why the results are different from Badger and Andrews (1982), who used a CO₂-bubbling technique. These results confirm that the outcomes of ocean acidification studies are dependent on the method used to generate acidic conditions. Since *H. akashiwo* lacks a CCM, explanations cannot be extended to this species and warrants further investigation.

Keeping in mind that a drop in pH represents an increase in H⁺ ion concentrations, the rise in H⁺ ions could alter intracellular pH, membrane potential, energy partitioning and enzymatic activity (Beardall and Raven 2004, Giordano *et al.* 2005). Oxygen evolution rates were predicted to be higher at high pH levels since pH affects the efficiency of CCMs that are most efficient in alkaline environments of 8.2 (Badger 1982). In these optimal alkaline environments, HCO₃⁻ is the primary source for inorganic carbon uptake and intracellular inorganic carbon storage, utilized by cyanobacteria (Badger and Andrews 1982). With an acidified ocean comes a decrease in pH which could result in a decrease in the amount of inorganic carbon available as HCO₃⁻ and, therefore, less inorganic carbon for cell uptake and less efficient photosynthesis.

Diatoms are important for the productivity of our oceans because they contribute roughly 45% of global marine primary production (Mann 1999). For the diatom examined in this study, *T. weissflogii*, there were no difference in growth rates, cell yield, photosynthetic efficiency (F_v/F_m), chlorophyll production, or fluorescence at any pH level examined regardless of the Fe or N nutrient enrichment. There was only an elevated maximal photosynthetic capacity from cell cultures grown in ambient pH (8.1) at a high Fe concentration, but no changes were found in photosynthetic efficiencies of any

treatments. These findings are supported by a study on *T. pseudonana* where Crawford *et al.* (2011) found that under an elevated pCO₂ of 760 µ-atm (equivalent to pH 7.8) compared to the ambient pCO₂ 380 µ-atm (equivalent to pH 8.1), there was no change detected in photosynthetic efficiency (F_v/F_m). The similarities between the results from the two studies confirm that this diatom species will not likely be at a disadvantage in the acidifications conditions predicted for the future ocean. However, the real question lies within the species intracellular carbon sequestration pathway. In the future ocean, is *T. weissflogii* able to accumulate sufficient lipids that would benefit the marine food web, compared to *Synechococcus* sp. and *H. akashiwo*?

3.5.3 Lipid production response to ocean acidification

Our present understanding of ocean acidification impacts for food web interactions are limited. Indirect effects of ocean acidification on higher marine organisms can be expected for consumers by changing the intracellular nutritional quality of their prey, being phytoplankton. Although increasing atmospheric CO₂ can stimulate carbon fixation by photosynthetic algae, it is the nutrient content relative to the carbon content that determines the quality of food available for trophic transfer since essential fatty acids (EFA), such as DHA and EPA, cannot be produced by heterotrophic organisms and must be obtained through diet (Urabe *et al.* 2003; Engel *et al.* 2008; Bellerby *et al.* 2008). DHA and EPA production were not found to be the prevalent fatty acids produced by phytoplankton under elevated CO₂ (low pH). Rather, it was neutral (or saturated lipids) that accumulate under an acidic ocean regime predicted for the future ocean. However, it will be necessary to complete a fatty acid profile of cultures grown under different conditions of acidity, iron and N to confirm this observation.

A study by Rossoll *et al.* (2012) found that there was a significant decline in total EFAs under elevated CO₂ (low pH) in the diatom *T. pseudonana* compared to present-day ambient pH. Additionally, the study found a decrease in copepod growth and egg production, from 34 to 5 eggs per female per day under elevated CO₂ (low pH). Since copepods play a critical role in the diets of fish, changes in growth and egg production has serious ramifications for the productivity of marine fisheries. Results can be extended here, where *T. weissflogii* – that exhibited no changes in growth rates under low pH – showed a decline in lipid production under low pH (7.4). These results were compounded by low Fe enrichments. A plausible explanation can be attributed to the notion that high environmental *p*CO₂ (low pH) decreases the internal cell pH, therefore the increased amount of fatty acids could be a mechanism to control the internal cellular pH (Mayor *et al.* 2007; Rossoll *et al.* 2012). This mechanism, however, is poorly understood. Results presented here suggest that when N became depleted, an increase in intracellular lipids resulted. It would be interesting to assess if excess nitrogen can mitigate the negative effects of lipid accumulation in phytoplankton. This idea can be a starting point for future investigations. Overall, this experiment showed that lipid production was only elevated for the diatom *T. weissflogii*. *Synechococcus* sp. and *H. akashiwo* did not demonstrate a drastic increase in lipid production under any pH condition, meaning that *T. weissflogii* may play an important role in marine food web dynamics under increased CO₂ conditions, whereas *Synechococcus* sp. and *H. akashiwo* may represent poorer food choices in the future ocean.

Most of the experiments conducted on marine phytoplankton have been short term and have not provided sufficient time for any genetic modifications that might allow them

to adapt to the changing ocean conditions. Further long-term experiments are required to determine if the organisms will evolve to take advantage of the increased CO₂.

3.6 References

- Anderson, D.M., Glibert P.M., Burkholder, J.M. 2002. Harmful algal blooms and eutrophication: Nutrient sources, composition, and consequences. *Estuaries*. **25**: 704-726.
- Apple, J.K., Strom, S.L., Palenik, B., and Brahamsha, B. 2011. Variability in protest grazing and growth on different marine *Synechococcus* isolates. *Appl. Environ. Microbiol.* **77**: 3074-3084.
- Badger, M.R. and Andrews, T.J. 1982. Photosynthesis and inorganic carbon usage by the marine Cyanobacterium, *Synechococcus* sp. *Plant Physiol.* **70**: 517-523.
- Bellerby, R.G.J., Schulz, K.G., Riebesell, U., Neill, C., Nondal, G. 2008. Marine ecosystem community carbon and nutrient uptake stoichiometry under varying ocean acidification during the PeECE III experiment. *Biogeosci.* **5**: 1517–1527.
- Berges, J.A., Franklin, D.J. and Harrison, P.J. 2001. Evolution of an artificial seawater medium: Improvements in enriched seawater, artificial water over the last two decades. *J. Phycol.*, **37**: 1138-1145
- Burkhardt, S., Amoroso, G., Riebesell, U., Sültemeyer, D., 2001. CO₂ and HCO₃ uptake in marine diatoms acclimated to different CO₂ concentrations. *Limnol. Ocean.* **46**: 1378-1391.
- Burkholder, J.M., 1998. Implications of harmful microalgae and heterotrophic dinoflagellates in management of sustainable marine fisheries. *Ecol. Appl.* **8**: 37–62.
- Capone, D.G., Burns, J.A., Montoya, J.P., Subramaniam, A. 2005. Nitrogen fixation by *Trichodesmium* spp.: an important source of new nitrogen to the tropical and subtropical North Atlantic Ocean. *Global Biogeochem. Cycles*. **19**: 20-24.
- Crawford, K.J., Raven, J.A., Wheeler, G.L., Baxter, E.J. and Joint, I. 2011. The response of *Thalassiosira pseudonana* to long-term exposure to increased CO₂ and decreased pH. *PLoS ONE*. **6**: 26-95.
- Elzenga, J.T.M., Prins, H.B.A., and Stefels, J., 2000. The role of extracellular carbonic anhydrase activity in inorganic carbon utilization of *Phaeocystis globosa* (Prymnesiophyceae): a comparison with other marine algae using the isotopic disequilibrium technique. *Limnol Ocean* **45**: 372-380.
- Engel, A., Schulz, K.G., Riebesell, U., Bellerby, R. and Delille, B. 2008. Effects of CO₂ on particle size distribution and phytoplankton abundance during a mesocosm bloom experiment (PeECE II). *Biogeosci.* **5**: 509–521.
- Feely, R.A., Sabine, C.L., Hernandez-Ayon, J.M., Ianson, D. and Hales, B. 2008. Evidence for upwelling of corrosive "acidified" water onto the continental shelf. *Science* **320**: 1490-1492.

- Fu, F.X., Warner, M.E., Zhang, Y., Feng, Y. and Hutchins, D.A. 2007. Effects of increased temperature and CO₂ on photo- synthesis, growth and elemental ratios of marine *Synechococcus* and *Prochlorococcus* (Cyanobacteria). *J. Phycol.* **43**: 485–496.
- Fu, F.X., Zhang, Y. M. E., Warner, M.E, Feng, Y., Sun, J. and Hutchins, D.A. 2008. A comparison of future increased CO₂ and temperature effects on sympatric *Heterosigma akashiwo* and *Prorocentrum minimum*. *Harmful Algae* **7**: 76–90.
- Guillard, R.R.L. and Ryther, J.H. 1962. Studies of marine planktonic diatoms. I. *Cyclotella nana* Hustedt and *Detonula confervacea* Cleve. *Can. J. Microbiol.* **8**: 1-14.
- Guillard, R.R.L. 1973 Division rates, p. 289-312. *In* Stein, J.R. [ed.] Handbook of Phycological Methods: Culture Methods and Growth Measurements. Cambridge University Press, Cambridge.
- Guillard, R.R.L. 1975. Culture of phytoplankton for feeding marine invertebrates, p. 26-60. *In* Smith W.L. and Chanley M.H [Eds.] *Culture of Marine Invertebrate Animals*. Plenum Press, New York, USA.
- Hallegraeff, G.M., 1993. A review of harmful algal blooms and their apparent global increase. *Phycologia* **32**: 79–99.
- Hallegraeff, G.M. 2010. Ocean climate change, phytoplankton community responses, and harmful algal blooms: a formidable predictive challenge. *J. Phycol.* **46**: 220–235.
- Harrison, P.J., Waters, R.E. and Taylor, F.J.R. 1980. A broad spectrum artificial seawater medium for coastal and open ocean phytoplankton. *J. Phycol.* **16**: 28-35
- Hein, M., Sand-Jensen, K., 1997. CO₂ increases oceanic primary production. *Nature* **388**: 526-527.
- Held, P. and Raymond, K. 2011. Determination of Algal Cell Lipids Using Nile Red. Winooski, Vermont, USA: BioTek Instruments, Inc.
- Hutchins, D.A., Mulholland, M.R. and Fu, F.X. 2009. Nutrient cycles and marine microbes in a CO₂-enriched ocean. *Oceanography* **22**:128–145.
- Lomas, M.W. and Glibert, P.M. 1999. Temperature regulation of nitrate uptake: A novel hypothesis about nitrate uptake and reduction in cool-water diatoms. *Limnol. Ocean.* **44**: 556-572.
- Lomas, M.W., Hopkinson, B.M., Losh, J.L., Ryan, D.E., Shi, D.L., Xu, Y. and Morel, F.M.M. 2012. Effect of ocean acidification on cyanobacteria in the subtropical North Atlantic. *Aquat. Microb. Ecol.* **66**: 211-222.

- Mayor, D.J., Matthews, C., Cook, K., Zuur, A.F., Hay, S. 2007 CO₂-induced acidification affects hatching success in *Calanus finmarchicus*. *Mar. Ecol. Progr. Ser.* **350**: 91–97.
- Moore, S.K., Mantua, N.J., Hickey, B.M., Trainer, V.L. 2009. Recent trends in paralytic shellfish toxins in Puget Sound, relationships to climate, and capacity for prediction of toxic events. *Harmful Algae* **8**: 463–477.
- Morgan-Kiss, R.M., Ivanov, A.G., Huner, N.P.A. 2002. The Antarctic psychrophile *Chlamydomonas subcaudata*, is deficient in state I–state II transitions. *Planta*. **214**: 435–445.
- Nimer, N.A., Iglesias-Rodriguez, M.D. and Merrett, M.J., 1997. Bicarbonate utilization by marine phytoplankton species. *J. Phycol.* **33**: 625-631.
- Parker, M.S. and Armbrust, E.V. 2005. Synergistic effects of light, temperature, and nitrogen source on transcription of genes for carbon and nitrogen metabolism in the centric diatom *Thalassiosira pseudonana* (Bacillariophyceae). *J. Phycol.* **41**: 1142-1153.
- Portis, A.R. and Parry, M.A.J. 2007. Discoveries in rubisco (ribulose 1,5-bisphosphate carboxylase/oxygenase): a historical perspective. *Photosynth. Res.* **94**: 121-143.
- Riebesell, U. 2004 Effects of CO₂ enrichment on marine phytoplankton. *J. Oceanogr.* **60**: 719–729.
- Riebesell, U. and Tortell, P.D. 2011. Effects of ocean acidification on pelagic organisms and ecosystems. p. 291-311. *In* Gattuso, J.P., Hansson, L. [Eds.], *Ocean Acidification*. Oxford University Press, New York.
- Reinfelder, J.R., Kraepiel, A.M.L. and Morel, F.M.M. 2000. Unicellular C₄ photosynthesis in a marine diatom. *Nature* **407**: 996-999.
- Rost, B., Zondervan, I. and Wolf-Gladrow, D. 2008. Sensitivity of phytoplankton to future changes in ocean carbonate chemistry: current knowledge, contradictions and research directions. *Mar. Ecol. Progr. Ser.* **373**: 227-237.
- Trimborn, S., Wolf-Gladrow, D.A., Richter, K.U. and Rost, B. 2009. The effect of pCO₂ on carbon acquisition and intracellular assimilation in four marine diatoms. *J. Exp. Marine Biol. Ecol.* **376**: 26-36.
- Tortell, P.D., Rau, G.H. and Morel, F.M.M. 2000. Inorganic carbon acquisition in coastal Pacific phytoplankton communities. *Limnol. Oceanogr.* **45**: 1485-1500.
- Urabe, J., Togari, J., and Elser, J.J. 2003. Stoichiometric impacts of increased carbon dioxide on a planktonic herbivore. *Global Change Biol.* **9**: 818–825.

Wu, Y.P., Gao, K.S. and Riebesell, U. 2010. CO₂-induced seawater acidification affects physiological performance of the marine diatom *Phaeodactylum tricornutum*. *Biogeosci.* **7**: 2915-2923.

CHAPTER 4

4. The combined effects of pH and pCO₂ on the growth and photosynthetic capacity of *Heterosigma akashiwo*

4.1 Introduction

Harmful algal blooms (HABs) have become an international concern over the past few decades, as the number of HAB events with resulting ecologic and economic consequences has increased in frequency (Anderson 1989). In particular, *Heterosigma akashiwo* blooms have been a concern because of their ability to kill fish, thus, negatively impacting our lucrative fisheries. The mechanism causing these blooms, however, is still unknown. It has been suggested that a lack of a carbon concentrating mechanism (CCM) in *H. akashiwo* might result in an increase in HAB events with the predicted rise in temperature and CO₂ expected in the future from anticipated global warming and ocean acidification (Nimer *et al.* 1997; IPCC 2007).

The oceans have been the primary sink for anthropogenic CO₂, and as more CO₂ dissolves in the seawater, increasing the DIC pool, the primary form of DIC is expected to shift equilibrium from HCO₃⁻ and CO₃²⁻ to CO₂ and HCO₃⁻ while CO₃²⁻ will decrease to coincide with the drop in pH (Zeebe and Wolf-Gladrow 2001). While this change has been shown to be detrimental for marine calcifying organisms, it is generally thought that phototrophs/phototrophic phytoplankton will not be limited by carbon because of the larger DIC pool available in seawater. Despite this expected outcome, growth and photosynthesis have been shown to be sensitive to CO₂ enrichment in diatoms, chlorophytes, cyanobacteria, and raphidophytes (Riebesell *et al.* 1993; Gordillo *et al.* 2003; Fu *et al.* 2007; Fu *et al.* 2008). This has been attributed to the low affinity of the primary carboxylating enzyme RuBisCo for CO₂. For example, Rost *et al.* (2003) found

that certain species of bloom forming algae are close to carbon saturation under present-day CO₂ levels because of their efficient CCMs. For species such as *H. akashiwo* that lack a highly effective CCM, increasing DIC might allow for increases in growth and photosynthesis, which would reduce the competitive advantage of phytoplankton that use CCMs, therefore possibly changing the phytoplankton community (Raven 1991). However, the underlying processes of ocean acidification might be strongly influenced by nutrients, temperature, light and salinity, as demonstrated in Chapters 2 and 3.

Within the scientific community, there is currently no consensus on the optimal method for manipulating ocean acidification events within a laboratory setting. There is considerable debate regarding the various methods of pH adjustment: acid/base buffering or bubbling CO₂ gas, and which method is best to apply. Notably, methods would differ depending on the objective of the study and the organism in question. With the two most commonly used methods, there is considerable evidence supporting that a *p*CO₂ type of system as most representative of a natural environmental acidification scenario, while other studies report that an acid/base manipulation type of system is sufficient for most purposes (Gattuso and Lavigne 2009; Shi *et al.* 2009). Both methods were examined and can have different effects on the carbonate system of seawater, which was anticipated to result in contradictory results. For instance, adding a biologically benign buffer to an acid (or base)-adjusted culture would control pH, and is advantageous as it would leave the amount of DIC constant when it becomes depleted during culture growth, but lower total alkalinity and pH. However, bubbling *p*CO₂ gas would change the DIC, but has the advantage of maintaining constant culture total alkalinity, yet increases total CO₂ and lowers pH (Hurd *et al.* 2009; Schulz *et al.* 2009; Shi *et al.* 2009). Therefore, acid/base methodology experiments are suggested to be advantageous to use when examining non-

calcifying organisms where saturation states are no concern, however, cell growth using this method is limited by a designated CO₂ concentration and may be problematic, as this change is not expected under a true ocean acidification scenario. CO₂-bubbling experiments are optimal to employ when examining calcifying organisms that rely on calcite and aragonite saturation states, which are dependent on stable alkalinity and steady carbonate concentrations and is more representative of the predicted future climatic change event (Berge *et al.* 2010). It is accepted that phytoplankton use HCO₃⁻ as their main source of carbon, therefore, the difference in total CO₂ between the two methods employed is suggested to represent only a small difference in HCO₃⁻ concentrations, which is suggested to not affect growth or photosynthesis (Brewer 1997; Hurd *et al.* 2009).

Fluctuations in ocean carbon chemistry with the resulting changes in HABs can influence the health and vigor of our marine ecosystem. With increases in HAB events over the past millennium, there is absolute need to assess the cause and dynamics of bloom formation. This Chapter outlines growth and photosynthetic capacity changes of one *H. akashiwo* isolate under the combined effects of low pH and high CO₂ expected under our global climate change scenario, using a CO₂ bubbling approach to creating an acidic environment.

4.2. Materials and methods

4.2.1 Phytoplankton species selection

The flagellated algal raphidophyte species used in this experiment, *Heterosigma akashiwo* NWFSC 513, was isolated from the waters of Clam Bay, Washington (June 16, 2010). Individual cells were physically isolated from the natural community by Brian Bill

(National Marine Fisheries Service, NOAA). This strain was maintained as uni-algal, non-axenic cultures throughout all experimentation.

4.2.2 *Heterosigma akashiwo* culturing conditions

Cultures of *H. akashiwo* NWFSC 513 were maintained in batch cultures of Enriched Seawater Natural Water (ESNW) medium (Guillard 1975, Appendix I), prepared with 0.2 µm Whatman polyethersulfone sterile-filtered seawater collected from Half-Moon Bay, California, USA (2010). Seawater salinity was measured with a YSI Incorporated 85D Meter, and found to be at 33.6 Practical Salinity Units (PSU).

ESNW seawater enrichment was amended with 200 µM of nitrate (NaNO₃) and 12.12 µM of phosphate (K₂HPO₄), to provide the optimal nitrogen to phosphate drawdown ratio of 16.5:1 at 20°C for the maximal growth of this algal species (Ikeda, unpublished results). Additional nutrient additions were provided (Appendix I), with the notable exception of iron, which was not added pre-experimentation.

Cultures were grown and maintained in a SANYO Versatile Environmental Test Chamber on a 12:12 h, light:dark cycle, with cool white lights at an intensity of 265 µmol photons m⁻² s⁻¹ (as measured with a QSL 101 light meter made by Biospherical instruments). Temperature was maintained at 20 ± 0.05 °C. Cells were acclimated for 14 days in medium adjusted to either an ambient seawater pH of 8.1 (representing the average current ocean pH) or an acidified seawater medium at a pH of 7.4 (representing predicted future oceanic pH for the year 2100), prior to all experimentation (Feely *et al.* 2008).

4.2.3 Seawater acidification and carbonate chemistry measurements

4.2.3a Monitoring pH and acidification using pCO₂ bubbling

The pH of the medium in the experimental cultures was monitored and recorded every 2 seconds, and regulated using the Queen's University Biological Instrumentation and Technology (QUBIT) D207 pH and pCO₂ Regulation System, by Loligo Systems (QUBIT Systems, Ontario, Canada). Each culture was individually controlled with a pH 3310 instrument meter and a WTW SenTix pH probe that was directly submerged in experimental cultures to continually monitor and record culture pH conditions throughout the duration of all experimentations. This automated feedback system determined pCO₂ indirectly as a function of culture pH, and regulated the release of 15% CO₂ gas that was routed through a series of computer-controlled solenoid valves. Bubbling cultures with pCO₂ gas changed the dissolved inorganic carbon (DIC) concentration, but maintained alkalinity- a change concomitant to our present-day climatic change conditions. The flow rate of CO₂ gas was held constant with Cole Palmer flow meters at $3.0 \pm 0.05 \text{ mL min}^{-1}$, where the CO₂ gas was then diffused through a glass sparger submerged directly into the experimental culture, keeping the culture at the desired pH levels of 7.4 ± 0.1 and 8.1 ± 0.1 to ensure pH shifts were no larger than those expected *in situ*. The windows CapCTRL software (Loligo Systems) monitored the calibrated values for pH in a real-time plot (pH vs. time) and controlled pH set-point levels automatically. With this setup (see diagram Appendix II), the two desired levels of pH remained stable during all experimentation at the precision level needed for the study. The pH of cultures were monitored daily using freshwater probes, and the colorimetric spectrophotometric method for correcting to representative seawater pH values using temperature, salinity and the Seacarb R-script code created by the Dickson laboratory (Scripps Institution of Oceanography, San Diego, CA) was used to determine true seawater pH values for three given time points during all

experimentation: the initial experiment commencement, exponential growth, and the third day of stationary growth.

4.2.3b Colorimetric pH measurements

Acidification followed recommended procedures from Dickson *et al.* (2007). Samples (30 mL) were collected and filtered through a 0.45 μm Millipore syringe driven filter unit fixed with an 8 cm silicon tube. The silicon tube was placed at the bottom of an acid-washed 20 mL glass scintillation vial and filtered through the silicon tube where excess sample was allowed to overflow from the vial to eliminate any potential bubbling or interaction with ambient air that could influence the carbonate chemistry of the sample. Samples were then sealed with an inverted poly-cone cap to ensure no headspace in the sample vial and stored in a water bath at a fixed temperature of 25°C and analyzed spectrophotometrically within a few hours following the procedure outlined in the Standard Operating Procedure (SOP) 6b Version 3.01 (Dickson *et al.* 2007) to alleviate any artifactual changes that might occur over time to obtain the pH of the seawater samples colorimetrically. Accuracy of the pH measurements was determined with a Tris buffer Certified Reference Material (CRM) from Dr. Andrew Dickson of Scripps Institution of Oceanography (Appendix III). The accuracy of the direct colorimetric pH measurement was a function of the chemical properties of the *m*-cresol purple indicator dye, not on the calibration of standards. For this reason, colorimetric measurements of pH were used alongside measurements of DIC to monitor the progress of ocean acidification (Appendix IV).

4.2.3c Dissolved Inorganic Carbon (DIC) determination

Samples (30 mL) for DIC determination were filtered through a 0.45 μm Millipore syringe driven filter unit fixed with an 8 cm silicon tube. The silicon tube was placed at

the bottom of an acid-washed 20 mL combusted (450°C for 6 hours) glass scintillation vial and filtered through the silicon tube where excess sample was allowed to overflow from the vial to eliminate any potential bubbling or interaction with ambient air that could influence the DIC of the sample. The samples were then immediately preserved with 300 μ L of 5% w/v mercuric chloride (HgCl_2) and sealed with an inverted poly-cone cap to ensure no headspace in the sample vial (Parker *et al.* 2006). Sample vials were stored in the dark at room temperature

DIC was measured in the Dugdale-Wilkerson laboratory at the Romberg Tiburon Center for Environmental Studies (SFSU) with an acid-sparging non-dispersive infrared (NDIR) gas analyzer developed at the Monterey Bay Aquarium Research Institute, MBARI (Friederich *et al.* 2002). Each scintillation vial provided treatments that were averaged to determine the measured DIC. Precision of the measurements was determined by comparing values with standard analytical material (CRM from Dr. Andrew Dickson of Scripps Institution of Oceanography).

4.2.4 Experimental design: Iron replete and deplete experiment

The culture medium with amendments was designed to allow cell growth until nitrogen was consumed and growth rates were reduced to 0-division cultures (representing nitrogen limited cultures). For this experiment, treatment cultures were conducted in duplicates (to obtain a sample size of $n=2$) and were inoculated at a modest cell density (200 μ M particulate nitrogen starting concentration) to ensure they were nitrogen limited, as expected *in situ*. The iron content of the medium was modified to provide both an iron (Fe) –replete and Fe-deplete medium, to represent an upwelling regime that is nutrient rich and nutrient poor. The Fe-replete cultures contained an optimal Fe final concentration of 6.6 μ M, whereas the Fe-deplete cultures contained no

added Fe stock solutions, yet a 100 nM final desferrioxamine-B (DFB) concentration was added to chelate and remove any Fe that might be found in the filtered natural seawater used to prepare the medium (the DFB concentration used was chosen based on the results from a preliminary experiment; Appendix V). The chelated-iron does not remove iron from the seawater but the complex is energetically less available to the growth needs of the cells, resulting in iron-limited cellular growth. The Fe-replete medium and Fe-deplete medium were both split in half to be inoculated with pre-acclimated *H. akashiwo* NWFSC 513 cultures to a pH condition of 7.4 and a pH condition of 8.1. Each experimental culture was then mixed gently, ensuring minimal cellular lysis, and inoculated to 5L volumes in autoclaved 6L round, flat-bottom Pyrex boiler flasks. All labware used for experimentation was cleaned according to Appendix VI to deduce the risk of iron and nitrogen contamination. Flasks were placed on a stir plate (Corning Stirrer, Scholar 171) and stirred constantly at 60 RPM in the SANYO Versatile Environmental Test Chambers on a 12h:12h, light: dark cycle with cool white lights at an intensity of 265 $\mu\text{mol photons m}^{-2}\text{s}^{-1}$, and at a constant temperature of $20\pm0.05^{\circ}\text{C}$.

Bubbling cultures with CO_2 (gas) changed dissolved inorganic carbon (DIC) but maintained alkalinity, consistent with natural climate change effects. Each flask contained a SenTix pH probe (calibrated and cleaned both before and during the experiment, according to Appendix VII) and through direct 15% pCO_2 (gas) bubbling, QUBIT Systems maintained the pH of treatment cultures at 7.4 ± 0.1 and 8.1 ± 0.1 , in replicates for both the Fe-replete and Fe-deplete conditions (replicates meaning, duplicates of each of the following treatments: pH 7.4+Fe, pH 8.1+Fe, pH 7.4+DFB and pH 8.1+DFB). To verify the parameters of the carbonate system for each experimental flask, colorimetric pH measurements, salinity and DIC measurements were taken at 3 time points: 24 hours

after experimental inoculation (lag phase), exponential (nutrient replete phase), and stationary (nutrient deplete phase).

4.2.5 Methods of analyses: growth measurements

Cell biomass for all experiments was measured by direct cell counts via microscopy, flow cytometry cell counts and cell chlorophyll fluorescence.

4.2.5a Cell counts

Prior to performing cell counts, a 0.5 mL subsample of each experimental culture was pipetted into 8 mL FloTubes™ in a sterile laminar flow hood. Direct cell counts were performed using a Sedgewick-Rafter to calculate cell density (cells mL⁻¹) using an Olympus IX83 Microscope during the exponential and stationary growth phases. Cells were counted by fixing a 1 mL sample of the experimental culture to the Sedgewick-Rafter using a prepared Lugol's solution, to obtain a final Lugol's solution concentration of 0.5%. The sample was enumerated on a Sedgewick-Rafter counting slide such that the number of columns counted was a function of counting a minimum number of 100 cells (adapted from IOC, 2010). The cell density (cells mL⁻¹) was then determined according to the following equation:

$$\text{Cell Density} = (\text{cell count} \times 1000) / (\text{number of columns counted} \times 20 \text{ nm})$$

Direct cell counts were performed in order to normalize nutrient, trace metal and lipid analyses to an exact cell number.

4.2.5b Flow Cytometry

Prior to Flow Cytometer counts, a 0.5 mL subsample of each experimental culture was pipetted into 2 mL Eppendorf® Safe-Lock microcentrifuge tubes in a sterile Laminar Flow Hood. Throughout experimentation, daily cell counts were performed beginning

with the day of inoculation throughout stationary growth phases using the PhytoCyt™ Flow Cytometer (Turner Designs, Inc.). Detection endogenous fluorophores common to *H. akashiwo* NWFSC 513 were detected by running 50 µL of the samples through the flow cytometer to obtain a proxy number for cell counts. Maximal yield ($\text{yield}_{\text{max}}$ in units of cells mL⁻¹) was averaged from analytical triplicates of all experimental treatments. Maximal growth rate (μ_{max} in units day⁻¹) was determined from the slope of a linear regression (the coefficient of correlation $[R^2] \geq 0.95$) of the natural logarithm of cell density versus time during exponential growth (Guillard, 1973). For selected experiments, the length of the lag phase was determined based on the number of days preceding exponential growth.

4.2.5c Chlorophyll Fluorescence- Raw Fluorescence Units (RFU)

Chlorophyll-based biomass estimations were generated *in vitro* and obtained daily by pipetting 6 mL of each experimental culture into 8 mL FloTubes™ in a sterile Laminar Flow Hood. Chlorophyll was measured on a Turner Designs 10-AU Fluorometer according to the protocol outlined in Appendix VIII. Raw fluorescence output was given in raw fluorescence standard units (RFU) and a growth curve was generated alongside the obtained cell counts.

4.2.6 Photosynthetic performance

Cellular fluorescence capacity using variable fluorescence (F_v/F_m) to measure photosystem II (PS II) efficiency was assessed *in vivo* during exponential and stationary growth phases according to the 3-(3,4-dichlorophenyl)-1,1-dimethylurea (DCMU) protocol outlined in Appendix VIII. DCMU is a specific inhibitor of photosynthesis and acts by blocking the plastoquinone-binding site of PS II, preventing electron flow from

the generation site in photosystem II, to the plastoquinone. This process interrupts the photosynthetic electron transport chain in photosynthesis and blocks the ability of the cells to turn light energy into chemical energy. DCMU only blocks electron flow from PS II and has no effect on photosystem I or other reactions in photosynthesis making the method an effective metric for determining PS II efficiency. The DCMU method effectively measures the quantum efficiency of PS II, which is an indicator of nutrient stress (Samuelsson and Öquist, 1997).

4.2.7 Nutrient analyses

4.2.7a Particulate Nitrogen (PN) and Phosphate

In a sterile laminar flow hood, 12 mL samples were collected daily in 15 mL polypropylene BD Falcon Conical Centrifuge Tubes (previously rinsed three times with D.I. (18.2 M Ω ·cm)), and stored in the freezer at -20 °C for future nutrient analyses.

Nutrient analyses were performed using a flow injection auto analyzer (Lachat Instruments QuickChem 8000 Series), for nitrate, nitrite and ortho-phosphate using standard colorimetric techniques (Smith and Bogren 2001; Knepel and Borgen 2002).

4.2.7b Particulate Carbon (PC)

Particulate Carbon (PC) samples were collected in 20 mL volumes on combusted (450 °C for 6 hours) Whatman glass fiber filters (GF/F) at 3 time points: 24 hours after experimental inoculation (lag phase), exponential (nutrient replete phase), and stationary (nutrient deplete phase). Samples were stored in acid-cleaned 47-mm petri dishes prior to analysis.

4.2.8 Trace metal analyses

A sample volume (100 mL) for each treatment was collected for Fe and Copper analyses at 3 time points: time zero (before the addition of cell culture to the medium),

exponential (nutrient replete phase), and stationary (nutrient deplete phase). Filtrate of the treatment samples were collected in 50 mL Teflon-lined GoFlo sample bottles by filtration through 1.0 μ M polycarbonate filters using a Nalgene polysulfone filtering apparatus. All bottles and filters were acid-cleaned and packaged in a trace-metal clean laboratory by The University of Maine using established protocols.

Samples were stored at 15°C prior to being returned to The University of Maine for analysis by Inductively Coupled Plasma Mass Spectrometry (Lohan *et al.*, 2005)

4.3 Results and discussion

Employing CO₂-bubbling to acidify laboratory cultures was examined as a more representative technique to mimic the ocean acidification changes that are occurring in a natural environmental system. Results from this methodology were used to compare differences in algal growth and photosystem efficiencies with the acid/base acidification methodology (Chapter 3) to explore any physiological differences among the two most common techniques used for ocean acidification studies.

To determine true seawater pH values for three given time points during all experimentation: the initial experiment commencement, exponential growth, and the third day of stationary growth, pH values were measured using freshwater probes and was corrected to representative seawater pH using the colorimetric method for determining seawater pH (Table 4.1).

Time	pH 7.4 (+Fe)	pH 8.1 (+Fe)	pH 7.4 (-Fe)	pH 8.1 (-Fe)
Initial	7.55	8.25	7.45	7.98
Exponential	7.35	7.97	7.40	7.97
Stationary	7.35	7.84	7.41	8.00

Table 4.1 True Salinity and temperature corrected pH values within the four experimental treatments during three algal growth stages.

4.3.1 Algal growth

All CO₂-bubbling experimentation was conducted at an initial particulate nitrogen concentration of 200 µM to ensure growth would not be N-limited, yet still able to induce an appropriate time to reach stationary growth (Fig. 4.1).

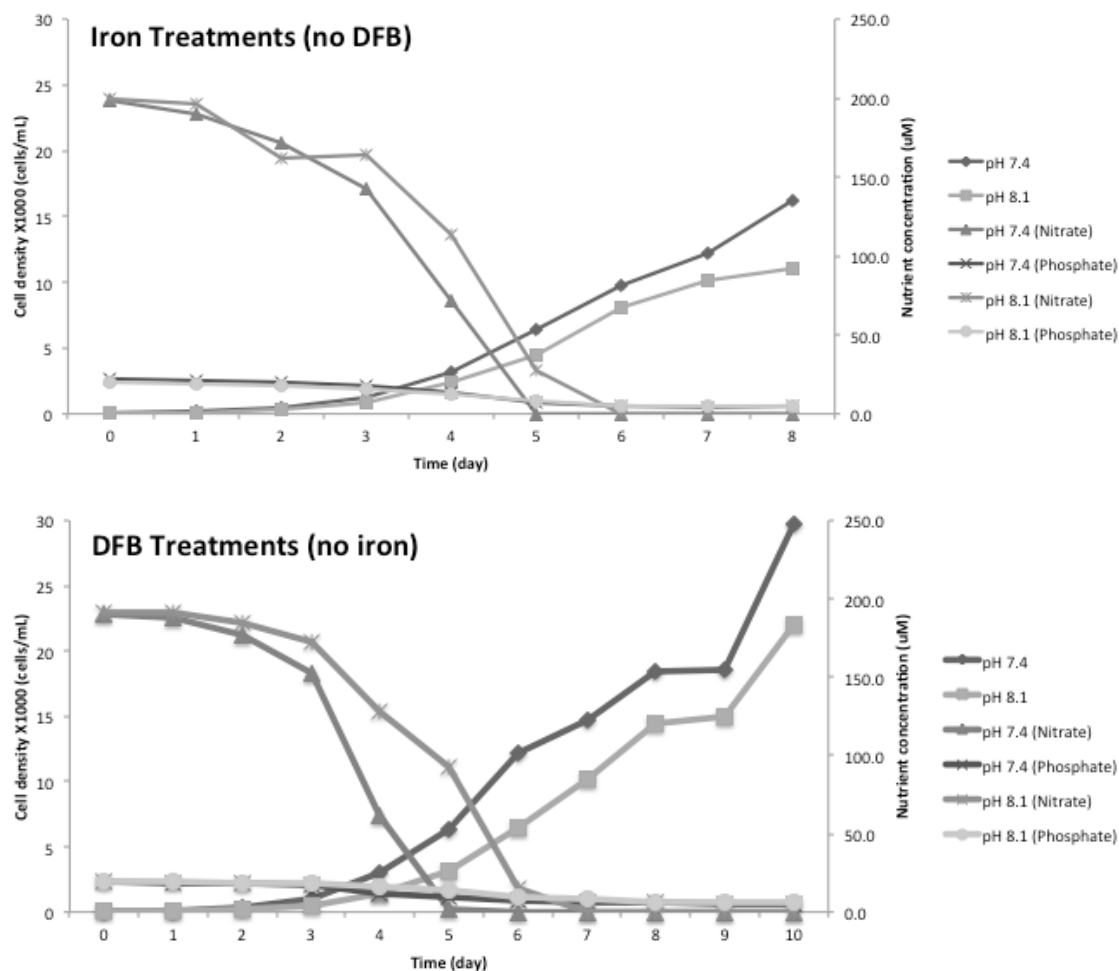


Figure 4.1 Nitrate and phosphate drawdown concentrations (μM), with corresponding cell density increases (cells mL^{-1}) in *H. akashiwo* NWFSC 503 at pH 7.4 and 8.1 grown in filtered seawater at a nitrate concentration of $220 \mu\text{M N}$. The iron treatment was at a concentration of $6.6 \mu\text{M Fe}$ and the treatment with DFB had no iron, but rather an enrichment of 125 nM DFB ($n=2$).

In Chapter 3, *H. akashiwo* cultures were acidified using acid/base methodologies with an N-addition of 80 μM N, where there was no resulting growth curve differences between any of the Fe or pH treatments. These results mimicked the CO_2 -bubbling system with an initial N-addition of 220 μM , where no growth differences were observed among treatments (Fig. 4.2).

Exponential growth rates are one important factor to consider when assessing for phytoplankton fitness. There was a considerable increase in exponential growth rates for *H. akashiwo* cultures reared under the CO_2 -bubbling experiments compared to the acid/base buffering experiments, suggesting that a surplus of carbon enabled the cells to increase their maximal growth rates. Comparing exponential growth rates in the CO_2 -bubbling methodology to the acid/base buffering methodology, there was an overall faster growth rate in cells grown using CO_2 -bubbling (high pCO_2) than acid/base buffering, but no differences among growth rates between any of the Fe or pH treatments within each experiment. Even with the addition of carbon in the low pH (high pCO_2) treatments, the CO_2 -bubbling experiment resulted in no growth rate differences between any of the Fe or pH treatments (Fig. 4.3). In other studies, CO_2 -limitation was not found to be the main factor associated with differences between growth and photosynthesis from these two acidification methods examined (Riebesell *et al.* 1993; Chen and Durbin 1994).

Heterosigm akashiwo growth rates under low and ambient pH treatments using the CO_2 -bubbling methodology were not statistically different. These results contradict other studies that used similar methodologies. For example, Lohbeck *et al.* (2012) assessed growth rate effects on phytoplankton using a CO_2 -bubbling technique and noted that populations had adapted to a low pH environment by increasing their exponential

growth rates when CO₂ levels were higher than control populations reared at ambient pH for the same duration of time. The differences between the two results can be partially explained by the different phytoplankton species examined in each study, concluding that ocean acidification effects on growth rates will vary among algal species as well as isolates- owing to the notion that ocean acidification effects on phytoplankton are not unified.

These results indicate that a surplus of nutrients (carbon, nitrogen or iron), does not change growth rates of *H. akashiwo*, indicating that these cells cannot acclimate to acquiring a surplus of nutrients under a short-term, stress-induced, environmental change scenario. This study suggests that ocean acidification (that is, an excess of bioavailable carbon), will not likely change growth rates of the harmful algal bloom, *H. akashiwo*, and is not an immediate threat to the productivity of this alga.

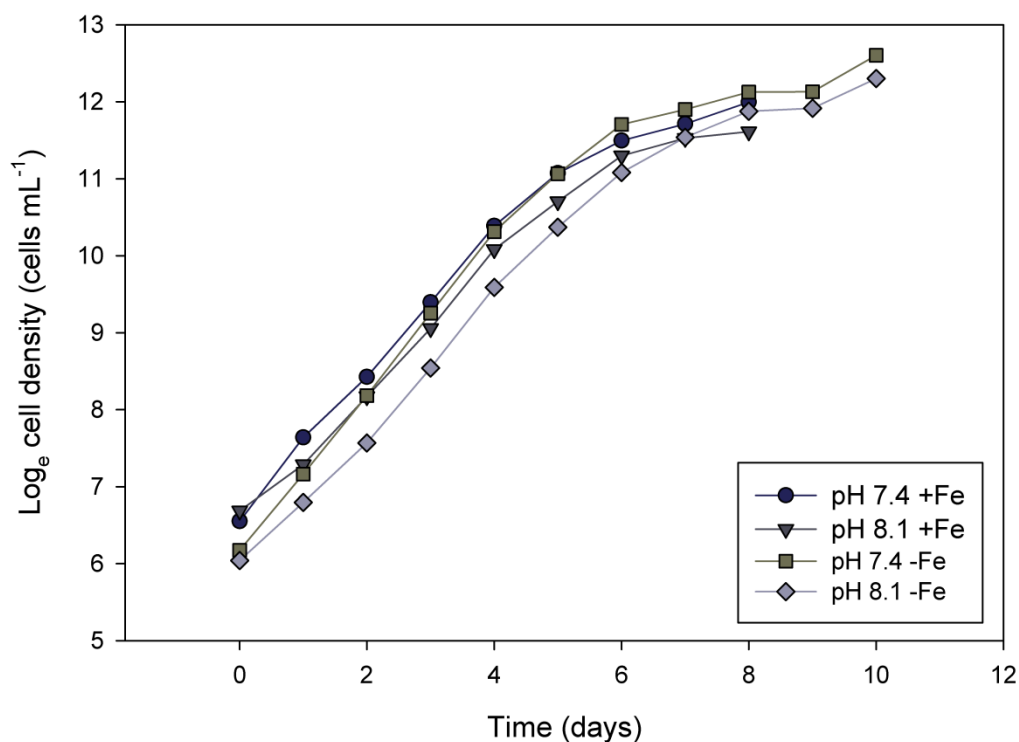


Figure 4.2 LN growth curve of *H. akashiwo* NWFSCS 503 grown in ESNW medium with 220 μM N, at a pH of 7.4 (± 0.5) and 8.1 (± 0.5), with the addition of 6.6 μM Fe (+Fe) and without the addition of any Fe (-Fe). The -Fe treatments contained a DFB concentration of 125 nM to chelate any Fe found in the natural seawater medium used for experimentation ($n = 2$).

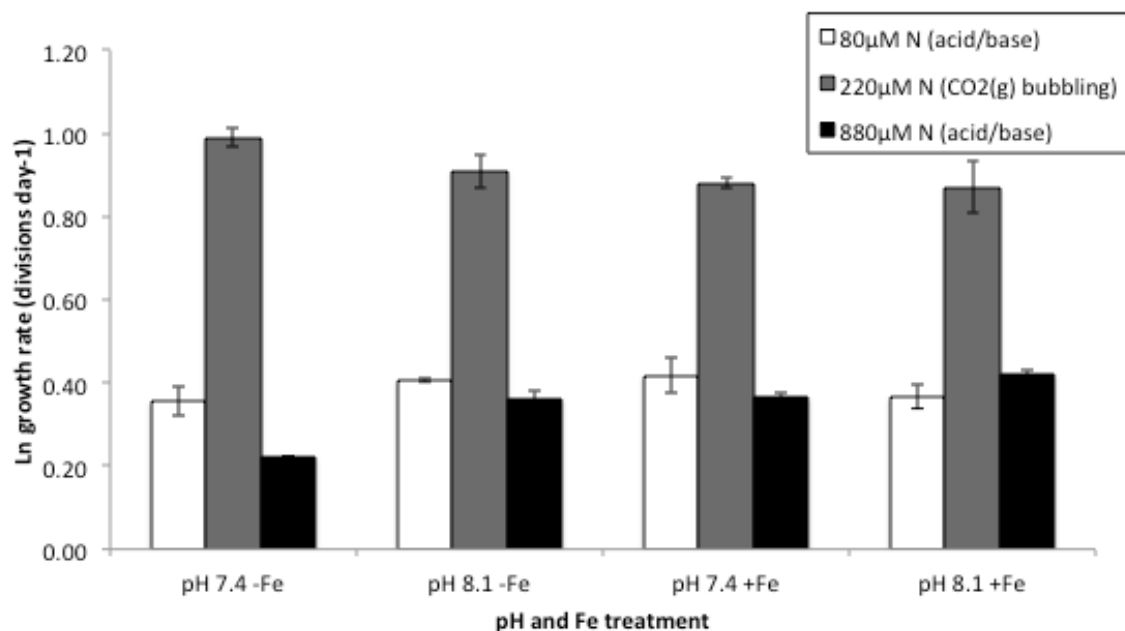


Figure 4.3 Comparison of growth rates (divisions day⁻¹) of *H. akashiwo* NWFSC 503 grown in ESAW with 80 μM N using an acid/base titrated system (n = 3), grown in ESNW with 220 μM N using a CO₂(g) bubbling system (n = 2) and grown in ESAW with 880 μM N using an acid/base titrated system (n = 3). Please note the data from treatments with 80 and 880 μM N was taken from Chapter 3 where experiments were conducted using the acid/base acidification method. All treatments were included here to compare growth rate results with the CO₂(g) bubbling system. Bars are representative of standard error.

4.3.2 Cell yield

For the CO₂(g)-bubbling system, maximal cell yield was calculated among all treatments and compared to the yield of treatments from the acid/base acidification methodology outlined in Chapter 3. In the CO₂(g)-bubbling system where initial particulate N was 220 μM, highest cell yield occurred in the following order: pH 7.4 (-Fe), pH 8.1 (-Fe), pH 7.4 (+Fe) and pH 8.1 (+Fe). This trend was different compared to all acid/base acidified treatments (Chapter 3) where experiments with an N-addition of 80 μM resulted in no difference in maximum cell yield among any treatments, and experiments with the N-addition of 880 μM resulted in a lower cell yield in only the

combined low pH and Fe treatment- the same trend that was noted with growth rates (Fig. 4.4).

Cell yield for all species remained constant at each pH in acid/base experiments, but was lower in Fe limited treatments- indicating that growth may have been limited by carbon or potentially another nutrient, namely, N or Fe. Since C was not limited in the CO₂-bubbling experiments, this accounted for cell yield being highest at low pH and lowest when pH increased for *H. akashiwo*. It is important to take note that despite the increased growth rates in the CO₂-bubbling experiments over the acid/base experiments, stationary phase was still induced implying that maximum cell density was not limited by carbon, but rather another underlying factor. The addition of DIC from CO₂-bubbling resulted in an additional carbon nutrient source for the culture, where stationary growth was thereby likely induced once the N-source was depleted. The lack of variability in growth rates between pH levels in the acid/base experiment (Chapter 3) may suggest that pH (that is, high pCO₂) alone will not have an effect on *H. akashiwo* growth yield. It is well known that the marine environment is complex and a shift in pH is only one consequence of acidifying waters. What this does not explain, however, is why there was an overall higher yield in the DFB (-Fe) treatments over the +Fe treatments?

As one might expect, using DFB (an Fe-binding chelator), would render any dissolved Fe unavailable for cellular acquisition and utilization. With Fe being unavailable, it is reasonable to assume that this missing key element would result in overall decreased cell yield. As shown in Fig. 4.4 however, cell yield was highest in all DFB treatments. In most laboratory studies, EDTA (a common metal chelator) is added to media in a 1:1 ratio with metals, enabling the metals to be bound and suspended in solution. Typically, most EDTA is bound up to calcium and magnesium when added to

seawater and as metals are drawn-down, this EDTA to metal ratio is changed. DFB, an Fe specific metal chelator, keeps Fe soluble in solution. With most phytoplankton, this would hinder their ability for Fe-uptake. This study, however, proposes that *H. akashiwo* cells behave differently than other phytoplankton species, in that they might have a common binding site and affinity for DFB. Adding a surplus of DFB in *H. akashiwo* medium would then aid in Fe acquisition by increasing the bioavailability of Fe to cells, essentially providing them Fe on a “silver platter”.

Although growth rates were not different between pH and Fe treatments, maximal cell yield was highest at low pH and decreased with increasing pH in the CO₂-bubbling experiments. The increase in cell yield at low pH (or high CO₂) is a result of the additional carbon source supplemented to the cultures. Unlike most phytoplankton species, *H. akashiwo* isolates lack a known carbon concentrating mechanism (CCM), which explains the potential for population increases (or bloom formation) with a predicted rise in CO₂ under a global change scenario (Nimer *et al.* 2007). For this reason, the CO₂ –bubbling methodology is more representative of a true environmental ocean acidification event. A major setback of employing the CO₂-bubbling method for flagellates in particular is the stress induced by the bubbles, which negatively affects growth (Chen *et al.* 1994).

Results shown in *H. akashiwo* may not be typical for other phytoplankton isolates, as most species possess a CCM and are only limited by total carbon at very low CO₂ concentrations (Hurd *et al.* 2009). Since oceans are presently at limiting levels for the enzyme RuBisCo- essential in the first step of photosynthesis, most phytoplankton species can increase their CO₂-uptake to saturate photosynthesis using their CCM, unlike *H. akashiwo*, (Beardall and Raven 2004; Giordano *et al.* 2005). Raven (1991) suggested

that increased dissolved CO₂-availability might benefit phytoplankton species that rely on diffusive CO₂ entry (rather than CCM) or those that have the capability to suppress their CCM. Species that depend on diffusive entry of CO₂ might develop higher intracellular CO₂ concentration that may match the concentrations required to saturate RuBisCo. This can help explain why cell yield was drastically higher in cultures reared at a low pH (higher CO₂ concentration) than ambient pH.

Since phytoplankton commonly use CCMs and actively take up both CO₂ and HCO₃⁻, most species may benefit from reduced CCM activity- meaning a reduction in CCM mechanisms- resulting in fewer CCM proteins. (Giordano *et al.* 2005; Reinfelder 2011). A reduction in CCM proteins could reduce the nitrogen requirement for CCM protein synthesis and could result in a concomitant reduction in the energy requirements for protein synthesis (Raven, 1991, Crawford *et al.* 2011). With these potential benefits in terms of energetic costs to the cell, one would assume that the savings could be sufficient to influence processes such as growth rate; however, this was not the case as growth rate remained unchanged in all treatments.

Although higher CO₂ did not act as a fertilizer to increase growth rates, we should not assume that there would be a uniform response in all species. In comparison, a *Thalassiosira* sp. community in the Californian upwelling region did not have an altered growth rate response when CO₂ concentrations were elevated (Tortell *et al.* 1997). Several studies have demonstrated that in diatoms there is no variation in the expression of the rubisco transcription gene when cultures were grown in high and low CO₂ treatments (Granum *et al.* 2009; Crawford *et al.* 2011). Growth of over 100 generations of diatoms did not provide any evidence for significant adaptation to high CO₂. Similarly, the diatoms demonstrated success in acclimating growth rates to a wide range of pH

conditions. If all species responded in a similar fashion, acidification may have little effect on phytoplankton productivity (Crawford *et al.* 2011).

Elevated pCO₂ has been predicted to be beneficial to diatoms due to reduced cost of CCMs by modulating CO₂ supply to RuBisCo, rather than forcing cells to regulate their expression of this enzyme. However, a recent study on the efficiency of CCM in marine diatoms suggested that active transport of bicarbonate into the chloroplast is what constituted the major energetic cost of the CCM, not the uptake of CO₂, leading one to the conclusion that ocean acidification and CO₂ would have little or have no effect on the growth and physiology of diatoms. Other studies have predicted that doubling atmospheric CO₂ could reduce energetic costs of carbon fixation for the CCM, yielding an energetic benefit to diatoms. However, such benefits were found to be marginal and not detectable as a change in growth rate, supporting the findings presented in this study (Hopkinson *et al.* 2011). From the results presented here, ocean acidification is therefore expected to impose no growth or physiological changes in marine diatom species as they have been shown to be unaffected by environmental acidification from both laboratory acid/base and CO₂–bubbling methodologies.

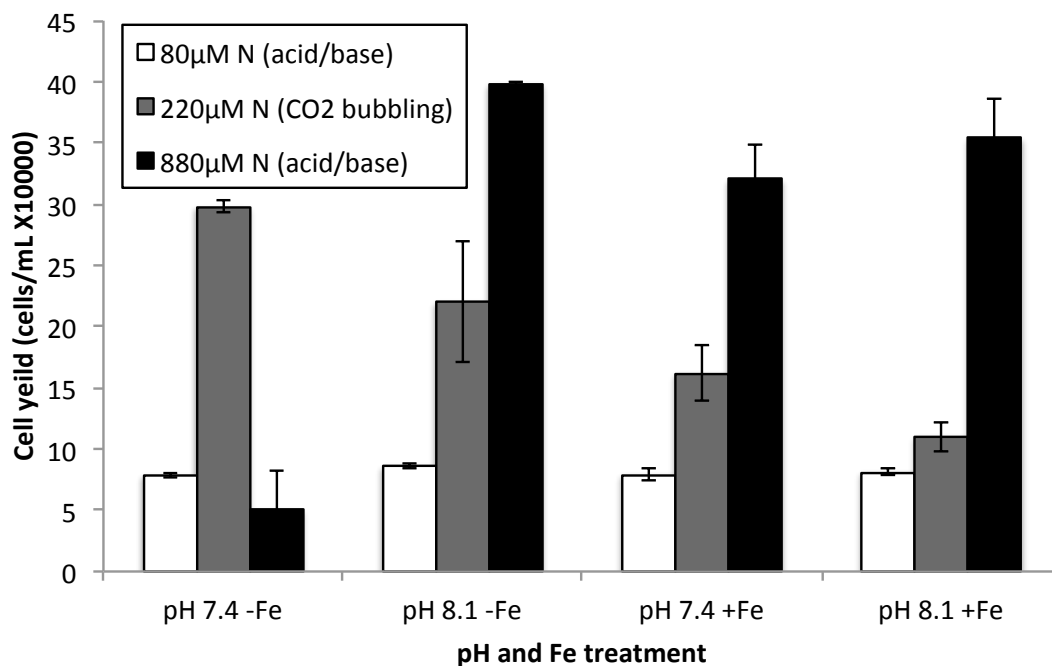


Figure 4.4 Comparison of maximum cell yield of *H. akashiwo* NWFSC 503 grown in: ESAW with 80 μM N using an acid/base titrated system (n=3), grown in ESNW with 220 μM N using a CO₂(g) bubbling system (n=2) and ESAW with 880 μM N using an acid/base titrated system (n = 3). Please note the data from treatments with 80 and 880 μM N was taken from Chapter 3 where experiments were conducted using the acid/base acidification method. All treatments were included here to compare growth rate results with the CO₂(g) bubbling system. Bars are representative of standard error.

Discrepancies resulted from obtaining daily cell counts using either the PhytoCyt flow cytometer, or taking true cell counts under the microscope. These cell count differences are noted in Fig. 4.5 where total cell densities between the two counting methods are compared.

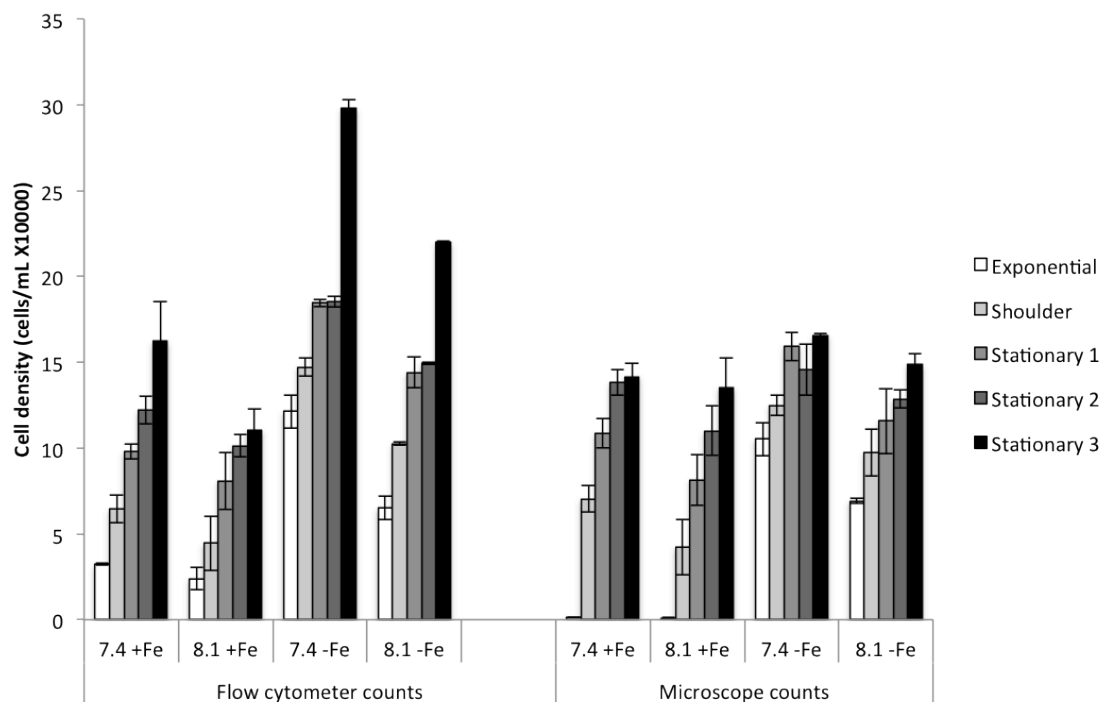


Figure 4.5 Total cell density differences in *H. akashiwo* NWFSC 503 as a result of cell counting using the flow cytometer and direct microscope counts. Bars are representative of standard error (n=2)

4.3.3 PSII efficiency

For all phytoplankton isolates examined, total photochemical (PSII) efficiency examined using variable over maximal fluorescence (F_v/F_m) was not drastically different between the +Fe and -Fe treatments, however, there were differences between the pH levels examined (8.1 and 7.4) (Fig. 4.6). To measure F_v/F_m , the DCMU protocol was used to block the transfer of electrons from QA to QB, thereby closing all PSII reaction centres, (thereby blocking linear electron transport), providing a measure of F_m . This value alongside an untreated raw fluorescence value (F_v) gave the F_v/F_m ratio, a measure of the light-harvesting ability of PSII. When pH was low, dark-acclimated *H. akashiwo* cultures were less effective at harvesting photons from a saturating pulse of actinic light to generate electron flow. The result suggests that when stationary phase is induced, as

one would expect in a bloom event, ambient pH (low CO₂) encourages *H. akashiwo* to acquire light energy for photosynthesis more effectively. These results indicate that electron transport proteins either function optimally at ambient pH, or are damaged at low pH.

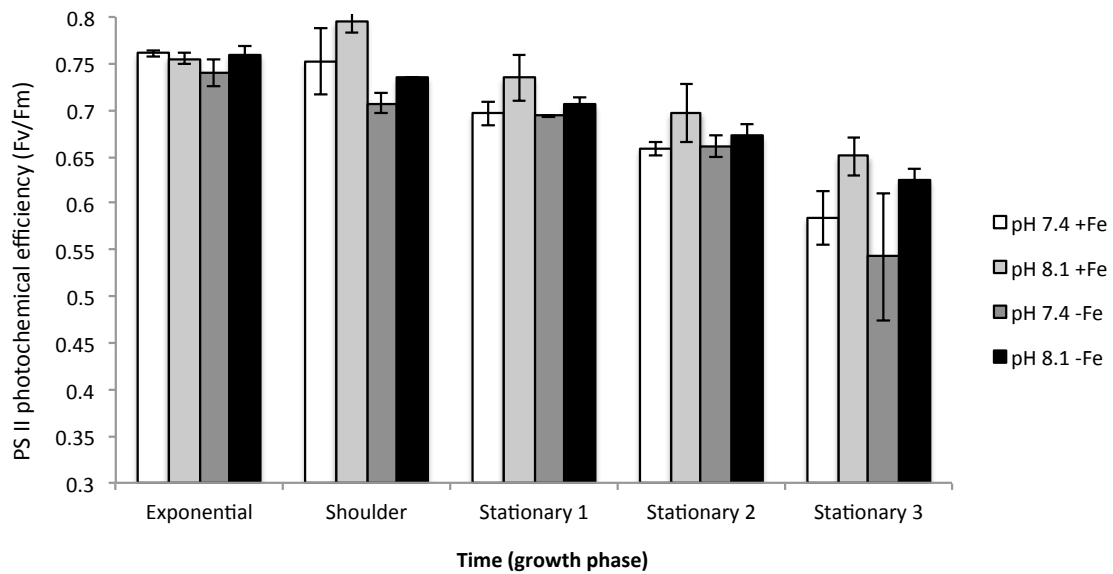


Figure 4.6 PSII efficiency was examined using a DCMU protocol with the alga, *H. akashiwo* NWFSC 513, grown in ESNW medium at a pH of 7.4 (± 0.5) and 8.1 (± 0.5), with the addition of 6.6 μM Fe (+Fe) and without the addition of any Fe (-Fe). The -Fe treatments contained a DFB concentration of 125nM to chelate any Fe found in the natural seawater medium used for experimentation ($n = 2$). Bars are representative of standard error.

4.4 Conclusion

Overall, examining *H. akashiwo* under the combined effects of low pH and high CO₂, as expected under the future global climate change scenario demonstrated that this HAB species appears to show no difference in growth rates. The most unexpected outcome arose in examining cell yield results, where the low pH (high CO₂) environment resulted in the greatest cell yield when Fe was limiting, compared to ambient pH (low CO₂) when Fe was present in abundance. Future experimentation should examine whether the intracellular composition of *H. akashiwo* cells within the high CO₂ and low Fe environment is altered, and how this compositional change might affect the nutritional value of phytoplankton cells available for higher trophic levels.

4.5 References

- Anderson, D.M. (1989) Toxic algal blooms and red tides: A global perspective. In T. Okaichi, D.M. Anderson, & T. Nemoto (Eds.), *Red Tides: Biology, Environmental Science and Toxicology* (pp. 11–16). Elsevier, New York, New York, USA.
- Crawford KJ, Raven JA, Wheeler GL, Baxter EJ, Joint I (2011) The Response of *Thalassiosira pseudonana* to Long-Term Exposure to Increased CO₂ and Decreased pH. *PLoS ONE* 6(10): e26695. doi:10.1371/journal.pone.0026695
- Dickson, A.G., Sabine, C.L. and Christian, J.R. (Eds.) (2007). Guide to best practices for ocean CO₂ measurements. PICES Special Publication 3, 1991 pp.
- Feely, R.A., Sabine, C.L., Hernandez-Ayon, J.M., Ianson, D. and Hales, B. (2008). Evidence for upwelling of corrosive "acidified" water onto the continental shelf. *Science*, 320: 1490-1492.
- Friederich, G. E., Walz, P. M., Burczynski, M. G. and Chavez, F. P. (2002). Inorganic carbon in the central California upwelling system during the 1997-1999 El Nino-La Nina event. *Prog. Oceanogr.* **54**(1-4), 185-203.
- Guillard, R.R.L. (1973) Division rates. In: Stein, J.R. (ed.). *Handbook of Phycological Methods: Culture Methods and Growth Measurements*. Cambridge University Press, Cambridge. pp. 289-312.
- Guillard, R.R.L. (1975). Culture of phytoplankton for feeding marine invertebrates. pp 26-60. In Smith W.L. and Chanley M.H (Eds.) *Culture of Marine Invertebrate Animals*. Plenum Press, New York, USA.
- Intergovernmental Oceanographic Commission (IOC) (2010). Microscopic and molecular methods for quantitative phytoplankton analysis. Manuals and Guides.
- Knepel, K. and K. Borgen, 2000. Determination of ammonium by flow injection analysis colorimetry. QuikChem® Method 10-107-06-1-C (revised by K. Bitzan). Zellweger Analytics, Inc., Lachat Instruments Division, Milwaukee, WI.
- Lohan, M. C., A. M. Aguilar-Islas, R. P. Franks, and K. W. Bruland. 2005. Determination of iron and copper in seawater at pH 1.7 with a new commercially available chelating resin, NTA Superflow. *Anal. Chim. Acta.* 530:121-129.
- Parker A. E., Fuller J., and Dugdale R. C. (2006). Estimating dissolved inorganic carbon concentrations from salinity in San Francisco Bay for use in ¹⁴C-primary production studies. Interagency Ecological Program for the San Francisco Estuary (in press).
- Samuelsson, G., Oquist, G. (1977). A method for studying photosynthetic capacities of unicellular algae based on *in vivo* chlorophyll fluorescence. *Physiol. Plant.* 40: 315-319.

Smith, P., Bogren, K., 2001a. Determination of nitrate and/or nitrite in brackish or 254 seawater by flow injection analysis colorimetry. QuikChem Method, 31–107: 255 Saline Methods of Analysis Lachat Instruments, Milwaukee, WI.

CHAPTER 5

5. Conclusions: tying it altogether

Over the past few decades, HAB outbreaks, particularly fish-killing flagellates and the corresponding losses to fisheries and tourism, have been at the forefront of coastal management concerns (Harness 2005). While it has been suggested that a larger number of recorded blooms are the result of community education and a greater community awareness (Hallegraeff 1993), there is reason to acknowledge that the effects of global change as outlined in this thesis may also be a primary contributor to the exacerbating HAB appearances, as several environmental factors can dynamically interact and attribute to marked increases in bloom populations.

Higher nutrient levels from increases in coastal populations, aquaculture, and observed anthropogenic climate changes have all interacted to influence bloom outbreaks. In an effort to understand HABs and predict their likely occurrences, studies examining the abiotic and biotic factors to likely impact the dynamics of bloom events are critical. Being able to anticipate how members of the phytoplankton community respond to anthropogenic effects depends on our knowledge of their key growth and physiological responses under several combined environmental factors: light, temperature, nitrogen, iron, carbon dioxide, pH and salinity. This thesis conducted multifactorial experiments where more than one interaction was measured, in an effort to tease apart the mechanisms that are likely to influence *H. akashiwo* blooms in future. In light of the increasing effects of global climate change, multifactorial studies included in this thesis are essential to predicting long-term effects of *H. akashiwo* HABs, and how these blooms might influence our overall oceanic ecosystem. Not only is this information economically

valuable to the sustainability and productivity of global fisheries, it is also useful in helping to anticipate the prosperity of global tourism industries that rely on the beauty of our coastal waterways.

Chapter 2 confirmed the phenomena that light, temperature and salinity changes can have a profound effect on *H. akashiwo* growth rates and cell permeability, where permeability might be linked to the formation of toxic blooms. Future studies should be focused at examining the mechanisms leading to *H. akashiwo* toxicity, and whether cellular permeability under the aforementioned abiotic factors is the outcome of these toxic blooms. By examining the effects of pH changes using both acid-titration (Chapter 3) and CO₂ (g) (Chapter 4) methodologies, I was able to highlight key differences in the two pH manipulation techniques. Additionally, by experimenting with the combined influences of N and Fe nutrient enrichments, along with the interaction that these nutrients have with pH, I was able to outline key areas of interest in *H. akashiwo* bloom predictions and how the occurrence of this species might compare to other key phytoplankton: *T. weissflogii* and *Synechococcus* sp.

The pH consistency in ESAW medium verified the expectation that the natural buffer of sodium bicarbonate (NaHCO₃) present in ESAW medium would maintain a nearly constant pH level when no cell culture was present. This pH consistency in ESAW medium was due to the lack of photosynthetic activity in the flask. When cell culture was added in the altered pH environments, there was a steady increase in pH- as growth yield increased in the closed environment of the flask, photosynthetic levels also increased. However, being a closed system, there was a lack of constant addition of CO₂ and cell growth requires inorganic carbon to be present in the flask in order to carry out photosynthesis. These phenomena decreased the partial pressure of CO₂ and therefore

increased the pH levels in solution from the original pH adjustment. This expected result indicated that an acid-titrated system is insufficient for maintaining culture pH during experimentation, and additional buffer is required to maintain pH in solution.

Although the natural buffer, sodium bicarbonate (NaHCO_3), decreased the pH rise over time, the buffering capacity of a bicarbonate buffer is reduced despite the natural benefit. Additional buffer was desired; therefore a supplemental buffer, HEPES was used. HEPES buffer is commonly used with cell cultures over a range of biological pH of 6-8, which is useful when CO_2 is produced during photosynthesis. The pH range of HEPES explains its efficiency at maintaining a constant pH under given conditions. HEPES buffer does not provide any nutritional benefit to cell cultures and therefore did not have an impact on growth measurements or chlorophyll fluorescence. However, it is well known that the marine environment is complex and shift in pH is only one consequence of acidifying waters.

In the case of algal photosynthetic capabilities under an acid-titrated system (chapter 3), *H. akashiwo* behaved more like the cyanobacterium *Synechococcus* sp. than the diatom *T. weissflogii*, at high nitrate levels $880\mu\text{M N}$, which surprisingly showed an increase in photosynthetic capacity with low Fe and low pH. This finding alludes to the plasticity that HAB species tend to have in our aquatic ecosystem, where they can thrive under extreme or unpredictable environmental conditions. Although it was evident that *H. akashiwo* produce an abundance of neutral (saturated) lipids in a low nitrate environment ($80\mu\text{M N}$), when the pH and Fe variables were included, *H. akashiwo*, coinciding with *Synechococcus* sp., did not demonstrate a dramatic change in intracellular lipid accumulation compared to the diatom *T. weissflogii*, that showed dramatic lipid accumulation at ambient pH and high Fe enrichments. This finding, again, highlights the

resilience of *H. akashiwo* grown in extreme nutrient or pH environments that are unlikely to influence the intracellular lipid concentrations, and thus will have a negligible effect on the nutritive value for fish and higher trophic levels. However, CO₂ manipulation experiments highlighted that intracellular carbon accumulation is likely to occur within *H. akashiwo* as they fill their internal carbon stores when pH is low and *pp*CO₂ is high. Future experiments should focus on the types of fatty acids that *H. akashiwo* produce under a high CO₂ scenario, which will help determine whether or not this HAB species will be a valuable food source at the base of our marine ecosystem.

Since nitrate is ultimately the key driver in cellular growth and yield, changing Fe concentrations would not affect the growth capabilities of *H. akashiwo*, rather photosynthetic changes are more probable when Fe is variable. These findings allude to the idea that when the environment is both N and Fe-limiting, cells designate more energy toward acquiring key nutrients for survival and sacrifice their affinity for carbon resulting in less photosynthesis, as evident in the decreased photosystem II efficiency at low Fe. When growth of *H. akashiwo* was explored in the acid-titrated conditions (chapter 3), at 880 µM N, pH adjustment resulted in a decreased final cell yield at low pH (7.4) compared to high pH (8.1). However, when nitrate levels were lowered and adjusted to 80 µM N, there was no change in growth rate or cell yield, which coincided with all other species examined. In comparison to a CO₂ (g) bubbling system (Chapter 4), the low pH environment resulted in no changes in growth rates, yet a higher cell yield at a low pH likely resulted from the high CO₂ (g) in the system that alleviated the cell's need to utilize their CCMs. In the case of the acidic ocean predicted in future, these results indicate that the rise in atmospheric CO₂ may result not in an excess of *H. akashiwo* blooms, rather larger cells with greater internal pools of carbon.

There are many changes in ocean chemistry that are associated with global climate change. Due to the various biological and chemical systems in the ocean, it is crucial to understand the effects that these changes have in relation to one another in order to recognize the threats posed to the future marine environment. In simulating a natural environmental system, results presented in this thesis could be used to further investigate how abiotic and biotic factors affect the mechanisms of carbon, nitrogen and iron sequestration, along with the resulting toxicity mechanisms and fatty acid production in the raphidophyte, *H. akashiwo*. Although the marine system is complex and ecophysiological changes can be attributed to several combined factors, this thesis approached our understanding of the future ocean from many angles to highlight the complexity of oceanographic research and to exemplify that any number of variables can change expected outcomes. The importance of understanding our future marine ecosystem is invaluable in protecting our natural resources. *Heterosigma akashiwo* is a mischievous HAB and unlocking the factors driving its metabolic demands will allow for the proper management of our future ocean.

5.1 References

Hallegraeff GM (1993) A review of harmful algal blooms and their apparent global increase. *Phycologia* 32: 79-99

Harness (2005) Harmful Algal Research and Response: A National Environmental Science Strategy 2005-2015, Washington DC

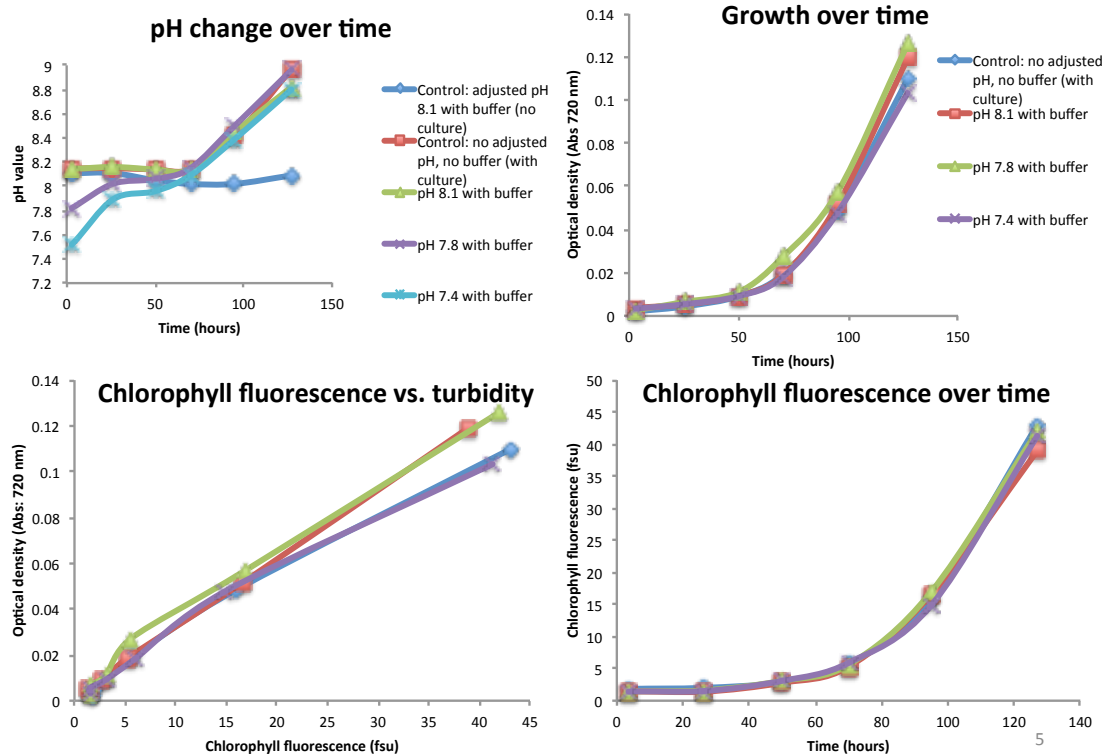
APPENDICES

CHAPTER 3 APPENDICES

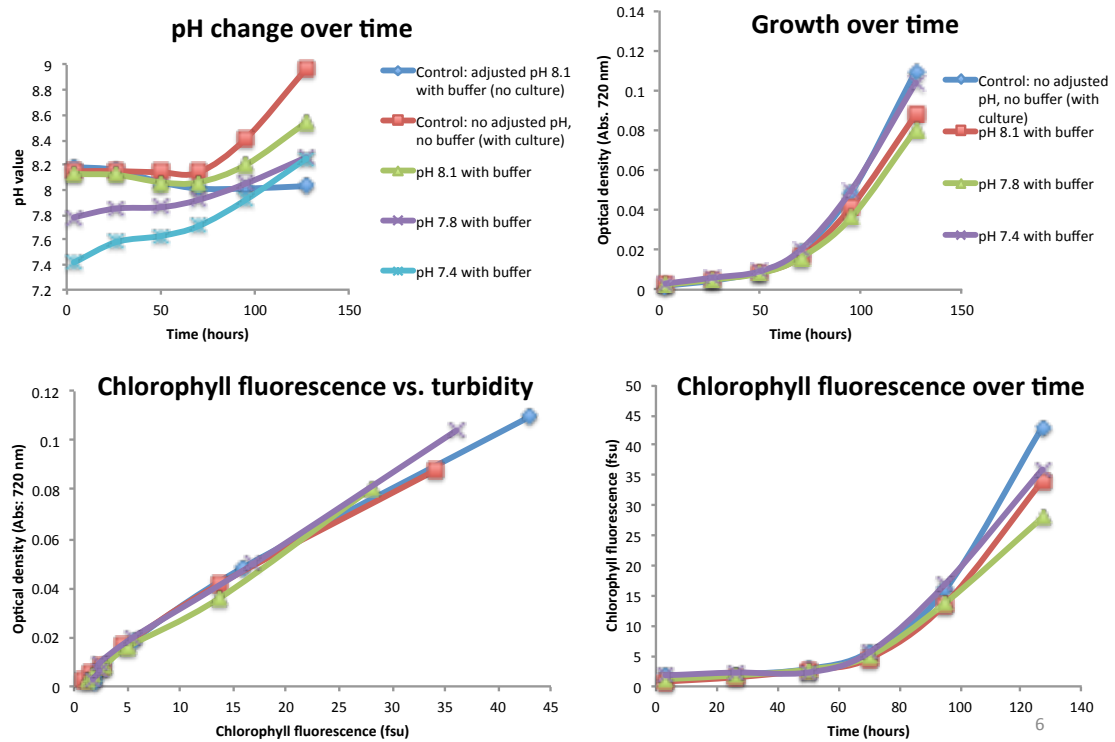
Appendix I: Stable pH readings with buffered and acidified cultures

Preliminary buffer experiments were carried out with Tris, Tricine and HEPES buffers at three different buffer concentrations. HEPES buffer was found to be the most effective buffer at maintaining culture pH over the duration of growth for each culture. The example outlined below is for the three HEPES buffer concentrations examined, using *Synechococcus sp.* CMPP 833.

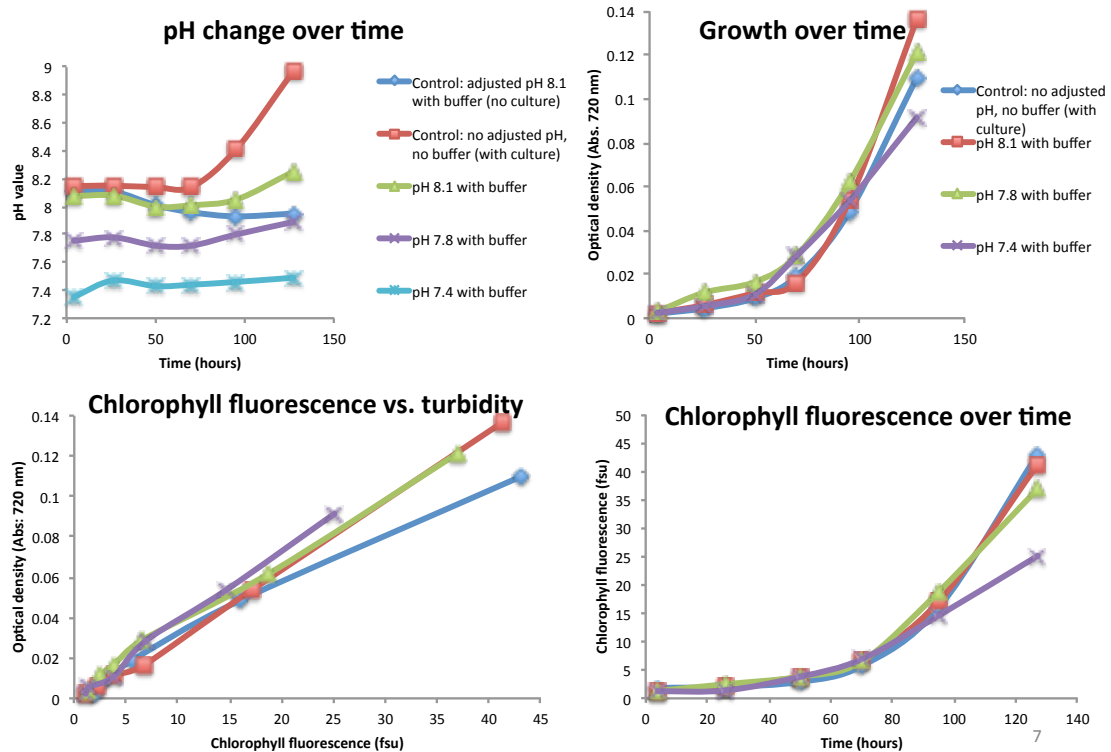
[0.133 g/L] HEPES buffer experiment with *Synechococcus spp.* 833:



[0.665 g/L] HEPES buffer experiment with *Synechococcus* spp. 833:



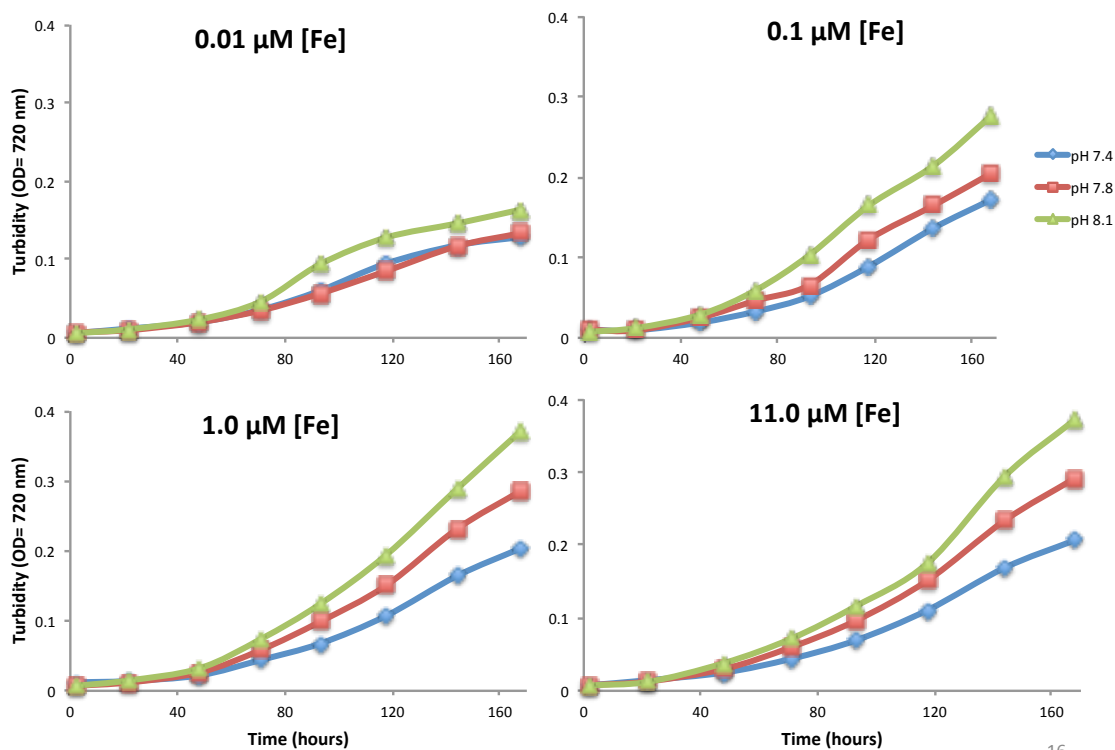
[2.659 g/L] HEPES buffer with *Synechococcus* spp. 833:



Appendix II: Selection of Fe enrichment

Based on a sample of preliminary results outlined below (with *Synechococcus* sp. CCMP 833), a divergent Fe growth trend was noted. The same divergent trend was noted with all other species examined, whereby the 0.01 μM Fe enrichment resulted in the same growth pattern as 0.1 μM Fe enrichment, and the 1.0 μM Fe enrichment resulted in the same growth pattern as 11.0 μM Fe enrichment. Therefore, experiments were carried out at two of the Fe concentrations: 0.01 μM Fe and 11.0 μM Fe.

Optical density measurements (OD=720nm):



Appendix III: Oxygen evolution rationale

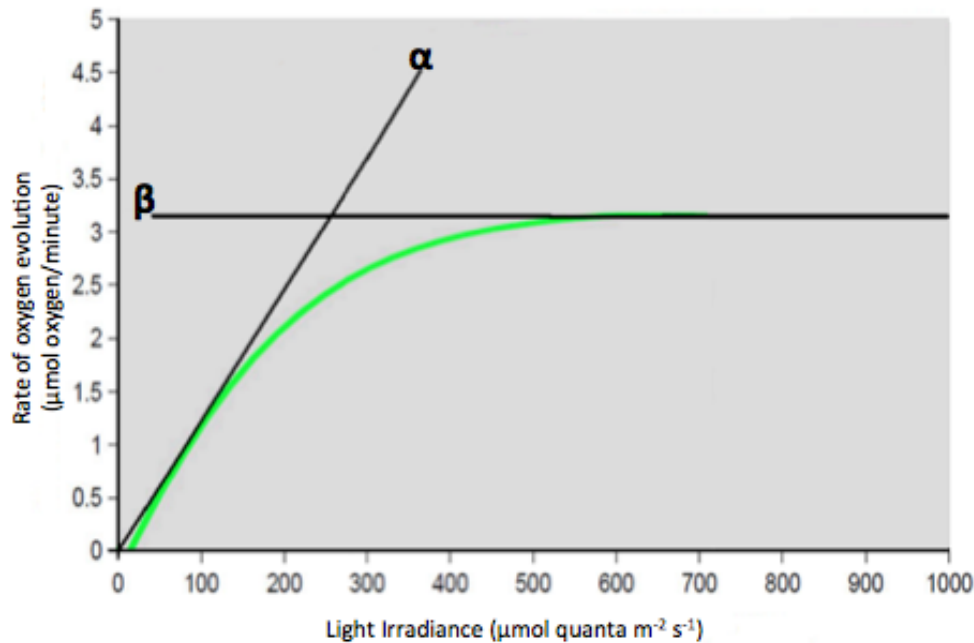







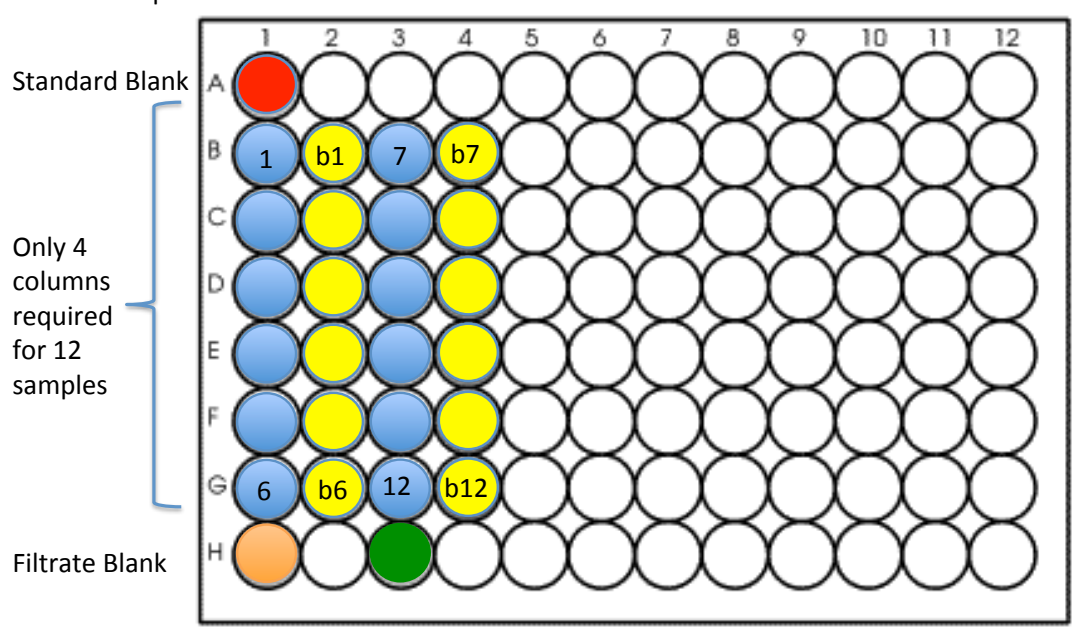
Figure. Appendix III: Depiction of a theoretical increase in the rate of oxygen evolution ($\mu\text{mol oxygen/minute}$) for phytoplankton cells as light irradiance ($\mu\text{mol quanta m}^{-2} \text{s}^{-1}$) increases. In cells under photosystem stressors, the α -value and β -value were expected to be altered.

The theoretical photosynthesis versus irradiance curve (Fig. Appendix III) generated from data obtained through oxygen electrode analysis illustrated that with increasing light irradiance (on the x-axis), there is a gradual increase in the rate of oxygen evolution from the cell (α) until the photosystem hits the critical point. This critical point is where the curve begins to plateau, and represented the point where the cellular photosystem is working at its maximum ability (β). At this point, there is no additional increase in light irradiance that can accelerate the photosynthetic electron pathway. Damage to the photosystem was denoted by a gentle slope (α), and damage to the carbon-enzyme RuBisCo system was denoted by a drop in the plateau (β).

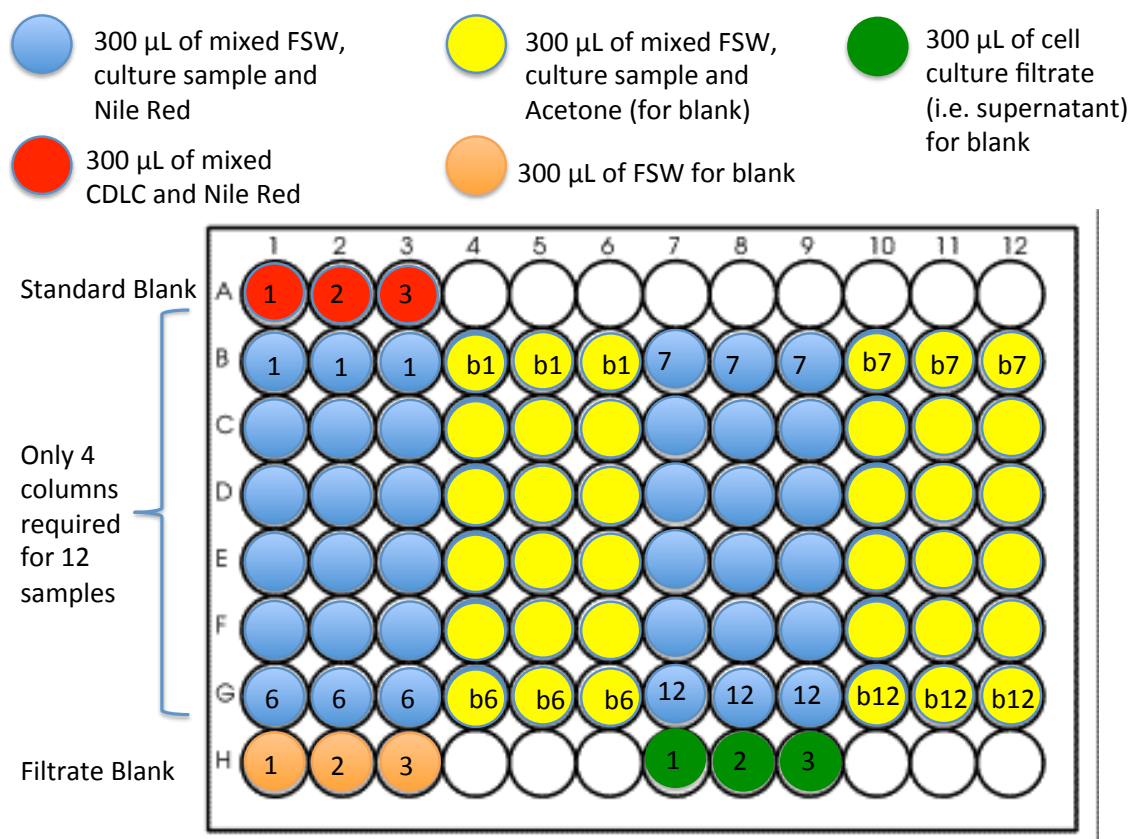
Appendix IV: Nile red plate reader organization

2mL, 96 MWP:

-  Add 880 μ L of FSW
Add 220 μ L of culture sample
Add 3 μ L of Nile Red
-  Add 880 μ L of FSW
Add 220 μ L of culture sample
Add 3 μ L of Acetone for blank
-  Add 1.1 mL of cell culture filtrate (i.e. supernatant) for blank
-  Add 1.1 mL of CDLC
Add 3 μ L of Nile Red
-  Add 1.1 mL of FSW for blank



300 μ L, 96 MWP:



CHAPTER 4 APPENDICES

Appendix I: Enriched Seawater, Natural Water (ESNW)

Recipe was developed by Andersen (2005) but altered by the Cochlan Lab, RTC-SFSU, to best suit the culturing and growth requirements of the alga used for experimentation, *H. akashiwo* NWFSC 513.

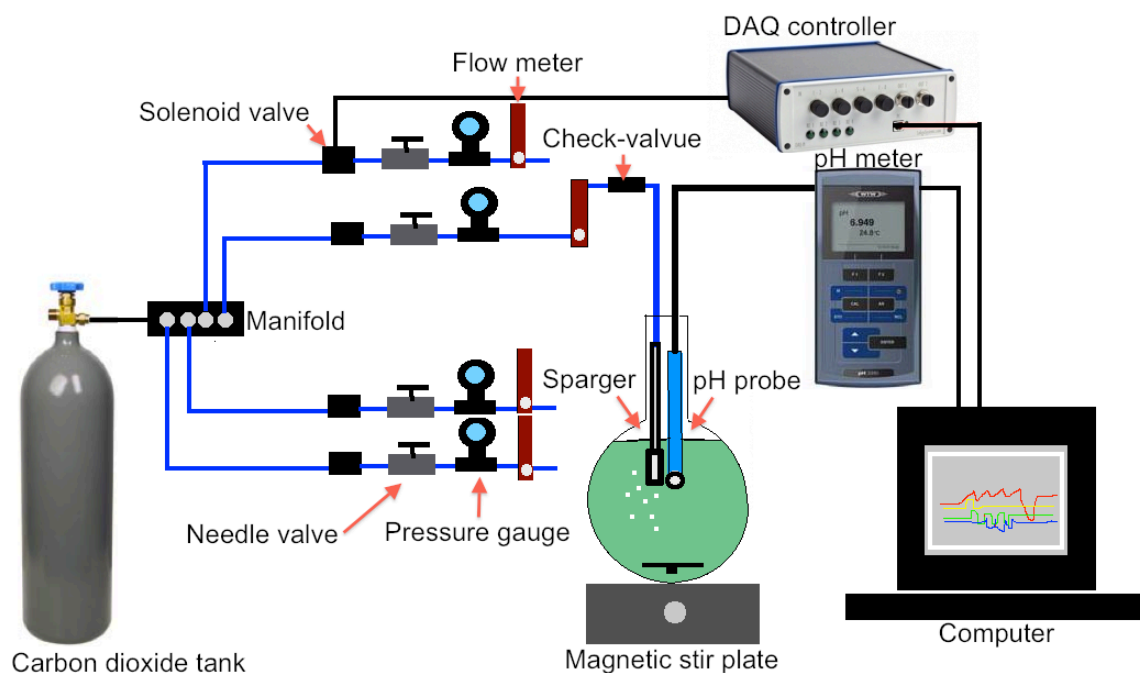
Nitrogen Stocks	g/L stock	f.w.	[stock] M	[media] M	[media] µM
NaNO ₃	0.8499	84.99	5.99E-02	5.00E-04	189.1
Enrichments	g/L stock	f.w.	[stock] M	[media] M	[media] µM
Na ₂ HPO ₄	1.4196	141.96	0.0099	5.00E-05	19.1
C ₁₀ H ₁₄ N ₂ O ₈ Na ₂ •2H ₂ O (EDTA)	2.4419	372.2	6.56E-03	6.56E-06	6.6
FeCl ₃ •6H ₂ O	1.7717	270.32	6.55E-03	6.55E-06	6.6
C ₁₀ H ₁₄ N ₂ O ₈ Na ₂ •2H ₂ O (EDTA)	3.0860	372.2	8.291E-03	8.29E-06	8.2912
MnSO ₄ •H ₂ O	0.4090	169.02	2.42E-03	2.42E-06	2.4198
ZnSO ₄ •7H ₂ O	0.0730	287.56	2.54E-04	2.54E-07	0.2539

CoSO ₄ •7H ₂ O	0.0160	281.10	5.69E-05	5.69E-08	0.0569
Na ₂ MoO ₄ •2H ₂ O	0.0148	241.95	6.12E-05	6.12E-08	0.0612
NiCl ₂ •6H ₂ O	0.0149	237.69	6.27E-05	6.27E-08	0.0627
Total metals bottle #4:			2.85E-03	2.85E-06	
CuSO ₄ •5H ₂ O	0.0098	249.68	3.93E-05	3.93E-09	0.0039
Na ₂ SeO ₃	0.0022	172.9379	1.27E-05	6.36E-09	0.006
Thiamine HCl (Vit. B1) C ₁₂ H ₁₇ ClN ₄ OS•HCl	0.1000	337.27	2.96E-04	2.96E-07	0.296
Cyanocobalamin (Vit. B-12) C ₆₃ H ₈₈ CoN ₁₄ O ₁₄ P	0.0020	1355.37	1.48E-06	1.48E-09	0.001
Biotin (Vit. H) C ₁₀ H ₁₆ N ₂ O ₃ S	0.0020	244.31	8.19E-06	4.09E-09	0.004

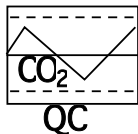
Notes:

- 1) All stock solutions were prepared using ultrapure D.I. water (18.2 MΩ·cm)
- 2) Completed medium was stored in the dark and bubbled with 0.2 µm filtered ambient air for a minimum of 24 hours to allow for the adjustment of the seawater pH to reach 8.0±0.1.

Appendix II: Diagrammatic representation of QUBIT



Appendix III: Tris Buffer CRM Certificate



<http://andrew.ucsd.edu/co2qc/>

University of California, San Diego
Scripps Institution of Oceanography
Marine Physical Laboratory
9500 Gilman Drive
La Jolla, CA 92093-0244

Certificate of Analysis

pH reference material (tris buffer in synthetic seawater)

Batch 13 (Bottled on June 18th, 2012)

This reference material consists of a buffer solution containing nominally equal concentrations (0.04 moles per kilogram of water) of tris (2-amino-2-hydroxymethyl-1,3-propanediol) and tris-HCl in a synthetic seawater with a nominal salinity of 35. It was prepared in accordance with the recipe described in DelValls and Dickson (1998), with the exception that the tris used was certified ACS alkalimetric standard obtained from Fisher Scientific (cat. # T3951) instead of certified material from NIST.

Analysis Results

The pH

$$\text{pH} = -\log_{10} \left(\frac{[\text{H}^+]}{\text{mol kg-soln}^{-1}} \right)$$

was determined on the total hydrogen ion scale using a hydrogen / silver – silver chloride cell (DelValls and Dickson, 1998). Four separate samples were measured in triplicate, on two different dates

The pH estimated at 25 °C was 8.0947 ± 0.0018 (12; 4).

The cited uncertainty represents the standard deviation. Figures in parentheses are the number of analyses made (total number of analyses; number of separate bottles analyzed).

Note: the value given in DelValls and Dickson (1998) for such a buffer is 8.0936. The small discrepancy (0.0011 in pH) is essentially negligible.

Estimated Overall Uncertainty

Although the measurements are capable of high precision, the overall uncertainty will be significantly greater. We are working to understand this value better, but presently expect it to be of the order of 0.005 in pH.

Stability

These buffer solutions have been shown to be stable to within 0.001 in pH for a period of a year (Nemzer and Dickson, 2005). However, they have not been poisoned, and an opened bottle should not be expected to remain stable for more than a few days at most.

A. G. Dickson
December 1, 2012

References

DelValls, T. A. and Dickson, A. G., 1998. The pH of buffers based on 2-amino-2-hydroxymethyl-1,3-propanediol ('tris') in synthetic sea water. *Deep-Sea Research I* **45**, 1541–1554.

Nemzer, B. V. and Dickson, A. G., 2005. The stability and reproducibility of Tris buffers in synthetic seawater. *Marine Chemistry* **96**, 237–242.

Appendix IV: Colour changes from the colorimetric pH measurement procedure



Colorimetric changes in pH from the spectrophotometric Dickson pH measurement protocol. The colour on the left indicates an acidified culture (pH 7.4) and the culture on the right represents a culture at ambient pH (pH 8.1). Colour changes ranged from yellow-orange in acidified cultures, to dark purple in ambient pH samples.

Appendix V: Comparison of in vivo fluorescence from Heterosigma akashiwo NWFSC 513, with different DFB concentrations

Objective:

This experiment was conducted to determine the appropriate concentration of the iron chelator, desferrioxamine B (DFB), necessary to induce an iron-limited environment for *Heterosigma akashiwo* 513, in a batch cultures with Enriched Seawater Natural Water (ESNW). The results will be used in subsequent studies involving iron-limitation.

Methods:

Cultures of *H. akashiwo* NWFSC 513 were grown in 50 mL borosilicate glass test tubes with teflon-lined caps at a 1.5% inoculum. The medium, with the omission of the

micronutrients iron and silica, and its preparation are described in Algal Culturing Techniques (Anderson *et al.* 2002).

The following experiment was conducted in duplicates using sterile techniques for all culturing work. Five DFB concentrations were added separately to five test tubes at the following concentrations: 0 nM, 50 nM, 100 nM, 150 nM, 200 nM. Cultures were grown at $20^{\circ} \pm 2^{\circ}$ Celsius at 250 $\mu\text{mol photons/m}^2/\text{s}$ 12h:12h light:dark cycle. Determinations of *in vivo* fluorescence were measured at 24 hour intervals by inserting the entire tube into a Turner Designs model 10-AU fluorometer, after mixing by three inversions.

RFU values: #1

	0 nM	50 nM	100 nM	150 nM	200 nM
	DFB	DFB	DFB	DFB	DFB
Day	0X	1X	2X	3X	4X
0	2.86	2.98	3.1	3.04	2.75
1	5.39	5.06	5.28	4.87	5.1
2	7.71	8.37	6.9	8.91	6.52
3	12.7	17.9	10.8	11.8	10.2
4	21.4	24.3	16.5	18.6	14
5	31.4	41.7	26.4	25.8	21.6
6	64.7	86.2	46.5	51.7	23.7
7	OVER	OVER	74.9	OVER	38.5

RFU values: #2

REPEAT	0 nM	50 nM	100 nM	150 nM	200 nM
2	DFB	DFB	DFB	DFB	DFB
	0X	1X	2X	3X	4X
0	2.98	3.02	2.89	2.89	2.87
1	5.16	5.41	5.47	4.73	4.66
2	8.41	7.45	7.77	9	7.77
3	15.1	12.7	13.7	17.8	11.3
4	24.9	19.1	18.7	15.2	16
5	43.3	36.4	27.8	25.8	18.4
6	77.8	60.5	45.4	37.5	26.1
7	OVER	OVER	71	62.3	39.6

Cell counts (cells/mL)

[DFB]	0 nM	50 nM	100 nM	150 nM	200 nM
Day 1:					
Repeat 1	888	2090	4300	1294	1150
Repeat 2	1075	1189	1539	977	1035
Day 3:					
Repeat 1	2430	3225	2250	2400	2170

Repeat 2	3500	2825	2360	2988	2060
----------	------	------	------	------	------

Day 5

Repeat 1	6300	6275	4317	4267	3867
Repeat 2	10125	6175	8175	5600	10400

Appendix VI: Lab-ware cleaning protocol

Cochlan Ecophysiology Laboratory
 Romberg Tiburon Center for Environmental Studies
 Updated: April 9, 2013 by J. Herndon

Background

Ensuring that laboratory glassware and plastic-ware are clean is essential for the successful outcome of laboratory experiments and chemical analysis.

Safety

Read the MSDS's for all chemicals used for cleaning.

Hydrochloric acid (HCl) can cause severe burns. The fumes can damage the lungs and eyes. Strong bases like potassium hydroxide (found in Contrad laboratory detergent) are corrosive.

Personal Protective Equipment (PPE): Lab coat, goggles and gloves should be worn in addition to closed toe/heel shoes. A face shield may be worn if there is concern about splashing. Note: a face-shield may NOT be worn in place of goggles/safety glasses. Larger nitrile gloves (green dishwashing gloves) may be worn to provide better coverage of the wrists and forearms.

Collect used acid and dispose of by mixing with algal cultures to be killed (acid will be neutralized during this process) or label as hazardous waste and dispose of appropriately.

Cleaning Process (LIVE)

- 1) Remove any tape or labels; use a razor blade if necessary.
- 2) Rinse with deionized water (DI) to remove salts and other residue. Note for bottles and flasks containing algae culture residue: pour the residual culture in the 20L "Acid Kill" carboy. Add a small volume of 10% HCl (vol/vol) to the container to kill the culture, use a brush if necessary to remove any organic culture residue (be careful not to scratch the container). Pour this sludge into the acid kill carboy also then rinse with DI before placing in the Contrad bath.
- 3) Place item in ~2-5% vol/vol Contrad bath for 2 to 24 hours. Note: Do not place polycarbonate items, rubber or Viton O-rings/gaskets, silicone stoppers as these will be damaged. See addendum #1 below for cleaning these types of items. DO NOT place any "Dead" items used with toxic chemicals or preservatives in the "LIVE" Contrad bath.
- 4) Remove items from Contrad bath and rinse with DI to remove detergent residue. Avoid dripping the detergent on the floor or your shoes. You may place the items in the bottom of the "LIVE" sink (previously rinsed), however, be mindful that the bottom of the sink is not "clean", small items should be placed inside beakers or other lab-ware to prevent contact with the bottom of the sink.

- 5) Place items in 5% vol/vol (~1.8% actual concentration) HCl bath. Allow them to soak for 2 to 24 hours. Observe the same cautions as stated for the Contrad bath.
- 6) Remove the items and rinse 3 times with ultrapure water (18.2 MΩ·cm, Milli-Q). You may choose to save on Milli-Q and do the first 2 rinses with DI. Ensure that all the internal surfaces of the items are contacted by the rinses. Remember to thoroughly rinse the inside of the caps and threads. Observe the same cautions as stated for the Contrad bath.
- 7) Allow the items to air dry, inverted on a previously cleaned drying rack or on kim-wipes laid out on a clean section of lab bench. Make sure to cover items such as magnetic stir-bars, plastic connectors, glass air diffusers, etc. that may get dirty from dust settling on them. Rinse your dishwashing gloves and allow them to dry before storing in a bag labeled with your name. If necessary, items may be dried in the drying oven.
- 8) Once dry, cover openings with aluminum foil and put the items away in their clean storage area. Small items may be stored in clean, labeled plastic bags. The aluminum foil cover is an indication to all lab members that the item has been through the proper cleaning procedure.

Note: when not in use, close the lids on the 10% vol/vol acid, DI and Milli-Q carboys. This will keep the water cleaner and reduce acid vapors in the lab.

Note: DEAD lab-ware (items used with toxic chemicals or preservatives) should be cleaned in the “DEAD” sink inside the Fume Hood. The Contrad step is typically omitted.

Refilling Cleaning Carboys

There are three 20L carboys over the sink. They contain DI, Milli-Q and 10% vol/vol HCl

- 1) DI and Milli-Q carboys can be re-filled directly from the DI hose and Milli-Q Gradient directly. If you have not obtained water from these sources, ask a knowledgeable lab-member first. Flush the DI hose and Milli-Q dispensing gun for a few seconds before collecting water for the carboy. Read the instructions for the Milli-Q before obtain water from it.
- 2) 10% HCl: Using scissors cut a strip of white lab mat and place it (plastic side down) in the fume hood.
- 3) Move the “10% hydrochloric acid” carboy to the DI water outlet and fill it with DI water to the 18L mark.
- 4) Place the carboy on the white lab mat in the fume hood.
- 5) Obtain a bottle of concentrated Hydrochloric acid (36-38%) from the acid cabinet and place it in the hood. Note: remember to adjust the sliding glass door to provide adequate access and protection from harmful vapors or splashes.
- 6) SLOWLY pour two liters of concentrated HCl into the container so that it reaches the 20L mark. Note: the reaction is highly exothermic and releases chlorine vapor so proceed slowly, but fast enough so that the acid won’t dribble down the side of the bottle as you pour. Wipe the bottle mouth/threads with a kimwipe to prevent acid dribbles on the outside. Return the concentrated HCl bottle to the acid cabinet and. Note: a full 20L carboy weighs 40 kilograms (about 88 pounds), so lift carefully to return it to the shelf above the sink.

Refilling Contrad and Acid Baths

Contrad bath:

- 1) Carefully pour the old Contrad down the LIVE sink while the faucet is running for dilution.
- 2) Rinse the soaking tank with DI and add DI until a depth of 10-15cm (4-6 in). Add a generous dollop of concentrated Contrad.

Acid bath:

- 1) Carefully pour (two people should do this part) portion of the used acid into the “algae acid kill carboy”. The rest should be collected in a waste carboy and tagged for appropriate disposal. Obtain a 20L waste carboy from the RTC Laboratory Coordinator (Brita Larsson).
- 2) Wheel the acid bath to the floor by the sink next to the Milli-Q.
- 3) Transfer the 10% hydrochloric acid carboy to the counter next to the Milli-Q and allow the spigot to hang over the edge, aimed into the acid bath.
- 4) Aim the DI water hose into the acid bath tub.
- 5) Turn on both the 10% hydrochloric acid carboy and the DI hose at roughly the same flow rate into the tank at the same time.
- 6) Fill to 10-15cm (4-6 in). Final concentration should be about 5% vol/vol HCl

Addendum #1 Cleaning specialized lab-ware

Silicone stoppers, Viton O-rings/gaskets and other delicate items: Follow the same process as described in the “Live Cleaning Process”, but limit the time in the Contrad and Acid baths to 5-10 minutes.

Polycarbonate bottles should be cleaned with a dilute solution (2-4mL/L) of Nalgene L900 cleaner for Polycarbonate. These bottles can be soaked for 2-24 hours. Then rinse with DI to remove the L900, rinse with 5-10% vol/vol HCl followed by three rinses with Milli-Q. For both the acid and Milli-Q rinses, ensure that the cap and threads are thoroughly rinsed. One way to do this is to pour the acid into the cap and then over the threads. The used L900 can be poured down the sink.

Volumetric flasks (glass and plastic) used for standards can be rinsed with 10% vol/vol HCl or soaked with 5% vol/vol HCL for 2-24 hours. Rinse three times with Milli-Q.

These items may also be stored full of Milli-Q to allow them to get cleaner. Volumetric flasks in the lab that are full all the way to the top when stored are full of Milli-Q.

Additional Reading:

Algal Culturing Techniques. R. A. Andersen, Ed. Chapter 5. Elsevier 2005.

Appendix VII: Care and maintenance of pH probe

Over time, probes become de-sensitized to the culture solution that they are contained in and were shown to develop a biofilm that would alter the true pH reading of the culture. Therefore, prior to the commencement of all experiments, pH probes were freshly cleaned and calibrated according to the procedure below. After 5 days of growth during experiments, pH probes were once again cleaned and calibrated to ensure accuracy of all pH measurements.

- 1) Remove the pH probe from the electrolyte solution.

- 2) Rinse pH probe in D.I. water (18.2 MΩ·cm), and gently clean the end of the probe with a cotton-ended Q-tip.
- 3) Soak the pH probe in a beaker containing a 10% Hydrochloric Acid solution for 10 minutes.
- 4) Rinse the pH probe with D.I. water and soak the probe in a beaker containing D.I. water for 1 minute.
- 5) Return probe to electrolyte solution.
- 6) Re-calibrate the pH probes with a 3-point calibration method.

Appendix VIII: DCMU protocol

Cochlan Ecophysiology Laboratory
 Romberg Tiburon Center for Environmental Studies
 Updated: April 9, 2013 by C. Bronicheski

Background

The following protocol for measuring photosystem II efficiency is outlined specifically for the alga, *Heterosigma akashiwo*.

Safety

Read the MSDS for DCMU before use.

Personal Protective Equipment (PPE): Lab coat, goggles and gloves should be worn in addition to long pants and closed toe/heel shoes.

Process for measuring Fv/Fm using the Turner Designs 10-AU Fluorometer:

*Ensure the range of the Fluorometer is set to “AUTO”

1) Make a 10 mM DCMU solution in 95% EtOH:

FW = 233.1
 $C_9H_{10}Cl_2N_2O$

$(12.011)_9 = 108.099$
 $(1.00794)_{10} = 10.0794$
 $(35.453)_2 = 70.906$
 $(14.0067)_2 = 28.0134$
 $(15.9994) = 15.9994$
 233.0972

$233.1 \text{ g/L} = 1000\text{mM}/10\text{mM}$
 $= 2.331\text{g/L}$

$$2.331\text{g/L} = x/.250\text{ L}$$

x = 0.58275g into 250 ml bottle ---target volume

Goal: 95% ethanol and 5% Milli-Q therefore add 237.5 mL of ethanol to 12.5 mL of Milli-Q

- 2) Measure background fluorescence of your sample using filtered seawater as a blank
- 3) Measure again with DCMU (should result in the same value)
- 4) Record RFU from step #3
- 5) Take your first true sample and wipe the vial with a Kimwipe
- 6) Invert sample 3 times, insert in the Fluorometer and quickly re-cap the Fluorometer sample chamber
- 7) Wait for the Fluorometer to adjust to the proper range
- 8) Press “*” and record the resulting RFU value when the instrument reads “DONE” (which will be after 5 seconds + an additional 5 seconds)
- 9) Remove sample vial from sample chamber quickly, and re-cap the sample chamber
- 7) Add 2 drops or 100 μL , of DCMU to your sample vial and mix (cap and invert 3x). Avoid touching the centre of the tube (no need to re-wipe)
- 8) Record the resulting RFU, after you insert and observe:
 - A) If the value decreases but then increases: record the lowest value. This is a result of (1) light flooding the photomultiplier tubes or (2) the Fluorometer switching ranges because the initial signal is very high.
 - B) Value increases, pauses, then increases more: record the “pause” value.
- 9) Leave the sample in the chamber until ready to analyze the next sample. This ensures that the Fluorometer is in the correct “Range” for the next sample (to avoid switching ranges mid-sample).
- 10) You can calculate variable fluorescence as:

$$F_v/F_m = [(RFU + DCMU) - RFU] / (RFU + DCMU)$$

$F_v = F_m - F_o$, where F_v is variable fluorescence, F_o is background fluorescence of the cells (all of the PSII reaction centers are open), and F_m is the “maximal” fluorescence before photochemical quenching (e.g. xanthophylls cycling) is initiated. non-

Dark-adapting the sample removes the fluorescence signal associated with the growth irradiance, and makes it easier to interpret the data (you get the potential, or true, F_v/F_m , rather than the light-induced F_v/F_m)

Note 1: if your blank from step 2 is not zero, you should subtract it from all values.

Note 2: The maximum F_v/F_m value for the very healthy cells should be around 0.7. If it's higher than that, you probably waited too long to read the RFU value.

Note 3: Depending on the Fluorometer, the “background” fluorescence measured without DCMU can be too high. That can be corrected for later by doing a “dilution” with a known culture sample and stopping down the excitation light using either neutral-density filters or Turner Design light baffles.

Disposal:

Ensure samples with DCMU are disposed in proper waste containers.

Additional Reading:

Butrón, A., Madariaga, I., Orive, E., Tolerance to high irradiance levels as a determinant of the bloom-forming *Heterosigma akashiwo* success in estuarine waters in summer, *Estuarine, Coastal and Shelf Science* (2012), doi: 10.1016/j.ecss.2012.05.008.

Curriculum Vitae
CAYLA M. BRONICHESKI

EDUCATION

- Master of Science in Biology, Physiology & Biochemistry** 2013
Collaboration with the Centre for Environment & Sustainability
University of Western Ontario, London, ON, Canada
- Bachelor of Science, Honors Specialization in Environmental Science** 2011
University of Western Ontario, London, ON, Canada

RELATED WORK EXPERIENCE

- Teaching Assistant** 2011 - 2013
Departments of Biology and Business Management Operations
Courses: Biology laboratories, Ecology, Environmental Biology & Business Management
University of Western Ontario, London, ON, Canada
- Laboratory Technician** 2011
Department of Biology in collaboration with *Trojan UV Technologies*
University of Western Ontario, London, ON, Canada
- Research Assistant** 2008 - 2011
Robarts Research Institute, Department of Medical Sciences
London, ON, Canada

AWARDS

- Award of Excellence Scholarship, University of Western Ontario 2013
Best Presentation, Centre for Environment & Sustainability at Western 2013
Award of Excellence Scholarship, University of Western Ontario 2012
Western Graduate Research Scholarship, University of Western Ontario 2011 - 2013
3-Minute Thesis Competition Finalist, University of Western Ontario 2012
Dean's Honor List, University of Western Ontario 2009 - 2011
Western Scholarship of Distinction 2007

PUBLICATIONS

Submitted

Ikeda, C.E., **Bronicheski, C.M.**, Trick, C.G. & Cochlan, W.P. (2013) The combinatorial effect of salinity and temperature on cellular permeability and toxicity of *Heterosigma akashiwo*, from Puget Sound, WA. Submitted to: *Harmful Algae*.

Czikkel, B.E., Petri, B., **Bronicheski, C.M.** & Trick, C. (2013) The effect of germicidal UV on the survival of the marine phytoplankter, *Tetraselmis* spp. – establishing the proper metrics of viability. Submitted to: *Water Research*.

Czikkel, B.E., Petri, B., **Bronicheski, C.M.** & Trick, C. (2013) The effect of germicidal UV on the survival of the marine phytoplankter, *Tetraselmis* spp. – establishing the damage to the photosystem. Submitted to: *Environmental Sciences and Technology*.

CONTRIBUTIONS

Oral presentations

Ikeda, C. E., **Bronicheski, C. M.**, Trick, C.G. & Cochlan, W.P. (2013) The combinatorial effect of salinity and temperature on cellular permeability and toxicity of *Heterosigma akashiwo*, from Pudget Sound, WA. ASLO Ocean Science Meeting 2014, Honolulu, Hawaii, USA.

Bronicheski, C.M. & Trick, C.G. (2012) Assessing the impact of ocean acidification on the quality of phytoplankton- as a food source- for productive marine food webs. 25th Annual Western Graduate Research Forum, University of Western Ontario, London, ON, Canada.

Bronicheski, C.M. & Trick, C.G. (2012) Fast food or fine dining: what's for dinner in our acidic ocean?. 3-Minute Thesis Competition, School of Graduate and Postdoctoral Studies, University of Western Ontario, London, ON, Canada.

Bronicheski, C.M. & Trick, C.G. (2012) Fast food or fine dining: what's for dinner in our acidic ocean?. 9th Annual Earth Day Colloquium, University of Western Ontario, London, ON, Canada.

Bronicheski, C.M. & Trick, C.G. (2011) Investigation of germicidal UV impacts on the marine flagellates, *T. apiculata* and *H. akashiwo*. Ontario Biology Day, Wilfrid Laurier University, ON, Canada.

Bronicheski, C.M. & Trick, C.G. (2011) The impact of germicidal UV on the photosynthetic efficiencies of two marine flagellates. 8th Annual Earth Day Colloquium, University of Western Ontario, London, ON, Canada.

Bronicheski, C.M. & Trick, C.G. (2011) Investigation of germicidal UV impacts on the marine flagellates, *T. apiculata* and *H. akashiwo*. Environmental Science and Biology Day, University of Western Ontario, London, ON, Canada.

TEACHING DEVELOPMENT WORKSHOPS

Research on teaching symposium

2012

Fall perspectives on teaching conferences

2011 - 2012

COMMITTEES

Society of Graduate Students, Sustainability Committee, University of Western Ontario

Earth Day Colloquium Committee, University of Western Ontario

Environment and Sustainability Society, University of Western Ontario

Environmental Science Association, University of Western Ontario

The sea, once it casts its spell, holds one in its net of wonder forever.

Jacques-Yves Cousteau